Physical Layer Algorithms and Architectures for Accurate Detection and Classification in Cognitive Radios

NARENDAR MADHAVAN

SCHOOL OF COMPUTER ENGINEERING

A thesis submitted to the Nanyang Technological University in partial fulfillment of the requirement for the degree of Doctor of Philosophy

2014

I dedicate this work to my family- Madhavan, Hemalatha, Vidhya, and Mahendar.

Acknowledgements

They say that you are on your own in your Ph.D. They may be wrong. An outstanding group of people have come together to make this thesis possible. And I would like to thank all those people who have supported me.

First and foremost, I would like to express my gratitude to my supervisor, Dr. Vinod A. Prasad. Without his guidance, encouragement, and timely help I could never have finished my doctoral work in Nanyang Technological University. I remain amazed at his dedication and motivation towards work. He not only provided me technical guidance, but also helped me build my character and personality. I thank him for his patience and understanding and for giving me the freedom to explore. I am indebted to him for his discussions and personal advices that go beyond the academics. I hope I could take a leaf out of his book and emulate him in the future.

I am greatly indebted to my co-supervisor, Dr. A.S. Madhukumar, who bombarded me with technical questions whenever I went to discuss with him. This helped me in critically analyzing my research methods constantly.

I would like to take this opportunity to thank European Aeronautics Defense and Space (EADS) Company for sponsoring my Ph.D. I express my most sincere gratitude to Dr. Anoop Kumar Krishna, Senior Expert at EADS Innovation Works, for providing me precious technical guidance, support and care throughout my Ph.D. as well as an internship opportunity in the final stages of my work. The one year long internship at EADS Innovation Works, Singapore played a major role in shaping my thesis. I would also like to express my gratitude to Dr. Timo Bretschneider, EADS Innovation Works, for providing me with valuable advice on life and time management during my thesis writing.

My vote of thanks is inadequate without the special mention of my lab seniors, Dr. Mahesh, Dr. Smitha, and Dr. Kavitha, for all their untiring help and motivation. My heartfelt thanks to my fellow lab mates, Sumit, Navin, Neethu, Rakesh, Supriya, Prashob, Mengda, Sumedh and Abhishek, for always being ready for a technical discussion in the lab. I also would like to thank the CHiPES lab's technical staff, Mr. Jeremiah and Ms. Merilyn, for providing an easy and quick access to the resources and facilities.

Words fail me to express my love and appreciation to my best friend 'Basu' for her support, care and love. Past several years have not been an easy ride, both academically and personally. Reelina (her original name) was always beside me through thick and thin. She was not the wind beneath the wings, but the wings itself. I was also lucky to have a wonderful group of close friends in Hari, Mani and Manish. They always had my back, providing me help and advice about everything under the sun. Hari, for sticking with me for 9 years and being the pillar of strength whenever I went weak, providing me financial, academic and emotional support whenever I was in need, Manish for the 'brotherhood' he shared and for proof-reading my thesis, Mani for being the nonchalant, leg-pulling friend he always was. He never failed to bring a smile onto my face. I also have to thank a huge list of friends who were part of my social life here at NTU- Abhinav, Ravi, Maggi, Mrinal, Nandhu, Laxmi, Archana, Mukesh, Sid, Vaishu, Maith, Lea, Snehal for giving me the support I needed during times of distress. Vijay and Durga for giving me the most beautiful niece, Mithra, who uplifts my mood even when she is asleep. My cricket team mates for teaching me camaraderie and sportsmanship while playing cricket. My guitar partner, Vinay, who not only brought music into my life but also a multitude of progressive and rational thinking. Sharada, for all the love, support and care that she gave me unselfishly.

Finally, I would like to acknowledge the people who mean the world to me, my mom, dad, brother, sister and brother-in-law. My hard-working parents have sacrificed their lives for us and provided unconditional love, care and education. My dad, Madhavan who worked all his life (still is), so that we can have a comfortable life. He couldn't further his education because he was the sole bread winner although he was a bright student at school. My mother, who keeps tab on when I eat even when I forget, for the awesome woman she is, and for the love and sacrifice she has done for my family. My sister, Vidhya, for constantly keeping me grounded, pointing out my flaws and yet giving me freedom of thought, my brother-in-law Vishwa, for setting a great example of a bro-in-law and allowing me to stay at his place. My twin brother, Mahen for being the mirror, literally and figuratively and the new intake in our family, Ashu, for her love. Lastly, to all my role models- Dr. Richard Dawkins, Christopher Hitchens, Dr. V.S. Ramachandran, Mahakavi Bharathiyar, Thiruvalluvar, Ilayaraja, Kamal Hassan, Sachin Tendulkar, Che Guevara, and Bhagat Singh for keeping me inspired through their work.

Abstract

The new mobile broadband technology is rapidly growing towards a fifth generation (5G), as there is an increasing demand for high data rate devices. The advent of new wireless communication services renders the electromagnetic spectrum congested. This congestion, coupled with rigid allocation of spectrum to the new wireless systems, leads to inefficient spectrum utilization and causes an apparent spectrum scarcity. Cognitive radio (CR) is envisaged as a solution to tackle the problem of this apparent spectrum scarcity. It is a conscious radio, which opportunistically uses the spectrum of a licensed user known as primary user (PU) while causing minimal interference to them. It utilizes software-defined radio (SDR) to adapt its transmission properties to match the required standards. In order to determine the spectral vacancies, the CR has to locate the PU signals accurately with the help of a spectrum sensing unit. In addition, after detecting the signal, the CR must be able to classify the detected signal into a known user type. This thesis presents methods for accurate wideband detection and modulation classification for a stand-alone CR scenario in the physical layer domain. These methods operate with partial knowledge about the PUs' signal and/or the noise environment. The proposed algorithms can also extract certain features of the signal spectrum such as edge frequencies and modulation scheme in a robust manner. In general, the research problem of signal detection and classification is addressed in this thesis using three methods- filter bank based detectors, higher order statistics and fractional lower order statistics.

In the first work, a filter bank based detection method that helps in determining the location of the vacant bands, by locating the PU signal and its edge frequencies is presented. In order to increase the granularity and efficiency of detection, the method involves a new multi-stage discrete Fourier transform filter bank based energy detector. An algorithm is proposed that determines the edge frequencies of the PU channels using the properties of filter bank and the information from the energy detector. Simulation and computational analysis show that the proposed method gives a good balance between accuracy and complexity. The design example and simulations show that the gate count resource utilization of this detection scheme is 22.9% lesser than the wavelets based detection method at the cost of a slight degradation of 0.5% in detection accuracy. This

method provides a good foundation to understand the underlying problem of spectrum sensing and its challenges.

The algorithms in the first work are based on second-order statistics where the noise has a degrading effect on the signal. The sensing becomes even more challenging in the presence of strong interferers, noisy environment or under fading conditions. To mitigate this, the second work proposes a detection and classification algorithm based on higher-order statistics (HOS) and fractional lower-order statistics (FLOS). Spectrum sensing is performed using the proposed test statistic for detection that incorporates modified cumulants derived using fractional lower order statistics. The performance of the proposed method is compared with the conventional method based on higher-order statistics for various noise conditions. It is shown that the proposed method performs well in both Gaussian and non-Gaussian conditions as compared to the conventional method. An experimental data acquisition setup was employed to obtain real time signals from the wideband spectrum to analyze the noise characteristics. The main advantage of the proposed method is that the same statistic used for detection is also used for classification.

After locating the vacant bands, the CR is required to change its transceiver parameters to use the vacant band opportunistically, which is achieved using SDR technology. In the third work, a CR scheme including a policy engine, two-stage spectrum sensing unit and an SDR is elucidated. The focus is on the working of a real-time policy engine with a two-stage spectrum sensing unit that aids policy driven cognitive radio. A new two-stage filter bank based energy detector and cumulants method has been proposed for accurate spectrum sensing. The filter bank used for channelization is used for spectrum sensing as well, resulting in complexity reduction.

Furthermore, this thesis presents validation of some existing and proposed algorithms using real world signals captured using a USRP2 radio and GNURadio framework. The main contribution of the work is on improved sensing and classification methods for cognitive radios and military radios. By deploying SDR, an overall framework for spectrum sensing based policy-driven CR has been demonstrated.

Publications

Journals

1. **M. Narendar**, A. P. Vinod, A.S. Madhukumar and Anoop Kumar Krishna, "Robust Two-stage Spectrum Sensing and Policy Management for Cognitive Radios Using Fourth Order Cumulants" in Academic Publications, *International Journal of Information Engineering*, IJIE Vol. 3, Iss. 2, Jun. 2013, PP. 45-55.

2. **M. Narendar**, A.P. Vinod, A.S. Madhukumar, Anoop Kumar Krishna, A tree-structured DFT filter bank based spectrum detector for estimation of radio channel edge frequencies in cognitive radios, *Physical Communication*, Available online 19 June 2013, ISSN 1874-4907, http://dx.doi.org/10.1016/j.phycom.2013.06.001.

3. **Narendar Madhavan**, A.P. Vinod, A.S. Madhukumar, Anoop Kumar Krishna, "Spectrum sensing and modulation classification for cognitive radios using cumulants based on fractional lower order statistics," *AEU - International Journal of Electronics and Communications*, Available online 25 December 2012, ISSN1434-8411, 10.1016/j.aeue.2012.11.004.

Conferences

1. **M. Narendar**, A. P. Vinod, A.S. Madhukumar and Anoop Kumar Krishna, *"*Automatic Modulation Classification for Cognitive Radios Using Cumulant Based on Fractional Lower Order Statistics*".* in *Proc. of the XXX General Assembly and Scientific Symposium of the International Union of Radio Science (Union Radio Scientifique Internationale-URSI),* pp. 1-4, 13-20 August 2011, Istanbul, Turkey.

2. **M. Narendar**, A. P. Vinod, A.S. Madhukumar and Anoop Kumar Krishna, "A Tree-Structured DFT Filter Bank based Spectrum Sensor for Estimation of Radio Channel Edge Frequencies in Military Wideband Receivers", in *Proc. of*

10th International Conference on Information Science, Signal Processing and their Applications, pp. 534-537, Kuala Lumpur, May 2010, (ISSPA 2010).

3. **M. Narendar**, A. P. Vinod, A.S. Madhukumar and Anoop Kumar Krishna, "An Algorithm for Spectrum Sensing in Cognitive Radio using Tree-Structured Filter Bank", *in Proc. of 17th IEEE International Conference on Telecommunications*, pp. 418 - 424, Doha, April 2010 (ICT 2010).

4. **M. Narendar**, A. P. Vinod, A.S. Madhukumar and Anoop Kumar Krishna, "A Robust Two-stage Spectrum Sensing Method Using Filter Bank based Energy Detector and Fourth Order Cumulants for Cognitive Radios", in *Proc. of the 13th International Conference on Communications Systems (ICCS)*, pp.438-442, 21-23 Nov. 2012, Singapore.

This page is intentionally left blank

Contents

ACKNOWLEDGEMENTS ..... **II**

ABSTRACT ..... **IV**

PUBLICATIONS ..... **VI**

LIST OF FIGURES ..... **XII**

LIST OF TABLES ..... **XVI**

LIST OF ABBREVIATIONS ..... **XVII**

LIST OF SYMBOLS ..... **XXI**

CHAPTER 1 ..... **1**

INTRODUCTION **1**

1.1. BACKGROUND AND MOTIVATION 1
1.2. OBJECTIVES 3
1.3. CONTRIBUTIONS 4
1.4. OUTLINE 7

CHAPTER 2 ..... **8**

LITERATURE SURVEY **8**

2.1. OVERVIEW OF COGNITIVE RADIO AND DYNAMIC SPECTRUM ACCESS 8
2.2. SPECTRUM SENSING REQUIREMENTS, CHALLENGES, AND TECHNIQUES 12
2.3. SPECTRUM SENSING ALGORITHMS 16
2.3.1. Matched Filtering 18
2.3.1.1. Coherent Detectors 19
2.3.2. Energy Detection 19
2.3.2.1. Multi-Antenna Multi-Resolution Energy Detector 25
2.3.2.2. Frequency Domain Spectrum Estimation 25
2.3.2.3. Wavelet-based Spectrum Sensing 26
2.3.2.4. Forward Methods based Energy Detection 27
2.3.2.5. Adaptive Threshold based Energy Detection 28
2.3.3. Feature Detection 29
2.3.3.1. Cyclostationarity-based Detection 30
2.3.3.2. Multi-cycle and Single-cycle Spectral Correlation Detectors 31
2.3.3.3. Other Cyclic Detectors 33
2.3.3.4. Energy based Feature Detection 34
2.3.3.5. Correlation Feature Detectors for OFDM Signals 34
2.3.4. Waveform-based Sensing 34
2.3.5. Eigen Value Detection 36
2.3.6. Multiple Cumulants based Sensing 38
2.3.7. Two-Stage Spectrum Sensing 38

2.4. SUMMARY 39

CHAPTER 3 42

DATA MODELS AND EXPERIMENT SETUP 42

3.1. DATA AND NOISE MODELS 43
3.1.1. Symmetric-alpha stable model 43
3.2. DATA ACQUISITION USING USRP2 44
3.3. GNU RADIO FRAMEWORK 47
3.4. SUMMARY 52

CHAPTER 4 53

SPECTRUM SENSING BASED ON FILTER BANKS AND ENERGY DETECTION 53

4.1. INTRODUCTION 53
4.2. LIMITATIONS OF FILTER BANK BASED SPECTRUM SENSOR 56
4.3. PROPOSED FILTER BANK BASED SENSING 58
4.3.1. Problem Formulation 58
4.4. DESIGN AND SIMULATION RESULTS 64
4.5. FREQUENCY EDGE ESTIMATION ALGORITHM 68
4.6. COMPARISON WITH WAVELETS BASED EDGE DETECTION 74
4.6.1. Wavelets based Edge Detection 74
4.7. OVER-THE-AIR TESTS 80
4.8. COMPLEXITY COMPARISON WITH WAVELET EDGE DETECTION 84
4.9. SYNTHESIS RESULTS 87
4.10. SUMMARY 88

CHAPTER 5 90

FRACTIONAL LOWER ORDER AND HIGHER ORDER STATISTICS BASED SIGNAL DETECTION AND CLASSIFICATION 90

5.1. INTRODUCTION 90
5.2. PROBLEM FORMULATION 92
5.2.1. Generalized Gaussian (GG) distribution 94
5.2.2. Cauchy-Gaussian Mixture (CGM) distribution 94
5.3. PROBLEM DEFINITION AND PREVIOUS WORKS 95
5.3.1. Automatic Modulation Classification Methods 95
5.4. PROPOSED SCHEME FOR SPECTRUM SENSING AND AUTOMATIC MODULATION CLASSIFICATION 97
5.4.1. Estimation of FLOS based Cumulants for the Received Signal 98
5.4.2. Threshold Analysis 100
5.5. PROPOSED SCHEME USING FLOS BASED CUMULANTS 103
5.6. SIMULATIONS AND RESULTS 107
5.6.2. Performance Analysis of the Spectrum Sensing Method 110
5.6.3. Performance Analysis of the AMC Method 113
5.6.4. Complexity Analysis of the Proposed Method 121
5.7. SUMMARY 122

CHAPTER 6 ..... **125**

ROBUST TWO-STAGE SPECTRUM SENSING AND POLICY MANAGEMENT FOR COGNITIVE RADIOS **125**

6.1. INTRODUCTION 125
6.2. POLICY MANAGEMENT IN RADIOS 128
6.3. PROPOSED POLICY-BASED COGNITIVE RADIO 131
6.3.1. Proposed Sensing Policy Channel 133
6.3.2. Proposed Spectrum Sensing Method 134
6.4. SIMULATION RESULTS AND EXPERIMENTAL ANALYSIS 139
6.4.1. Analysis of the Proposed Two-stage Sensing Method 140
6.4.3. Experimental Setup and Analysis 145
6.5. SUMMARY 147

CHAPTER 7 ..... **149**

CONCLUSIONS AND FUTURE WORK **149**

7.1. CONCLUSIONS 150
7.2. FUTURE WORK 151

REFERENCES **155**

List of Figures

1.1. Contributions of this thesis. .....**Error! Bookmark not defined.**

2.1. A typical cognitive radio scenario. 11

2.2. Ideal and generalized interpretations of interference temperature model [16]. 14

2.3. Basic techniques for spectrum sensing. 17

2.4. A basic energy detector. 20

2.5. A basic Welch's periodogram [33]. 20

2.6. Trade-off between missed detections and false alarms [5]. 22

2.7. Implementation of a multi-cycles cyclostationary feature detector [74]. 33

3.1. USRP2 front view. 45

3.2. USRP2 top view. 45

3.3. RF antenna front view. 47

3.4. Block diagram of a USRP2 operating in GNU Radio framework. 48

3.5. Software architecture of GNU Radio. 49

3.6(a). Setup to capture signals using WBX antennae and USRP2. 51

3.6(b). Alternate setup for testing algorithms using Thomson DVB-T antenna and USRP2. 51

4.1. M -Channel DFTFB. 56

4.2. Spectral Scenario depicting the limitation of DFTFB spectrum sensor.

(a) Input spectrum to a DFTFB.

(b) Output spectrum as deciphered by a conventional DFTFB. 57

4.3. Proposed TDFTFB based sensing scheme. 60

4.4. Ratio of BWmax to BWmin vs number of stages. 62

4.5. Subband splitting of a DFTFB. 65

4.6. Realizable spectral region using all the subbands. 66

4.7. Example subband splitting using DFTFB 67

4.8. Subband splitting by the first-stage of TDFTFB..... 68

4.9. Algorithm for the edge detection process. 70

4.10. Simulation schematic of the proposed edge detection method. 71

4.11. Architecture for the energy detection in the edge detection process..... 72

4.12. PSD of Input Spectrum showing CH1, CH2 and CH3. 73

4.13. Percentage error versus number of stages, n, determined by $\log\left(\frac{BW_{\max}}{BW_{\min}}\right)$ 74

4.14. Multiscale wavelet products for scales 1 to 4 showing edges and irregularities..... 77

4.15. Multiscale wavelet sums for scales 2 to 5 showing edges and irregularities. 77

4.16. Over-the-air test setup. 81

4.17. A single frame of the PSD of the signal transmitted. 82

4.18. A frame of multiscale wavelet sums for scales 1 to 4 showing edges and irregularities. 82

4.19. A frame of multiscale wavelet products for scales 2 to 5 showing edges. 83

4.20. Complexity comparison of the proposed and wavelets methods (DWPT) for a ratio of BW_{max} to BW_{min} =5, for different length of input sequences, using a 40-tap filter. 87

5.1. Proposed scheme for sensing and modulation classification in a typical CR scenario. ... 97

5.2. Normalized theoretical cumulant value vs p for various modulation schemes. 100

5.3. Normalized theoretical cumulant value vs p for various noises. 101

5.4. Histogram of a typical non-Gaussian noise (slightly impulsive than Gaussian with p=0.9). 102

5.5. USRP2 Signal data flow. 108

5.6. USRP2 Radio setup to capture signals. 108

5.8. Comparison of probability of detection vs SNR in AWGN (p=1) for the proposed and conventional HOS method. 111

5.9. Comparison of probability of detection vs SNR in slightly impulsive noise (p=0.9) for the proposed and conventional HOS method. 112

5.10. Comparison of probability of detection vs SNR in highly impulsive noise (p=0.7) for

the proposed and conventional HOS method. 112

5.11. Comparison of probability of classification vs SNR in slightly impulsive noise (p=0.9) for the proposed and conventional HOS method in [128]. 114

5.12. Comparison of probability of classification vs SNR in highly impulsive noise (p=0.7) for the proposed and conventional HOS method in [128]. 114

5.13. Conditional probability of classification vs SNR in AWGN (p=1) for the proposed AMC method. 115

5.14. Conditional probability of classification vs SNR in AWGN (p=1) and multipath fading with L=4 without channel information for the proposed AMC method. 116

5.15. Confusion matrix as a bar plot showing probability of correct classification using the proposed AMC method for AWGN (p=1), multipath fading without channel information, and multipath fading with proposed channel correction for SNR= 7 dB and SNR= 10 dB. 118

5.16. Conditional probability of classification vs SNR in AWGN (p=1), and multipath fading with L=4 with channel correction for the proposed AMC method showing improved performance. 119

6.1. Proposed cognitive radio scheme with policy engine and spectrum sensing module.... 131

6.2. Proposed spectrum sensing module. 134

6.3. Proposed cumulant value and conventional cumulant value plotted against the channel numbers for BPSK, 16-QAM and 64-QAM signals at SNR=-10 dB. 140

6.4. Histogram comparisons of the proposed cumulant value and the conventional cumulant value for the binary hypothesis for a 64-QAM signal..... 141

6.5(a). Probability of detection and false alarm versus SNR for a 64-QAM signal using the conventional and proposed cumulants method. 142

6.5(b). Probability of detection and false alarm versus SNR for a 16-QAM signal using the conventional and proposed cumulants method. 143

6.5(c). Probability of detection and false alarm versus SNR for a BPSK signal using the conventional and proposed cumulants method. 143

6.6. Probability of detection versus SNR for various conventional methods and the proposed method. 144

List of Tables

Table 2.1. Comparison of various spectrum sensing algorithms 40

Table 3.1. Hardware Configuration of Data Acquisition 50

Table 4.1. Absolute average error in the estimation of edge frequencies of all the channels in the input signal using the proposed and wavelets method (500 simulations). 79

Table 4.2. Hardware Configuration for over-the-air tests 80

Table 4.3. Comparison of number of real multiplications of the proposed method and wavelets based method for input sequence length=2048, filter length=40 by varying the Ratio of BW_{max} to BW_{min} 86

Table 4.4. Comparison of hardware complexity in terms of power consumption for the proposed method and wavelets method with 42 taps using a coefficient wordlength of 12 bits. 88

Table 5.1. Hardware Configuration for Laboratory setup 107

Table 5.2. Comparison of the noise characteristics in various frequency bands 109

Table 5.3. Comparison of the probability of correct classification for the proposed modulation classification method and the conventional HOS method in the presence of AWGN and Rayleigh multipath fading (L=4) 119

Table 6.1. Hardware Configuration for over-the-air tests using USRP2 145

Table 6.2. Comparison of the Average decision time requirement for the proposed policy engine and XG DARPA engine [147] 146

List of Abbreviations

ADC	Analog-to-digital converter
ADT	Average decision time
AFE	Analog frontend
ALRT	Average likelihood ratio test
AMC	Automatic modulation classification
API	Application-programming interface
ATSCDTV	Advanced Television Systems Committee, digital television standard
AWGN	Additive white Gaussian noise
BPF	Bandpass filter
BPSK	Binary Phase Shift Keying
CDMA	Code division multiple access
CFAR	Constant false alarm rate
CGM	Cauchy-Gaussian Mixture
CLT	Central Limit theorem
CORBA	Common Object Request Broker Architecture
CR	Cognitive Radio
CRN	Cognitive radio network
DARPA	Defense Advanced Research Projects Agency
dB	Decibel
DDC	Digital Down Converter

DFE	Digital frontend
DFT	Discrete Fourier Transform
DFTFB	Discrete Fourier transform filter bank
DFS	Dynamic frequency selection
DSA	Dynamic spectrum access
DTV	Digital television
DWPT	Discrete Wavelet Packet Transform
DWT	Discrete Wavelet Transform
ED	Energy Detection
EEPROM	Electrically Erasable Programmable Read-Only Memory
EME	Energy with minimum Eigen value
FAM	FFT accumulation method
FBD	Feature based detectors
FCC	Federal Communications Commission
FFT	Fast Fourier transform
FLOS	Fractional lower order statistics
FPGA	Field Programmable Gate Array
GG	Generalized Gaussian
GPS	Global Positioning System
GLRT	Generalized likelihood ratio test
GNU	GNU Not Unix
GRC	GNU Radio Companion
GSM	Global System for Mobile
HLRT	Hybrid likelihood ratio test
HOS	Higher order statistics
IDFT	Inverse Discrete Fourier Transform

i.i.d	independent and identically distributed
ISM	Industrial, scientific, and medical
JB	Jarque-Bera
JTRS	Joint Tactical Radio System
LBD	Likelihood based detectors
LCD	Liquid Crystal Display
LPF	Low Pass Fitler
LTE	Long Term Evolution
MAC	Medium access control
MME	Maximum-minimum Eigen value
MRSS	Multi-Resolution Spectrum Sensing
MTM	Multitaper method
OFDM	Orthogonal Frequency-Division Multiplexing
PDC	Personal Digital Cellular
PDF	Probability density function
PE	Policy Engine
PHY	Physical layer
PN	Pseudo-random number
PSD	Power spectral density
PSK	Phase shift keying
PU	Primary user
QAM	Quadrature-amplitude modulation
QoS	Quality of service
QPSK	Quadrature Phase Shift Keying
RMT	Random matrix theories
$S\alpha S$	Symmetric alpha stable

SCA	Software Communications Architecture
SDR	Software defined ratio
SINR	Signal-to-interference-noise ratio
SNR	Signal-to-noise ratio
SPC	Sensing policy channel
SU	Secondary user
SWIG	Simple Wrapper and Interface Generator
TDFTFB	Tree-structured discrete Fourier transform filter bank
TETRA	Terrestrial Trunked Radio
TQMFB	Tree structured quadrature mirror filter bank
UE	User equipment
UMTS	Universal mobile telecommunications system
USRP2	Universal software radio peripheral2
UWB	Ultra-wideband
WBX	Wide bandwidth transceiver
WCDMA	Wideband Code Division Multiple Access
WiMAX	Worldwide Interoperability for Microwave Access
WLAN	Wireless Local Area Network
XG	Next Generation

List of Symbols

$r(t)$	Continuous time received signal
$\eta(t)$	Continuous time noise added in the channel
$s(t)$	Signal to be detected
H_0	Null hypothesis
H_1	Alternate hypothesis
P_d	Probability of detection
P_{fa}	Probability of false alarm
P_{md}	Probability of miss detection
Λ	Test statistic threshold
$r(n)$	Discrete time received complex signal
N	Number of samples/symbols
$\eta[n]$	Discrete time AWGN added to the signal
σ_s^2	Signal variance
σ_w^2 or σ_n^2	Noise variance
T	Time period of the signal
M	Number of subbands of the DFTFB
f_s	Sampling frequency

N	Minimum number of stages of a DFTFB
$h(n)$	Channel coefficients
$E(\ )$	Statistical expectation
$\gamma(\ )$	Gamma function
S	Sample skewness
K	Sample Kurtosis
$L_{pq}(x)$	Zero lagged p^{th} order-q^{th} conjugate cumulant

Chapter 1

Introduction

1.1. Background and Motivation

During the last decade, there has been an enormous boom in the utilization of electromagnetic radio frequency spectrum. With the advent of new wireless technologies and devices, and increase in the number of subscribers, there is an escalating demand for seamless, high data rate services. On the other hand, this has congested the limited radio spectrum available. However, recent survey studies on spectrum utilization revealed that this apparent spectrum scarcity is due to the rigid allocation policy adopted by many spectrum regulatory bodies such as the Federal Communications Commission (FCC) [1]. In the fixed allocation policy, each licensed user is allocated a part of the entire frequency spectrum. Dynamic spectrum access (DSA) is proposed as a technology to solve this spectral congestion problem by employing intelligent, self-adapting radios known as cognitive radios (CRs), which can utilize the spectrum efficiently. The CR scenario allows the unlicensed users known as secondary users (SUs) (called CR users) to use a frequency band allocated to licensed users or primary users (PUs) in an opportunistic and non-interfering basis [1].

Cognitive radio is a term coined by Joseph Mitola [2], that refers to an intelligent radio that has the ability to sense, learn and be aware of its surrounding spectral environment. Moreover, a CR is capable of adapting its parameters to the sensed environment providing better performance to the SU. In order to sense and learn about the

spectral environment, a CR-enabled SU has to perform spectrum sensing, i.e., detect the PUs and vacant bands (white spaces) for opportunistic usage. For the SUs to be able to identify potential spectral vacancies accurately, robust algorithms for signal detection, identification and classification are critical. CR also finds applications in civilian spectrum management. These applications may include, e.g., traffic analysis, public safety radio, jammer detection, identification, and characterization of interference sources.

In addition to the application in CR and DSA, signal identification and classification is a key feature in multi-mode software defined radios (SDRs), adaptive modulation and coding systems. Prior knowledge of the modulation scheme used by the transmitter can aid these radio receivers to perform signal demodulation. However, this information about the modulation scheme has to be transmitted along with the data. This overhead can be reduced using blind modulation classification techniques, thereby increasing the achievable data throughput [3]. In addition, in military communications, there is an inherent need to frequently scan the radio spectrum for detection of jammer or intruder signals. This includes, employing jamming interference cancellation, deploying adaptive frequency hopping, equalization etc. The present methods for the location of jammers and interference protection are substantially limited. Both these functions require radio awareness, statistical information about the interfering signal and the capability of signal identification [4].

A detailed study of the spectrum sensing techniques is given in the second chapter of this thesis [5-14]. Existing spectrum sensing methods focus mainly on improving the detection accuracy, but do not provide accurate information about the exact location of spectrum holes (channel center and edge frequencies). Therefore, the existing methods are mostly applicable to commercial wireless communication receivers where the channel locations are known to the user. On the other hand, in an ideal CR scenario, where the frequency allocations may not be rigid, accurate location of spectrum holes is a key task. Robust detection of a wideband signal with low complexity in low signal-to-noise ratio (SNR) scenario is a challenging task due to the large bandwidth of the signal and high input sampling rate. Moreover, the CR must be able to perform sensing and classification

in a blind fashion i.e., with limited or no prior knowledge of the signal of interest, statistics of the noise added in the communication channel and the fading experienced by the signal. Therefore, this thesis develops new blind techniques for sensing and classification in additive Gaussian and non-Gaussian noise processes.

1.2. Objectives

The main objective of this thesis is to develop reliable algorithms for detection and classification of signals in a cognitive radio scenario and to enable dynamic spectrum access. The objective is to develop algorithms and architectures that can perform spectrum sensing with minimal knowledge about the received signals. The algorithms should also be less complex than the conventional methods and robust in detection. The proposed work in the physical layer (PHY) of CR's focuses on accurate signal detection where a secondary user is trying to detect whether the primary user is active or not in a given frequency band. In cases of military applications, the CR needs to be radio aware, and hence modulation classification algorithms are the need of the hour.

The objectives of the work presented in this thesis are:

1. To propose new filter banks based spectrum sensing algorithm in cognitive radios (CR) that are reliable, fast and with high detection accuracy. Spectrum sensing is a challenging task due to the large bandwidth of the signal and high input sampling rate. Moreover, in order to locate accurate spectral vacancies, these sensing methods need to have a high spectral dynamic range of operation. While fast Fourier transform (FFT) is used as a channel sensing method, large side lobes of the frequency response cause interference to the adjacent channel. This poses a limitation on the accuracy and dynamic range of the method used for sensing. By using a filter bank based sensing algorithm, the side lobes can be made arbitrarily small by designing appropriate filters. Conventional filter bank based spectrum sensing consists of a uniform filter bank to split the wideband signal into multiple subbands followed by energy detection, which consists of a power estimator that compares the estimated power with a threshold to decide if the band has any signal. However, the low resolution of the filter banks proved to be erroneous for

the detection purpose which is discussed in Chapter 4 of this thesis. Therefore, in order to determine vacant bands accurately, there is a need for high resolution multiple band sensing using filter banks. This method acts as a foundation for various other methods proposed in this thesis.

2. To propose an algorithm with low complexity for detection and classification of the signal spectrum. In many applications, after sensing is performed, a CR must be able to identify the waveform with little knowledge about the signal or noise. The idea is to design an algorithm that works under adverse conditions such as fading and highly noisy environment. In other words, the method must be able to detect the presence of primary users in the spectrum and determine the modulation type of the received signal. This finds application in adaptive modulation coding systems, where the signal has to be demodulated further using the modulation scheme determined.

3. To implement a sensing methodology for a policy enabled CR that can be used on a policy basis in a software defined radio and validate its functionality and estimate the area, power and delay metrics. This would provide a good insight on the enabling CR technology in terms of implementation and feasibility.

1.3. Contributions

The main contribution of the work is focused on improved sensing and classification methods for cognitive radios and military radios. An energy detector based on tree-structured discrete Fourier transform filter bank (TDFTFB) is proposed for detecting the frequency edges of channels for accurate hole detection. Simulation results are presented to show that the proposed architecture performs better than the conventional DFTFB based spectrum sensor. The advantage of the proposed method is that, it works with limited knowledge about the signal and noise. The noise is assumed Gaussian in nature, to serve as a simple starting point for the detection problem addressed in this thesis. Ideal CRs emphasize that the PU signals be sensed accurately in order to locate the spectrum vacancies. In certain applications such as military and public radios, the PU

signals need to be identified and classified, in addition to sensing. Therefore, the second contribution is an integrated scheme for blind spectrum sensing and modulation classification in cognitive radios. Detection is performed using the proposed method based on cumulants and fractional lower order statistics. The detection performance is compared with the conventional higher-order statistics (HOS) based method for various noise conditions. It is shown through simulations that the proposed method performs well in both Gaussian and non-Gaussian conditions as compared to the conventional method. Over-the-air tests were conducted to obtain real time data from the wideband spectrum to analyze the noise characteristics in the communication channel. A new pattern recognition based automatic modulation classification algorithm based on fractional lower order statistics (FLOS) and cumulants, is proposed. The advantage of the proposed method is that, the same test statistic is used for both detection and classification. The main challenge in designing a classifier is the lack of prior knowledge about the signal and noise in the channel. In the proposed method, detection and classification were performed without any prior information about the signal, noise added in the channel and the fading experienced in the channel. The main advantage of the proposed scheme is that, it is applicable for a wide class of noises while most of the algorithms in the literature assume the noise in the channel to be additive Gaussian in nature. After performing sensing and classification, the CRs are expected to operate in the vacant band using certain policies that are usually decided by the network provider. These policies, which are determined based on the spectral usage information known to the base station of the network provider, are relayed to the CR through a separate channel.

As an alternative to the conventional network provider aided policy-based radio, the third contribution is a policy-based CR that loads configuration policies based on the sensing of a specific channel known as sensing policy channel. The sensing policy channel consists of signals at various pre-defined frequencies that are sensed in order to determine which waveform has to be loaded onto the SDR. Using the proposed model, many standards can operate in a reconfigurable fashion. By providing a dedicated channel for sensing, a policy strategy for CR based on sensing was elucidated. It allows policies to be dynamically changed and controlled. The proposed concept is implemented using an off-the-shelf Java Imperius policy engine and the SCA architecture.

The fourth contribution is focused on improving the detection accuracy of the CR using a two-stage detection method using filter banks and higher order statistics. The overhead in using a separate filter bank for sensing is reduced by using the same filter bank used for channelization. The two-stage spectrum sensing method involves subband splitting in the first stage and calculation of HOS based single valued fourth order cumulants at each subband in the second stage. These cumulant values are normalized using weights determined by the power estimated in the corresponding subband. Applying binary hypothesis testing, it is shown through simulations that the normalization method helps in improving the detection accuracy.

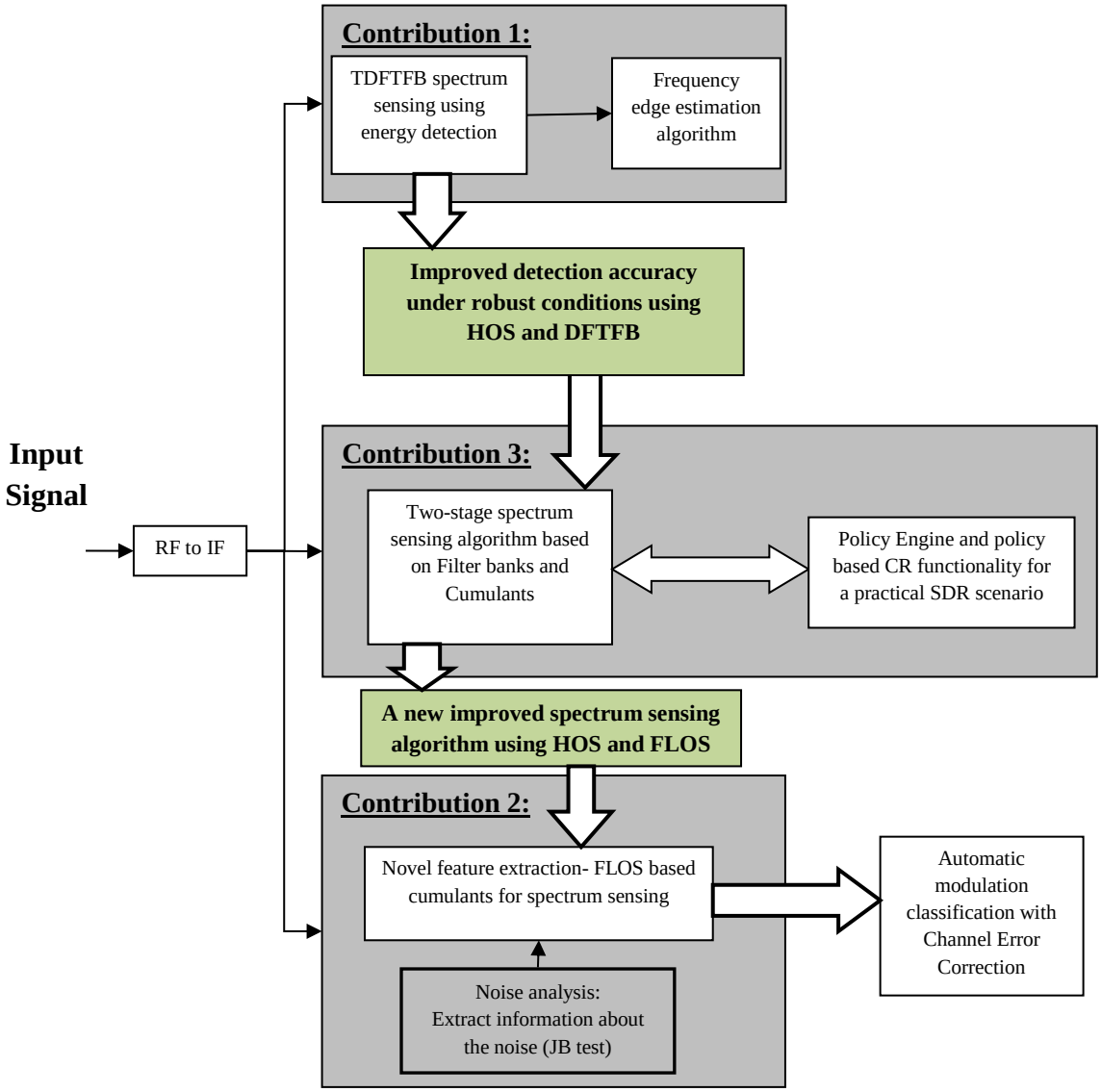

Figure 1.1. Contributions of this thesis.

1.4. Outline

This thesis is organized as follows: Chapter 2 presents the background knowledge and literature review pertaining to various spectrum sensing techniques available and highlights its challenges. Chapter 3 presents the data and noise model used in the thesis. It also provides detailed information on the experimental setup used in regard with the work presented in this thesis. In Chapter 4, the proposed TDFTFB based energy detector along with a reliable frequency edge estimation algorithm is proposed. Chapter 5 presents the proposed integrated scheme for detection and classification using fractional lower order statistics and higher-order statistics based cumulants. Chapter 6 presents the a policy based CR implemented on a JAVA platform that takes input for spectrum sensing. Additionally, a two-stage spectrum sensing method based on filter banks and cumulants is presented. Chapter 7 has the conclusions of the work presented in this thesis and possible future directions.

Chapter 2

Literature Survey

In Chapter 1, a brief discussion on the contents of the work in this thesis and its contributions towards the vast field of signal detection and classification in wireless communication systems was presented. This chapter presents existing methods, results, discussions and conclusions that provide the foundation for the contributions in this thesis. In the section 2.1, the basic concept of a CR receiver in DSA is presented. The emphasis of this chapter is to provide a good understanding of the conventional detection and classification algorithms along with their merits and demerits.

2.1. Overview of Cognitive Radio and Dynamic Spectrum Access

The current spectrum management and regulation is based on a static frequency allocation policy. This means that the radio frequency bands in the spectrum are allocated to different wireless standards in a rigid manner. Most of the existing electromagnetic spectrum has been allocated to many emerging wireless communication systems. However, there is rapid increase in the number of wireless systems and devices due to the high demand for ubiquitous, high data-rate communication systems. Since each wireless communication system operates in a specific frequency band allocated to them, the allocation is very inflexible. This has resulted in an apparent scarcity of spectral resources that effects heavy data traffic in certain frequency bands, in order to accommodate new wireless communication systems. However, these systems utilize the allocated spectrum

inefficiently, as many of the frequency bands are sparingly used. It has been shown through studies that the degree of utilization of a frequency band varies with respect to time and location. Consequently, depending on time, frequency band, and location, the radio frequency spectrum is utilized in a wasteful manner. With the exponential rise of new wireless communication services, there is an increasing need for more efficient ways of utilizing the spectral resource. Dynamic spectrum access provides a flexible way of utilizing the available resources more efficiently. Dynamic spectrum access is widely categorized into three models [5]: spectrum commons model, dynamic exclusive use model, and hierarchical access model. Similar categorization with slightly different terminology and more subcategories for the three main models has been given in [6].

In the dynamic exclusive use model, frequency bands are licensed to different legacy systems in a static fashion. However, in this case, spatial and temporal traffic analyses are utilized while the spectrum is allocated. Inflexibility is removed by allowing the licensed users to trade spectrum in a lease fashion. Different dynamic access models are elucidated in [5]. In the spectrum commons model, different users compete for the available electromagnetic resources in a fair manner and share the spectrum. This model is successful in the unlicensed industrial, scientific, and medical (ISM) bands. The spectrum commons model accommodates both the fully open model and the managed commons model. In the former, the spectrum is not owned by licensees, and the access is available to all users, whereas in the latter, the spectrum is licensed to a group of entities who own and control that spectral region [6]. In managed commons [7], there are stringent rules on spectral usage than the open sharing model.

The hierarchical access model adopts the structure, where primary systems are licensed to access specific frequency bands. The secondary users are allowed to use the licensed spectrum without causing interference to the primary systems. The interference level is determined by the regulating bodies. Hierarchical access model is broadly classified into two approaches- spectrum underlay and spectrum overlay [5]. Spectrum underlay approach does not require spectrum sensing to be performed, as the interference level is determined by imposing stringent constraints on the transmit powers of the secondary users. This is applicable to short range, low power ultra-wideband (UWB) devices. As opposed to spectrum underlay, spectrum overlay is based on spectrum

sensing aided secondary users. The interference to the primary users is kept below the threshold level by spectrum sensing and dynamic utilization of the band. This UWB approach for spectrum overlay has been approved by the FCC [8] in 2002 in the US, and is one of the first steps to improve spectrum utilization through sharing. However, the existence of white space or spectrum holes was not properly addressed by the UWB approach. After realizing UWB limitations and showing that some interference below the threshold level is acceptable, the FCC issued a Notice of Proposed Rule Making in [9]. This advanced CR technology was proposed as a candidate to implement opportunistic spectrum sharing as a solution to spectrum crowding problem.

The intention was to allow higher transmission power if the radio can reliably identify spectrum holes and prevent the interference to the licensed primary users. More importantly, flexibility in usage of available spectrum holes through opportunistic sharing would allow deployment of heterogeneous services based on location and application demands. This opportunity is particularly attractive for socially important services like public safety and emergency relief. Such services require a very large throughput and large number of wireless users during relatively short period of time. It also needs to work with low latency and high priority. These demands in the society could not be accommodated using fixed frequency allocation mainly because the cost and efficiency of spectrum resource usage would not be justified. Cognitive radio technology seems to be a perfect solution to address these emergency scenarios as it has the ability to utilize large bandwidths for communication, temporarily with high priority access, at virtually no cost per spectrum resource usage.

The work on spectrum sensing in this thesis focuses on the spectrum overlay approach, more so on spectrum sensing in the physical layer. The main challenges faced by the cognitive radios in spectrum sensing and obtaining awareness about spectral usage are briefly discussed. Due to the limitations in hardware and power constraints, the whole wideband spectrum cannot be simultaneously sensed by the CR. Hence, a sensing policy needs to be defined. This policy determines when and which frequency band to sense at a given time. Sensing policy may be implemented either individually or collaboratively. This is addressed in Chapter 6 of this thesis.

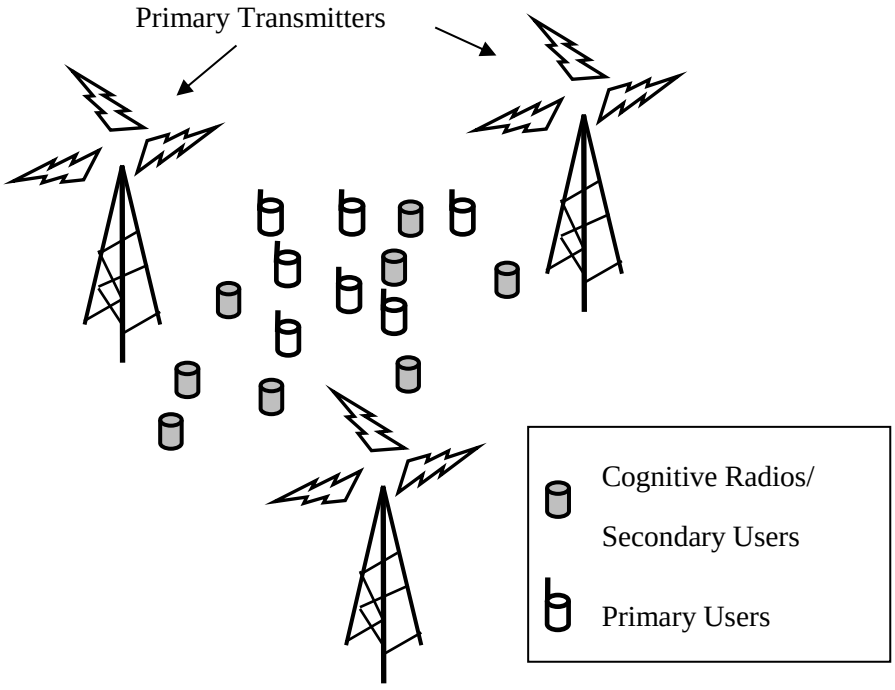

Figure 2.1. A typical cognitive radio scenario.

Figure 2.1 presents a typical cognitive radio scenario. It comprises of PU transmitters and PU receivers, while the CRs use the PU frequency band in an opportunistic manner. The operation of a CR for DSA consists of two main components: spectrum sensing and spectrum access.

The CRs sense the spectrum for vacant bands or holes and exploit them in a dynamic manner. However, in the case of collaborative sensing, the sensing periods are assumed to be synchronized with all the cognitive radios. This is inevitable because a CR cannot perform sensing and transmission simultaneously on the same frequency band. The sensing policy defines the sensing period, the channels to be sensed and whether a cognitive radio is idle or performs sensing in a given period. Due to the spatial diversity involved in sensing, collaborative sensing in the physical layer offers benefits over individually selected policies as the cognitive radios can share this information for accurate spectrum sensing.

After sensing and identifying the spectral opportunities, the cognitive radios need to exploit these available opportunities. For this purpose, depending on the channel

information, there are access policies that determine which channels have to be used for transmission. Similar to sensing policy, access policy can be decided individually or in a collaborative fashion. Interference management is also an integral part of spectrum exploitation. The CR system must ensure that the interference caused to the primary systems do not exceed the threshold set by the regulatory bodies. In addition to the issues mentioned above, the CRs also need to identify the employed modulation scheme, transmitting power, regulatory challenges etc. depending on the application.

In the following section, an overview of sensing algorithms for cognitive radios is presented. Firstly, a short discussion of the main requirements, challenges and techniques of physical layer spectrum sensing is provided.

2.2. Spectrum Sensing Requirements, Challenges, and Techniques

Cognitive radios are secondary users that do not have legacy rights to any frequency band. CRs communication is dependent on its ability to accurately locate primary user transmissions in their vicinity. Many approaches such as databases or beacons can be used to check the presence of primary user signals, but the only autonomous and flexible approach is based on measurements of the actual occupancy at a given location and time. Even in database and beacon approaches, spectrum sensing could add robustness and responsiveness to changes in the environment because it provides a real-time feedback. Therefore, spectrum sensing should be considered as an essential part of any cognitive radio systems.

Given that every cognitive radio has some sensing capability, the question that needs to be answered is the architecture design and implementation of this radio component. Different spectrum utilization regimes might require different spectrum sensing architecture designs. The most flexible architecture scalable to regimes with higher spectrum utilization should allow a cognitive radio to simultaneously sense the spectral environment over a wide frequency band [10]. Within a wide band of interest there could be different types of primary user systems with various ranges of operation

and traffic patterns. Based on these characteristics and actual sensing measurements, cognitive radios can apply suitable spectrum sharing strategies. For example, packet based primary systems bands might be suitable for time sharing, while broadcast system offers frequency reuse spectrum sharing at non-overlapping geographic locations. On the other hand, more sophisticated approaches could use spatial dimension in addition to time and/or location.

Even though there are a large variety of primary user systems, cognitive radio's knowledge of their characteristics and requirements for interference protection can be abstracted by a few generally applicable parameters. The three critical requirements for sensing in cognitive radio are the sensing time, the probability of detection and the minimum detectable signal level. The required detection time and probability of detection are set by primary user tolerances to quality of Service (QoS) degradation. While these are two conflicting requirements, a cognitive radio system's goal is to minimize the detection time in order to increase the time available to use the channel. Primary users can claim their frequency bands (channels) anytime while cognitive radio is operating at that band. In order to prevent interference to and from primary users, cognitive radio should be able to identify the presence of primary users as quickly as possible and should vacate the band immediately. Hence, the sensing method should be able to identify the presence of primary user within a certain duration. These requirements possess a limit on the performance of sensing algorithm and create a challenge for cognitive radio design. The minimum detectable signal level is determined by the sensitivity provided by the legacy users. For example, TV broadcast signals are much easier to detect than GPS signals, since the TV receivers' sensitivity is lower than that of GPS receivers [11]. Furthermore, a higher sensitivity in spectrum sensing could possibly allow cognitive radios to transmit at higher power.

Discussions regarding the requirements and implementation issues of spectrum sensing are found in [8, 12, 13]. In the following subsection, some of the most important concepts regarding spectrum sensing and opportunistic spectrum use are briefly discussed. Interference temperature concept has been introduced by the FCC as a model for measuring and limiting interference in wireless communications [3, 8, 14, 15].

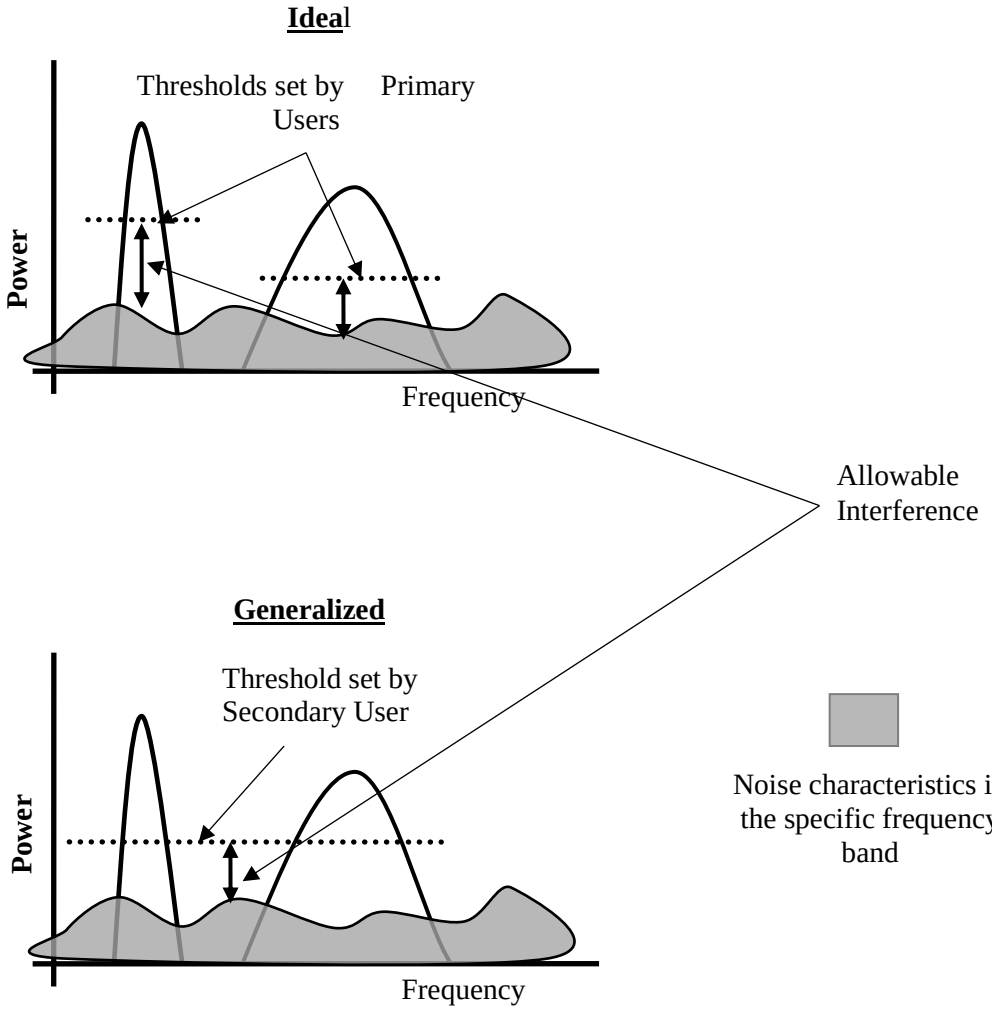

Figure 2.2. Ideal and generalized interpretations of interference temperature model [3].

Figure 2.2 illustrates two possible realizations of the interference temperature concept. The idea is that each primary receiver has an interference temperature limit that defines how much noise and interference it can tolerate. This opens up opportunities for secondary users that are consequently allowed to transmit, provided that the interference their transmissions cause to the primary receivers do not increase the interference temperature above the limit. However, the problem arises from measuring the interference temperature at the primary receivers that may be infeasible in practice [8]. The FCC has quite recently abandoned the interference temperature concept as unworkable. The generalized model applies to a situation where there is no prior

knowledge of the primary user signals. A more practical opportunistic access concept relies on secondary users identifying frequency bands unused by the primary users and transmitting at those frequency bands until a primary user becomes active. Such a frequency band or channel is called a spectrum opportunity [5, 16, 17].

Spectrum opportunity is a concept that is defined as follows [17]: *A channel is an opportunity to a secondary transmitter A and secondary receiver B if they can communicate successfully over this channel while limiting the interference to primary users below a prescribed level determined by the regulatory policy.*

The inherent requirement is that the secondary users must vacate the spectrum as quickly as possible when the primary user appears. Moreover, in order to guarantee low-interference operation of the primary users, the detection probability of the CR users has to be very high. Note that some interference must be tolerated otherwise opportunistic access based on spectrum sensing is not possible. There are many ways to improve the detection probability or sensitivity of a cognitive radio network (CRN). The sensitivity of the cognitive radios can be improved by enhancing the cognitive radio's RF front-end sensitivity, designing and employing powerful signal processing algorithms suited for the task, as well as by exploiting spatial diversity through collaborative sensing among multiple cognitive radios [12].

Another important consideration for the cognitive radios is the sensing policy. The sensing policy includes decisions such as when and how long to sense, and which frequency band to sense. In order to maximize performance, the sensing policies should be coordinated among the secondary users. As discussed earlier, simultaneous transmission and sensing on a given frequency is not possible in general. Hence, sensing and transmission have to be performed in an alternating fashion. Moreover, the sensing periods must be synchronized among the cognitive radios. Ideally, a cognitive radio user wants to minimize the time required for identifying spectral opportunities in order to maximize the time available for transmission. Different primary systems impose different constraints for sensing.

In addition to sensing, cognitive radios may benefit from using geolocation information for avoiding primary systems and managing interference [18]. Geolocation

database consisting of primary transmitter geolocations and employed channels would enable the cognitive radio that is aware of its own geolocation to avoid using those bands whenever the primary user could potentially be interfered by the secondary user's transmissions. Apart from the above discussed challenges and requirements, some other challenges need to be considered while designing effective spectrum sensing algorithms. These include implementation complexity of the proposed algorithm, presence of multiple secondary users, coherence times, multipath and shadowing, cooperation, competition, robustness, heterogeneous propagation losses, and power consumption. In the following subsections, an overview of spectrum sensing algorithms proposed in the literature is presented.

2.3. Spectrum Sensing Algorithms

The spectrum sensing algorithms proposed in the literature may be broadly divided to three classes: matched filters, energy based detectors, and feature detectors as shown in Figure 2.3. The detection problem can be formulated as a binary hypothesis test;

$$H_0 : r(t) = \eta(t) \tag{2.1}$$

$$H_1 : r(t) = s(t) + \eta(t) \tag{2.2}$$

where $r(t)$ and $\eta(t)$ denote the received signal and the noise respectively, and $s(t)$ denotes the signal to be detected. In traditional binary hypothesis testing, a null hypothesis, H_0 is tested against an alternative hypothesis, H_1 by performing experiments to reject the null hypothesis in favor of the alternative. Hypothesis testing is therefore a binary classification of the hypothesis under study. In a binary hypothesis test, there are two types of errors; type I and type II errors. A type I error is made if H_1 is accepted when H_0 is true. The probability of making a type I error is often called the probability of false alarm (P_{fa}). The P_{fa} of a detector is an important design parameter since false alarms lead to overlooking of spectral opportunities. A type II error is committed if H_0 is accepted when H_1 is true. Type II errors are a result of a missed detection and hence lead

to collisions with primary transmissions and reduced rate for both the primary system and the secondary system.

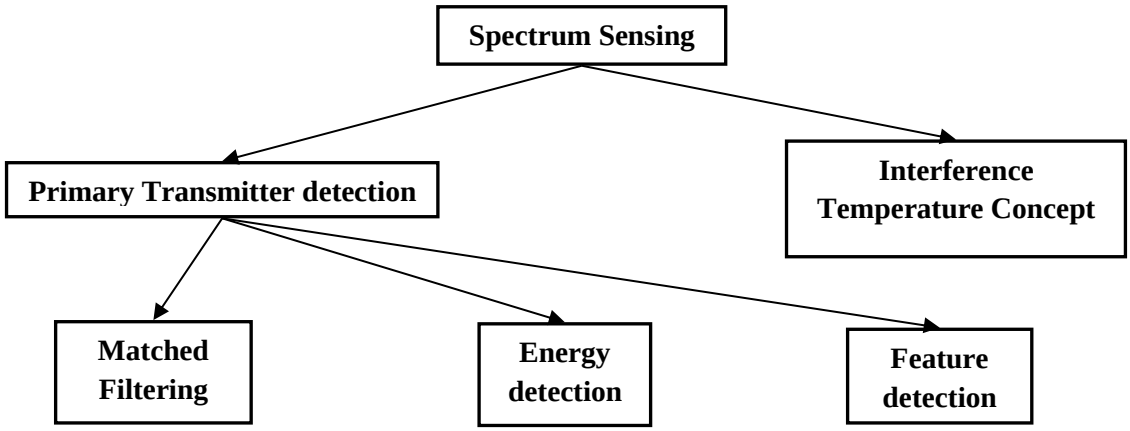

Figure 2.3. Basic techniques for spectrum sensing.

In general, a cognitive radio system should satisfy constraints on both the probability of false alarm and the probability of miss detection (P_{md}). The detection ability of the method is determined by the probability of detection (P_d), which occurs when H_1 is accepted when H_1 is actually true. Designing a detection rule presents a trade-off between these two probabilities, P_d and P_{fa} . However, if the detector behaves reasonably, i.e. the probability of error (the probability of false alarm and the probability of miss detection) decreases as the number of samples increases, both constraints can be satisfied by selecting a large number of samples. However, the drawback is that, the computation time and power increases with increase in the number of samples. From the implementation point of view, it is desirable to have algorithms whose threshold can be set analytically. This is because; the number of samples, which affects the working rate of the implemented system, also influences the probability of detection for a given threshold. Moreover, in practice the number of samples required to achieve a given probability of detection will have to be determined experimentally due to the large number of variables, such as the fading channel, synchronization errors, noise power uncertainty, etc.

2.3.1. Matched Filtering

Matched filter is the optimum detector of a known signal in the presence of additive white Gaussian noise (AWGN). The linear filter maximizes the signal-to-noise ratio (SNR) of the output.

The output of the matched filter is given by

$$y = s^H \sum_n^{-1} x \tag{2.3}$$

where x is the observation vector, s is the known deterministic signal to be detected, H is the Hermitian operation, and Σ_n^{-1} is the noise covariance matrix [19]. Assuming that the noise is AWGN, it follows that the output y is Gaussian as well since it is a linear transformation of a Gaussian random vector. The mean of y is zero under H_0 and $s^H\Sigma_n^{-1}s$ under H_1. The variance is $s^H\Sigma_n^{-1}s$ under both hypotheses. H_1 is true if $y \geq \lambda$, and H_0 is true if $y < \lambda$ where λ is the test threshold selected to obtain a specific false alarm rate.

From equation (2.3), it can be seen that the matched filter requires explicit knowledge of the transmitted signal and the noise covariance matrix. Hence, the usability of the matched filter is limited to cases where explicit information about the waveform such as pilot signals or preambles are known. When a secondary user has a priori knowledge of the primary user signal at both physical and medium access control (MAC) layers, such as the pulse shape, modulation type, and the packet format, the optimal signal detection method is a matched filter, since it maximizes the output signal-to-noise ratio [12]. The output of a matched filter has to be compared to a threshold to decide whether the PU signal is present. The main advantage is that the matched filter needs shorter time to achieve high processing gain due to coherent detection as compared to non-coherent detection methods [20]. For demodulation, cognitive radio has to perform timing and carrier synchronization and channel equalization [12]. When the SU has no accurate information on the PU signal, the matched filter performs poorly. However, most licensed systems include pilots, preambles, synchronization words or spreading codes to aid the coherent detection. A significant drawback in the use of matched filter is that it would require a dedicated sensing receiver for every PU signal type. Digital television (DTV) band is an example where matched filter detection can be performed [21]. Experimental

measurements of matched filter pilot detection performance with synchronization errors (frequency offset) have been provided in [22, 23]. In [24], an entropy-based matched filter method is proposed. The proposed detector compares the estimated entropy of the matched filter output with a threshold. The method can be applied when the variance of the assumed Gaussian noise is unknown.

2.3.1.1. Coherent Detectors

Coherent detectors for ATSC DTV (Advanced Television Systems Committee, digital television standard in North America) signals employing the field sync segment have been proposed in [25, 26]. The field sync segment includes a known 511 symbol pseudo-random number (PN) sequence that can be employed for detection. Detection times required for the field sync detectors are typically relatively long since the field sync is inserted to the data stream once every 24.2 ms. Asymptotic distribution of the field sync correlation detector under the null hypothesis has been established in [27]. The probability of detection at SNR of -13 dB exceeds 99 % for a false alarm rate of 10 % in good channel conditions [27].

2.3.2. Energy Detection

The most generic approach for detecting signals in the presence of noise is based on energy measurement. It is the most general technique since it applies to any signal type. It requires minimum prior information about the signal, i.e. only the signal bandwidth and carrier frequency. In communications and signal processing literature, energy detection is also studied as a hypothesis-testing problem as explained in Section 2.3. Energy detector (or radiometer) measures the received energy and compares it to a threshold. The test statistic for energy detector is given as [28, 29];

$$y_N = \frac{1}{N}\sum_{n=1}^{N}|r(n)|^2 \tag{2.4}$$

where $r(n)$ is the received complex valued discrete time signal, N is the number of observation samples. Figure 2.4 depicts the block diagram of the basic energy detector. First, the input signal is filtered with a bandpass filter (BPF) to select the bandwidth of interest. The filtered signal is squared and integrated over the observation interval.

Finally, the output of the integrator is compared to a threshold to decide whether the primary user is present.

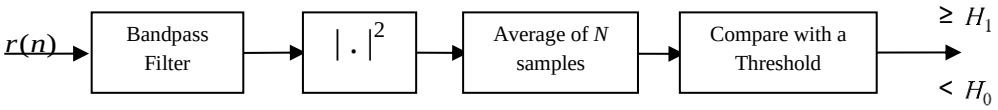

Figure 2.4. A basic energy detector.

When the spectral environment is analyzed in the digital domain, FFT based methods are usually used in order to obtain frequency response. FFT also generates the resolution in frequency domain. The periodogram method is used to estimate power spectrum and it is based on the FFT [30]. The periodogram is a poor spectrum sensing method because of the large variance and bias of the estimate.

Modified periodogram techniques have been developed to cope with such drawbacks [30, 31]. A practical energy detection method for cognitive radio is Welch's periodogram [32] which is depicted in Figure 2.5. The Welch's periodogram gives a better estimate to the energy in the spectrum as the method takes segments of input data and applies an *N*-point FFT on them.

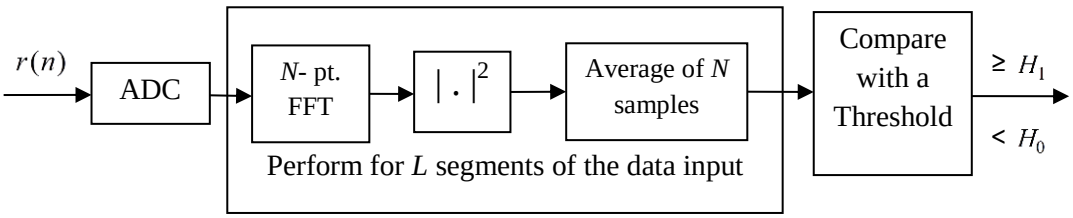

Figure 2.5. A basic Welch's periodogram [32].

A computationally feasible Thomson's multitaper method (MTM) [33] was proposed as a good candidate for spectrum sensing task. This method exploits multiple orthonormal windows for spectral estimation [14, 33]. The key advantage of energy detector is its low implementation complexity. However, its performance is highly susceptible to noise level uncertainty. Noise level uncertainty refers to a situation where the noise variance is only approximately known. Considerable noise uncertainty may result from thermal noise and nonlinearities of components, and from inaccuracy of the noise estimator (due to limited time of averaging). The noise uncertainty causes problems

especially in the case of a simple energy detector because it is difficult to set the threshold properly without the knowledge of the accurate noise level. A pilot tone from the primary transmitter can be used to alleviate this problem [25].

Noise level uncertainty renders robust detection below certain SNR impossible [34, 35]. To constrain the resulting false alarm rate, the detection threshold has to be set based on the worst-case noise level uncertainty. Consequently, if the signal power is below a certain level, the energy detector cannot distinguish the signal from a slightly larger noise power regardless of the detection time. This threshold is called the *SNR wall.* For example, for a real-valued signal, a 1 dB noise uncertainty renders robust detection below SNR of -3.3 dB impossible [35]. Consequently, the energy detector performance depends heavily on the accuracy and reliability of the noise level estimate. The noise level may be estimated from guard bands or the detection may be performed in the frequency domain using a channelized radiometer [36, 37] which divides the total frequency band to smaller channels and then integrates energy from each channel separately using a radiometer. In the end, a final global decision can be made for the whole frequency band by combining the radiometer outputs or decisions from the different channels (e.g., maximum or sum over outputs; sum or OR of decisions). If the noise bandwidth is significantly larger than the signal bandwidth, a reasonably accurate noise level estimate needs to be obtained. In addition, collaboration among secondary users that employ energy detection mitigates the effects of noise uncertainty when the users are experiencing fading or shadowing [38-40].

In addition, an energy detector cannot differentiate between modulated signals, noise and interference. Thus, it cannot benefit from adaptive signal processing for cancelling the interferer and it is prone to false detection triggered by unintended signals. The performance of an energy detector is clearly degraded in fading environments and secondary users may need to cooperate in order to detect the presence of primary users [18, 41]. One of the important challenges is setting the right threshold for detection. The problem is illustrated in Figure 2.6 where the probability density functions of the received signal with and without primary signal are shown.

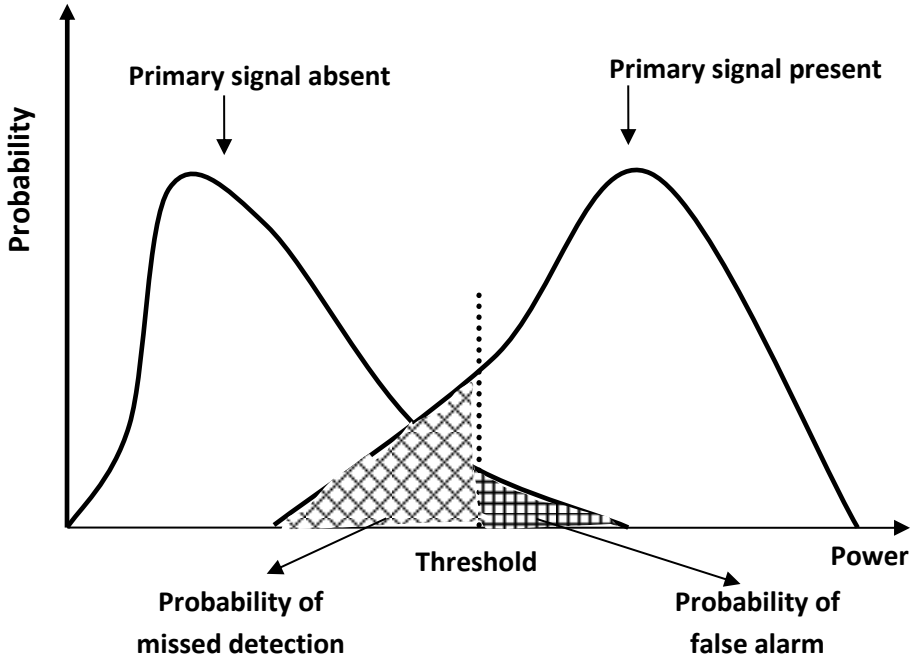

Figure 2.6. Trade-off between missed detections and false alarms [5].

When the probability of missed detections is very low, the probability of false alarms increases, resulting in low spectrum utilization. On the other hand, a low probability of false alarms would result in high missed detection probability, which increases the probability of interfering with the primary users. This trade-off has to be carefully considered while determining the threshold for energy detection. In most radar detectors, the threshold is set in order to achieve a constant level of a false alarm [42]. The threshold level is changed dynamically during detection to maintain a constant probability of a false alarm. This approach is known as constant false alarm rate (CFAR) detection.

As the threshold determination is crucial in the detection based on energy, the theoretical analysis is done first. The detection is the test of the following two hypotheses: under H_0, primary user signal is not present and there is only noise at input of the receiver, and under H_1, primary user signal and noise are present at the input of the receiver. Given that the center frequency *fc* and bandwidth *B* of the primary user signal are known, input signal is down converted and sampled at the Nyquist rate, $f_s = 2B$.

The discrete time model of this hypothesis test is:

$$H_0 : r[n] = \eta[n] \tag{2.5}$$

$$H_1 : r[n] = s[n] + \eta[n] \tag{2.6}$$

where *N* samples of the received signal are considered for each observation equivalent to the sensing time. Both signal $s[n]$ and noise $\eta[n]$ samples are modeled as independent Gaussian random variables with zero mean and variance, σ_s^2 and σ_w^2, respectively. The performance of the detection algorithm can be illustrated using P_d and P_{fa}. P_d describes the probability of detecting a signal on the considered frequency when it is truly present, while P_{fa} decides that the considered frequency is occupied when it actually is not. In order to compute these probabilities, the probability density function (PDF) of the decision statistic under both hypotheses needs to be determined. The test statistic is a sum of Gaussian random variables hence its PDF is chi-square. The detection is performed by a threshold test on the measured power values. There are a number of ways that a threshold can be set. In the spectrum sensing scenario, threshold is set to meet a fixed P_{fa}, as it depends only on the noise variance, making it regardless of the primary user signal level. These probabilities are obtained for energy detection in [29, 30]

$$P_d = P_r\left(\varepsilon(y) > \langle \gamma \,|\, H_1 \rangle\right) = Q_{X_N^2}\left(\frac{\gamma}{\delta_w^2 + \delta_s^2}\right) \tag{2.7}$$

$$P_{fa} = P_r\left(\varepsilon(y) > \langle \gamma \,|\, H_0 \rangle\right) = Q_{X_N^2}\left(\frac{\gamma}{\delta_w^2}\right) \tag{2.8}$$

If the number of samples used in sensing is not limited, an energy detector can meet any desired P_d and P_{fa} simultaneously. The minimum required number of samples in order to achieve a desired P_d, for a given P_{fa}, is a function of the SNR.

$$SNR = \frac{\delta_s^2}{\delta_w^2} \tag{2.9}$$

$$N = 2\left[\left(Q^{-1}\left(P_{fa}\right) - Q^{-1}\left(P_d\right)\right)SNR^{-1} - Q^{-1}\left(P_d\right)\right]^2 \quad (2.10)$$

In the low SNR regime, the number of samples required for the detection that meets specified P_d and P_{fa}, asymptotically scales as 1/SNR^2. This scaling law is characteristic for non-coherent detection, i.e. detectors whose sensing time scale is 1/SNR^2 will be termed as non-coherent.

A review of energy based detection literature has been provided in [43]. In [43, 44], through numerical examples, it has been shown that the cell-averaging strategy offers the desired false alarm probability, whereas a more conventional strategy gives too high values, especially with a small number of reference samples. The performance of a channelized radiometer, when different CFAR strategies are used to set the detection threshold [44], have been considered. Experimental measurements of energy detection performance with noise uncertainty have been provided in [22, 23]. Energy detection of WiMAX systems for ultra-wideband/WiMAX coexistence has been considered in [45]. UWB devices are used to detect and avoid WiMAX devices in certain regulatory domains. In [45], various obstacles faced in achieving robust detection and avoidance with an on-chip implementation of basic detect and avoid functionality was proposed. It highlights the problem of dealing with listen before speak systems where secondary users are allowed to interfere by blocking the primary user's access to the medium. The detection of wireless microphone signals using the maximum of the frequency domain energy measurements has been proposed in [46]. Energy detectors have been proposed for colored Gaussian [47] and independent non-Gaussian noises [48, 49]. A discrete Fourier transform filter bank (DFTFB) based sensing method for wideband spectrum sensing was proposed in [50]. It has been shown in [50] that DFTFB based energy detector is more promising in terms of accuracy over the low-level power spectral density (PSD) portions of the band than other techniques such as MTM, if the noise variance is known. More details about the filter bank based spectrum sending are dealt with in the Chapter 4 of this thesis, as the focus of the work is filter banks based spectrum sensing of a wideband input signal.

2.3.2.1. Multi-Antenna Multi-Resolution Energy Detector

In [51], a multi-resolution multiple antenna energy detector for spectrum sensing has been proposed. The proposed multi-resolution detector first performs the sensing at a coarse frequency resolution. The fine resolution sensing that follows the coarse sensing is performed only for a small range of frequencies that have the smallest power in the coarse sensing stage. Using multiple antennas allows for faster sensing, since in the coarse sensing stage each antenna block senses only a part of the spectrum. In the fine sensing stage, all the antenna blocks sense the same frequency band, thus achieving spatial diversity gain. In [52], multi-antenna energy detection schemes based on maximum ratio and selection combining have been considered. Maximum ratio combining is an optimal combiner for independent AWGN added channels. In this combining method, the signals from each channel are added together, by using weighted constants for each channel that maximizes the SNR. However, in selective combining, only selected channels are combined to obtain the received signal. Maximum ratio combining is difficult to implement in practice since it requires explicit channel information. In conclusion, using multiple antennas offers benefits through diversity but on the other hand, it also requires an expensive structure because of multiple antennas.

2.3.2.2. Frequency Domain Spectrum Estimation

Frequency domain energy detector estimates the power spectral density (PSD) using the periodogram or the Bartlett's method if block averaging in time is employed. Bartlett's method (also known as the method of averaged periodograms), is used for estimating power spectra. It provides a way to reduce the variance of the periodogram in exchange for a reduction of resolution, compared to standard periodograms. A final estimate of the spectrum at a given frequency is obtained by averaging the estimates from the periodograms (at the same frequency) derived from non-overlapping portions of the original series. Although Bartlett's method is the most popular, any other spectrum estimation method can be applied for this purpose. Introduction to spectral analysis and various spectrum estimation methods are found in [30, 53, 54]. Note, however, that the analysis and distributions derived for the energy detector apply in general only for the

periodogram or the Bartlett's method. In practice, one may need to resort to less rigorous ad-hoc techniques for setting the thresholds and detecting the spectrum holes.

Spectrum estimation methods may be divided into parametric and non-parametric methods. Parametric methods are a branch of statistics that assumes that the received data follows a type of probability distribution that is known a priori and makes inferences about the parameters of the distribution. On the other hand, the non-parametric methods are statistical methods in which the model structure is not specified a priori but is instead determined from the received data. Non-parametric methods are better suited for detecting an unknown signal than parametric methods. Hence, the focus for spectrum sensing has been on nonparametric methods. In [55], single-user and collaborative energy detection using Welch's periodogram has been considered. The theoretical analysis of the energy detection to the Welch's periodogram was analyzed along with cooperative spectrum sensing. Simulations were carried out to show that Welch's periodogram signal detection method operates well for narrowband signals. The main limitations of the periodogram method yield from the variance. The periodogram is an inconsistent spectral estimator which means that it continues to fluctuate around the true PSD with a non-zero variance. This effect cannot be eliminated even if the length of the processed sample increases without a bound. From the results on cooperative sensing presented in [55] it can be concluded that the highest increase in probability of detection is observed when two cooperating radios were considered.

Welch's periodogram is an extension of the Bartlett's method that employs window functions and possibly overlapping segments. In [56], a multi-resolution frequency subband detection algorithm based on frequency-smoothed periodograms has been proposed.

2.3.2.3. Wavelet-based Spectrum Sensing

Wavelets are a good tool for modeling and detecting singularities in the spectrum such as band edges. A wavelets based approach for spectrum hole detection has been proposed in [57]. In [58], the wavelet approach has been further developed: The PSD is first estimated for a wide bandwidth using compressive sampling and then the wavelet approach is applied for edge detection to locate the different spectrum areas in the

estimated PSD. Moreover, in order to reduce computational complexity, the edge spectrum whose peaks correspond to changes between different spectrum areas may be directly estimated from the compressed measurements without reconstructing the PSD.

In [59], another compressive sampling approach for wide-band spectrum estimation and spectrum hole detection has been proposed. The idea in the proposed scheme is to directly sample the signal at the information rate of the signal. Conceptually this can be viewed as an analog-to-digital converter (ADC) operating at the Nyquist rate, followed by compressive sampling. After the compressive sampling based PSD reconstruction performed using a wavelet edge detector along the approach of [58], the spectrum holes are detected using an energy detector in frequency domain. In [60], a collaborative detection approach based on the compressive sampling based spectrum sensing method of [59] has been proposed. The local autocorrelations of the compressed signal are transmitted to the fusion center that then performs spectrum reconstruction followed by energy detection in frequency domain. Another wavelets based multi-resolution approach has been proposed in [61]. The wavelet transform is performed in analog domain using an adjustable wavelet pulse to obtain the desired resolution. Detection is performed first at a coarse resolution after which the spectrum segments that appear to be unoccupied are sensed again using a finer resolution. Similar detector is presented in [62] where discrete wavelet packets transform based energy detector has been proposed for performing initial coarse sensing for wide bandwidths. The focus of the work presented in this thesis is on reliable detection of spectrum holes with edge/center frequency estimation. Hence, wavelets based method is compared with the proposed filter bank based methods, for complexity and functionality later in Chapter 4.

2.3.2.4. Forward Methods based Energy Detection

Spectrum sensing using forward methods has been proposed in [63, 64]. Forward methods are aimed at detecting outliers (i.e., highly-deviating samples) from a data set. In the cognitive radio context, the outliers are the occupied frequency channels in the frequency domain. The algorithm in [63, 64] is based on energy measurements in the frequency domain (i.e., channelized radiometer). Frequency channels are sorted in an increasing order of energy, and using an iterative algorithm, the number of occupied

channels is determined. Contrary to typical energy detection based methods, the algorithm does not require the knowledge of the noise level; the noise level is adaptively estimated. The method requires a few vacant channels, although their location does not need to be known in advance.

In addition, spectrum hole detection using localization algorithm based on double-thresholding has been proposed in [65]. The proposed method iteratively updates two thresholds for clustering energy measurements in frequency domain. In the basic algorithm, every cluster consisting of adjacent samples above the final lower threshold is considered to be a primary signal if at least one of the frequency domain samples is above the final upper threshold. This method is suitable only for narrowband signals with sufficiently high SNR. Furthermore, it means that if two different signals are present in a single frame of the energy detection, it cannot be separated.

2.3.2.5. Adaptive Threshold based Energy Detection

Algorithms for setting the threshold for mobile channels have been considered in [66, 67] that combines fixed and adaptive setting of threshold for energy detection. The adaptive algorithm sets the threshold as the average of the current threshold and the received signal energy. If the received energy is less than the current threshold, then the threshold is not changed and set to a fixed level. However, the operating SNR considered is positive and hence the performance of the algorithm at low SNR has not been provided.

In [68], a patent has been filed proposing an algorithm for adaptive setting of threshold for energy detection. In this method, the threshold is set arbitrarily and then updated with each sensing cycle. A new detection threshold, which is a function of the current detection threshold and the estimated energy of the received signal, is set if the received energy is below the current detection threshold. On the other hand, if the received signal energy is above the threshold, then the threshold is left unchanged. The advantages of the proposed method are that, there is no need to estimate the noise variance nor any information about the signal is required. Nevertheless, the method requires the calculation of the threshold with each sensing cycle that will in turn increase the computational complexity and sensing time in a practical scenario.

In [69], an adaptive threshold based on transmit power control is discussed. The threshold is calculated based on the transmission power of the PU, the transmission power of the SU, the distance between the PU and the SU, and the minimum decodable signal-to-interference-noise ratio (SINR). The threshold is changed adaptively by changing the transmission power of the SU. The whole issue of setting the threshold is observed from the perspective of power control with the main intention being the co-existence of the SU device with the PU. At the same time, it should also be ensured that the interference caused due to the SU at the PU should not in any case exceed the maximum SINR expected by the PU.

An adaptive setting of threshold which takes into account the interference due to signals in the adjacent bands have been discussed in [70]. The authors provide an insight on how the interference due to the presence of other channels can impact the performance of an ED based CR. However, there is no distinction made between noise power and adjacent channel signal power for calculating the threshold. The adjacent channel signal power has been added on to the noise power for all calculation purposes.

Adaptive setting of threshold in the context of cooperative sensing has also been dealt with in the literature [71, 72]. Here a two level threshold has been proposed wherein the decision as well as the data is sent by the CR nodes to the fusion centre. In [71], if the energy received by the individual CR node is below or above the two pre fixed threshold, then the final result alone is sent to the fusion centre. Otherwise, if the test statistic calculated based on the received energy is in between the two selected thresholds, then the test statistic itself is transmitted to the fusion centre. The CR node does not take any decision in that case. The improvement of this algorithm over the conventional technique has not been found to be significant. A similar algorithm is used in [72] with the difference that only the test statistic is sent to the fusion centre.

2.3.3. Feature Detection

Feature detection refers to extracting features from the received signal and performing the detection based on the extracted features. In a broad sense, a feature can be any measurement that can be extracted from the data. Typical features used for detection are, for example, correlation based features. Cyclostationarity-based detection

has received considerable attention [73-77] in the literature. The benefit of feature detection compared to energy detection is that it typically allows distinction among different signals or waveforms. In the following sub-section, different feature detection methods are reviewed. The main emphasis in this literature survey is on cyclostationarity-based detectors.

2.3.3.1. Cyclostationarity-based Detection

A process *x(t)* is said to be second-order cyclostationary in the wide sense if its mean and autocorrelation functions are periodic with some period $T > 0$ [78]:

$$E\left[x(t)\right] = E\left[x(t+T)\right] \tag{2.11}$$

$$E\left[x(t)x(t+\tau)\right] = E\left[x(t+T+\tau)\right] \tag{2.12}$$

for all t and τ . Most of the wireless communication and radar signals typically exhibit cyclostationarity at multiple cyclic frequencies. This may be related to the carrier frequency, symbol, chip, code, or hop rates, as well as their harmonics, sums, and differences. Exploiting these periodicities allows designing powerful feature detectors that possess very appealing properties. Cyclostationarity-based detectors have the potential to distinguish among the primary users, secondary users, and interference exhibiting cyclostationarity at different cyclic frequencies. Moreover, random noise commonly does not possess cyclostationarity property. In practice, however, the noise experienced in wireless communication and radar systems contains interference from various sources, such as ultra-wideband devices, device-to-device communication, leakage from adjacent channels, etc., that may exhibit cyclostationarity.

This is the case especially for interference limited wireless communication systems. In cognitive radio applications, it is reasonable to assume explicit knowledge of the cyclic frequencies of the primary users. This is because, their key parameters are specified in the wireless standards, and/or the regulatory bodies that allocate frequencies disclose such information. Cyclostationary properties of many common modulated waveforms and air interfaces have been established in [78-82]. The cyclostationarity-based detection is very sensitive to synchronization errors, such as carrier frequency and sampling clock frequency offsets. Moreover, sampling clock frequency offset may result

in smearing of the spectral correlation features if block averaging is used in the estimation [82]. However, this problem can be alleviated with noncoherent block averaging.

Cyclostationarity-based detection has received considerable amount of attention in the past [73-77, 83]. Two recent bibliographies on cyclostationarity, including a large number of references on cyclostationarity-based detection are provided in [80, 84].

In the following sub-section, an overview of cyclic detectors is provided. The detectors may be divided into single-cycle and multi-cycle detectors depending on the number of cyclic frequencies employed. Moreover, the amount of prior knowledge required by the detectors may be used to categorize them further.

2.3.3.2. Multi-cycle and Single-cycle Spectral Correlation Detectors

Optimum spectral correlation detector in AWGN noise using a multi cycle detector is presented in [73]. The test statistic for the multi-cycle detector, $z_{mc}(N)$ is given as follows

$$z_{mc}(N) = \frac{1}{N_0^2} \sum_{\alpha} \int_{-\frac{f_s}{2}}^{\frac{f_s}{2}} S_x^{\alpha}(f)^* \tilde{S}_y^{\alpha}(f) df \tag{2.13}$$

where the summation is over all the cyclic frequencies α for which the spectral correlation function $S_x^{\alpha}(f)$ of the transmitted signal *s(t)* is not identically zero. N_0 is the spectral density of the white noise and *f* denotes the frequency. The function, $\tilde{S}_y^{\alpha}(f)$, is called the cyclic periodogram or the spectral correlation function, denoted as

$$\tilde{S}_y^{\alpha}(f) = \frac{1}{N}\frac{1}{T}\sum_{n=0}^{N} Y_T(n, f + \frac{\alpha}{2}) Y_T^*(n, f - \frac{\alpha}{2}) \tag{2.14}$$

where,

$$Y_T(n, f) = \int_{n-T/2}^{n+T/2} y(u) e^{-j2\pi fu} du \tag{2.15}$$

The above multi-cycle detector is optimum in the sense that it maximizes the SNR of the regenerated spectral lines. However, it cannot be implemented without the

knowledge of the signal phase since the values of $S_x^\alpha(f)$ depend on it. For example, for a delayed signal $u(t) = x(t - \tau)$, the spectral correlation function is given by

$$S_u^\alpha(f) = S_x^\alpha(f) e^{-j2\pi\alpha\tau} \tag{2.16}$$

Hence, if the employed value for τ is wrong, the individual terms in (2.13) may add destructively. Consequently, in practice, one typically needs to resort to a suboptimum single-cycle detector [73]

$$z_{sc}(N) = \int_{-\frac{f_s}{2}}^{\frac{f_s}{2}} S_x^\alpha(f)^* \tilde{S}_y^\alpha(f) df \tag{2.17}$$

Although the signal phase is no longer required, utilizing (2.17) still requires knowledge of the modulation type and its parameters, such as carrier frequency, pulse shape and symbol rate, in order to calculate the spectral correlation function $S_x^\alpha(f)$. In addition, the noise spectral density N_0 may be replaced by its maximum likelihood (ML) estimate,

$$\tilde{N}_0 = \frac{1}{N} \sum_{k=1}^{N} |\eta(n)|^2 \tag{2.18}$$

where N is the number of received samples and $\eta(n)$ is the received signal which is purely noise [74].

The multi-cycle detector test statistic in (2.13) is asymptotically complex normal distributed under both hypotheses [74] while the single-cycle test statistic in (2.17) is asymptotically Rayleigh distributed under H_0 and Rician distributed under H_1 [77]. Figure 2.7 illustrates the implementation of a multi-cycle based cyclostationary feature detector [73]. Variants of the above detectors have been proposed recently for spectrum sensing in cognitive radios, e.g., in [85, 86]. Single-cycle detector has been proposed for detecting code division multiple access (CDMA) signals used in universal mobile telecommunications system (UMTS) in [86].

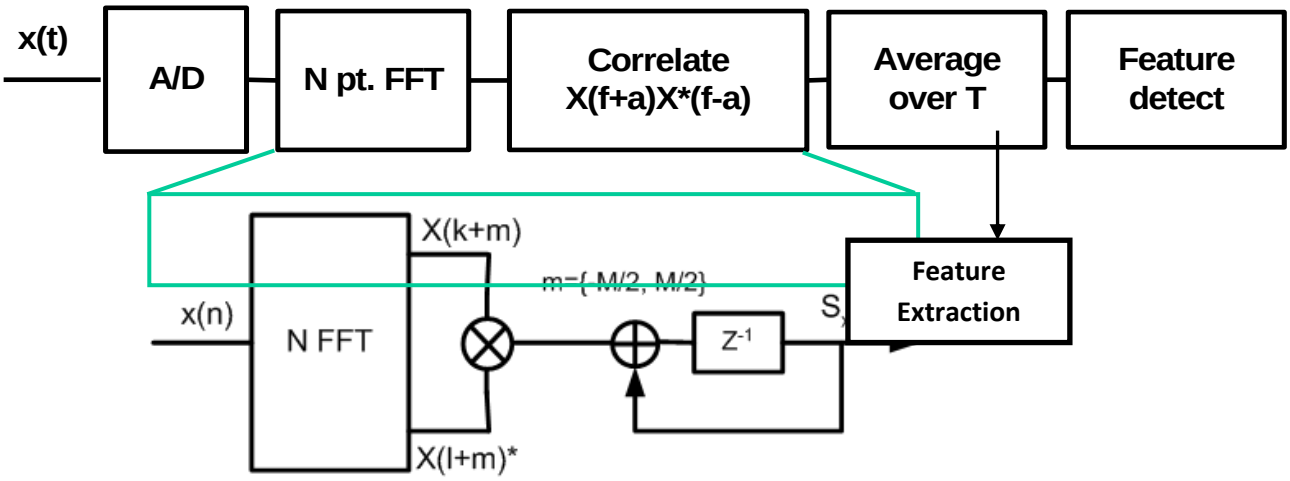

Figure 2.7. Implementation of a multi-cycles cyclostationary feature detector [73].

The estimate for the noise power is obtained from the cyclic spectrum areas where signal features do not exist. Furthermore, DVB-T signal detection using simplified versions of the single cycle detector has been considered in [85].

2.3.3.3. Other Cyclic Detectors

In [87], CFAR spectral correlation detectors based on the estimated cyclic spectrum that make no assumptions on the intercepted signal have been proposed. Thus, they are suited for unknown signal detection. However, the caveat is that, it is performed without any prior knowledge of the noise and signal. Hence, they cannot distinguish among different systems. The proposed method employs the computationally efficient FFT accumulation method (FAM) [88] for estimating the cyclic spectrum and uses the normalized peak values of the cyclic spectrum as the test statistic. A similar type of cyclic spectrum based CFAR detector has been proposed and applied for ATSC pilot tone detection in [89].

In [56], a multi-resolution frequency subband spectral correlation detection algorithm based on frequency smoothed periodograms has been proposed. The presence of spectral correlation is detected at a given cyclic frequency. In addition to signal detection, cyclostationarity may be used for modulation classification as well. This is especially helpful for characterizing unknown signals. In addition, many of the techniques could be used for detection as well. Many of the cyclostationarity-based modulation classification methods are based on the cyclic frequency domain profile [90].

2.3.3.4. Energy based Feature Detection

In [91], the authors propose a detector based on energy detection in frequency domain followed by a feature extraction of the bandwidths and center frequencies. The extracted features are used to classify the primary user system using a Bayesian classifier. Frequency correlation is exploited for obtaining better detection performance and for finding the transmission parameters using the energy detector output. Furthermore, partial match-filtering is used to detect the active primary users by matching to the extracted features.

2.3.3.5. Correlation Feature Detectors for OFDM Signals

In [92, 93], a correlation detector for cyclic prefix OFDM signals has been proposed. The proposed detector is based on the fact that the cyclic prefix which precedes every OFDM symbol is the exact copy of the end part of that same OFDM symbol. This creates intrinsic correlation within the OFDM signal that can be exploited for detection. Moreover, in [92, 94] a sequential collaborative detection approach based on the autocorrelation method of [93] for the fusion of local secondary user test statistics has been proposed.

2.3.4. Waveform-based Sensing

Most of the wireless systems use known patterns to assist in synchronization or for other purposes. Such patterns include preambles, midambles, regularly transmitted pilot patterns, spreading sequences, etc. Sensing can be performed in the presence of a known pattern, by correlating the received signal with a known copy of itself [95, 96]. This method is only applicable to systems with known signal patterns, and it is termed as waveform-based sensing. In [95], it is shown that waveform-based sensing outperforms energy detector-based sensing in reliability and convergence time. Furthermore, it is shown that the performance of the sensing algorithm increases as the length of the known signal pattern increases. As one of the methods for analyzing the Wireless Local Area Network (WLAN) channel usage characteristics, packet preambles of IEEE 802.11b [97] signals are exploited in [98, 99]. Measurement results presented in [22] show that

waveform-based sensing requires short measurement times, however, it is susceptible to synchronization errors.

Assume that the received signal has the following simple form

$$r[n] = s[n] + w[n] \tag{2.19}$$

where $s[n]$ is the signal to be detected, $w[n]$ is the AWGN, $y[n]$ is the known waveform model and n is the sample index. The waveform-based sensing metric can be obtained as in [96]:

$$S = \mathrm{Re}\left[\sum_{n=1}^{N} y[n]s^*[n]\right] \tag{2.20}$$

where N is the length of known pattern and 'Re' is the operation to determine the real part of the complex entity inside the brackets. In the absence of the primary user, the metric value becomes

$$H = \mathrm{Re}\left[\sum_{n=1}^{N} w[n]s^*[n]\right] \tag{2.21}$$

Similarly, in the presence of a primary user's signal, the sensing metric becomes

$$H = \sum_{n=1}^{N} |s[n]|^2 + \mathrm{Re}\left[\sum_{n=1}^{N} w[n]s^*[n]\right] \tag{2.22}$$

The decision on the presence of a primary user signal can be made by comparing the decision metric H against a fixed threshold λ_W. This is equivalent to distinguishing between the two hypotheses in (2.5) and (2.6). It can be formulated in a similar way as discussed in the energy detection section. P_{fa} should be kept as small as possible. The decision threshold λ_W can be selected for finding an optimum balance between P_d and P_{fa}. However, this requires the knowledge of noise and detected signal powers. The noise power can be estimated, but the signal power is difficult to estimate as it changes depending on ongoing transmission characteristics and the distance between the cognitive

radio and primary user. In practice, the threshold is chosen to obtain a certain false alarm rate. Hence, the knowledge of noise variance is enough for selection of a threshold.

2.3.5. Eigen Value Detection

Eigen values based spectrum sensing are a new class of blind sensing algorithms that do not require any prior knowledge of the signal structure or characteristics [100-102]. The technique builds on the latest random matrix theories (RMT) to quantify the distribution of the Eigen values and to calculate the probability of detection and probability of false alarm of the system. In order to calculate the Eigen values, the statistical covariance matrix of the received input vector *r[n]* needs to be computed first. Considering *L* consecutive samples of the received vector,

$$\mathrm{r}[\mathrm{n}] = \left[r(n) r(n-1) \ldots\ldots\ldots r(n-L+1) \right]^{T} \tag{2.23}$$

The statistical covariance is given by

$$R_x = E\left[r[n] r^{T}[n] \right] \tag{2.24}$$

Practically, the statistical covariance matrix can only be calculated by using a limited number of samples [103]. Thus, a sample covariance matrix is estimated by calculating the sample auto correlation of the received signals. This is given as

$$\psi(l) = \frac{1}{N} \sum_{1}^{N} r[n] r[n-l],\ l = 0,1,\ldots,L-1 \tag{2.25}$$

From the autocorrelation values obtained, the sample covariance matrix, $\hat{R}_x(N)$ can be obtained. From the sample covariance matrix, the statistical covariance matrix can be approximated [103].

$$\hat{R}_x(N) = \begin{bmatrix} \psi(0) & \cdots & \psi(L-1) \\ \vdots & \ddots & \vdots \\ \psi(L-1) & \cdots & \psi(0) \end{bmatrix} \tag{2.26}$$

It should be noted that the sample covariance matrix given by (2.26) is a symmetric matrix. To detect the presence or absence of the signal, the maximum and minimum Eigen values, ψ_{max} and ψ_{min} respectively, of the sample covariance matrix are calculated. Two algorithms proposed in [101] to detect are maximum-minimum Eigen value (MME) and Energy with minimum Eigen value (EME) ratio tests. In the MME technique, if ψ_{max}/ψ_{min} exceeds a threshold then the presence of the signal is hypothesized. Else, it is assumed that the spectrum is vacant. In the EME technique, the average power of the received signal is computed and a ratio of the computed power to ψ_{min} is taken. If this ratio exceeds the set threshold then the spectrum is occupied. The threshold for the MME and EME technique depends only on the number of samples *N*, the smoothing factor or the number of segments *L* and the probability of false alarm. Unlike the energy detector, the threshold can thus be pre-computed since it is independent of the signal and noise power. The major advantage of Eigen value detection is that it does not require any knowledge about the signal, channel or the noise power. It is a blind detection technique and yet it is more robust to fluctuations to noise than the conventional energy detector. The technique works best when the input signals are highly correlated, like wireless microphone signals, or DTV signals, etc. The disadvantage of the technique is that a high number of computations are required to arrive at the final decision. For a smoothing factor of *L* and an oversampling factor of *M*, the total time required to arrive at the result is approximately *M*L* times that required for an energy detection.

In [104], a detection method based on the estimated covariance matrix has been proposed. The proposed detector calculates the ratio of the sum of the absolute values of the correlation matrix and the sum of the diagonal elements. In essence, the detection is based on whether the absolute values of the non-diagonal elements are approximately zero. This allows detection of correlated signals since noise has diagonal covariance matrix. Two other detection algorithms using the same formulation have been proposed in [99]. These two detectors are based on the Eigen values of the sample covariance matrix: One calculates the ratio of the maximum and minimum Eigen values, i.e. the condition number, and the other calculates the ratio of the received signal energy and minimum Eigen value. The detection algorithms proposed in [101, 104] are robust against receiver noise uncertainty and can be implemented without the knowledge of the signal and

channel. However, these algorithms cannot distinguish among different signals or interference.

2.3.6. Multiple Cumulants based Sensing

In [105], a new spectrum sensing method based on multiple cumulants was proposed. In practice, due to the presence of a colored channel interferer or lower number of samples considered, the conventional AWGN may become colored. The energy detector fails and is not effective in cases of signals corrupted by correlated noise. Autocorrelation based detectors are also infeasible in this case. It is well known that cumulants higher than second order are zero for Gaussian distributions. Thus, cumulants can be used to extract non-Gaussian signals from Gaussian noise. Most of the existing literature usually uses a single cumulant of a certain order and a certain lag. This poses a disadvantage to the sensing method as they only make limited use of the rich statistical information contained in the signal. The spectrum sensing method in [105] is based on multiple cumulants of arbitrary orders and arbitrary lags. This makes it superior and flexible compared to other cumulants based methods. It also requires no extra information such as exact noise power or cyclic frequencies hence it is nonparametric. It is shown to be robust to noise uncertainty.

2.3.7. Two-Stage Spectrum Sensing

In order to determine spectrum holes efficiently, two-stage spectrum sensing algorithms have been proposed in the literature. At the beginning of the spectrum sensing process, a coarse sensing is performed over the entire frequency range with a wide bandwidth. This step uses a very simple method such as energy detection. In this step, the spectrum bands where the energy level is over the threshold level, possible spectrum holes for secondary users are identified. This coarse sensing result is reported to the medium access control (MAC). Then, for these possible empty bands, the fine sensing is performed that detects the unique features of the modulated signals. This fine sensing step is performed to confirm that the spectral band of interest was indeed unoccupied.

In [106], for the coarse sensing stage, a wavelet transform approach is used to reconstruct the power spectral density of the signal. By comparing the derived power

spectral density in each band with the threshold level, the vacant regions of the spectrum band can be determined. In [107], the authors use an energy detector for the first stage and cyclostationary feature detector for the second stage detection. The use of a two-stage detector for spectrum sensing in a CR device is justified because it leads to an improvement in the detection accuracy of the system. However, the improved detection accuracy comes at the cost of increase in sensing time and implementation complexity.

A two-stage method was proposed in [108] wherein it is shown that by pre-computing the lower bound of the SNR at which the energy detection still works satisfactorily, the second stage of a two-stage detector can be switched off when the channel SNR is higher, without any loss of performance. In other words, when the channel SNR is good, the results of the first stage energy detector can be trusted. This also leads to enormous savings in power consumption. Thus, the modified two-stage detector presented in [108] not only leads to savings in the mean detection time of the CR, but also leads to the reduction of the overall power requirements of the CR device which is a limiting factor for any battery operated device.

2.4. Summary

In this chapter, various spectrum sensing methods for identifying underutilized radio spectrum have been reviewed. Spectrum sensing methods are broadly categorized into three classes: matched filter, energy based detection, and feature detection. Different methods based on these three techniques were discussed in detail. Table 2.1 summarizes the comparison of various spectrum sensing methods available in the literature.

Although most of the existing spectrum detection methods provide good performance in terms of detecting the occupied channels, none of them provides accurate information about the channel center frequency, edge frequencies and/or the modulation scheme of the received signal. Therefore, the existing methods are mostly suited for commercial wireless communication receivers where the channel locations are predefined and known apriori to the secondary user. On the other hand, in an ideal CR scenario, accurate location of spectrum holes is a challenging task due to the high input sampling rate and large bandwidth of the signal.

TABLE 2.1. COMPARISON OF VARIOUS SPECTRUM SENSING ALGORITHMS

Algorithms	Features	Pros and Cons
Matched Filtering	• Optimum method for detection of a PU signal. • Requires *a priori* knowledge about the signal. It requires to demodulate the received signal. • When there is no accurate information about PU signals or the noise variance, it performs poorly.	Pros – Maximizes the receiver SNR. – Accurate in detection, as it demodulates the received signal Cons – Needs special receiver for each PU signal, hence very complex to implement. – Large power consumption as various receiver algorithms need to be executed.
Energy detection	• More generic method for spectrum sensing. • Requires no knowledge about PU signals. • Similar to a spectrum analyzer. Many methods like periodogram, Multi-Taper (MT) and filter bank method exist.	Pros – Non-coherent and easy to implement. – No priori knowledge about the signal is required. Cons – Not robust in low SNR conditions. – Fails to distinguish between noise, interference and modulation.
Feature detection (cyclostationary, Eigen values, higher order moments, cumulants etc.)	• Built in periodicity (for e.g. pulse trains, repeating spreading, hopping rates etc) can be used for extracting features of the spectrum. • Requires *a priori* knowledge about the transmitted signal and the communication channel used by the standard. • Spectral correlation function (SCF), Eigen values, higher order moments, and cumulants are some examples of features for feature detection.	Pros – More robust at lower SNRs than energy detector. – Can extract features from the received signals. – Higher detection accuracy Cons – SCF-highly complex 2-D FFT, higher order moments and cumulants, Eigen values are all highly complex operations. – Difficult to implement in hardware due to the highly complex computations involved. – Sensing time is higher.

The estimation of the location of the PUs' signals helps in determining the spectrum vacancies or holes, which can be used for opportunistic spectrum usage. However, in some cases of CR, if a spectral region is occupied, it is not evident if a primary user or a secondary user occupies it. There is also a possibility that more than one user is present in a frequency band. Moreover, in some applications such as military and public safety applications where there are needs for interoperability amongst various standards, there is a need to determine more details and characteristics of the received signal. In addition, for some military applications, the CR receiver needs to identify the modulation format employed in the enemy signal, as there is no information on it. Hence, there is a need to perform modulation classification to recognize the modulation format of the detected signal in various applications of CR. This is the intermediate step between the signal detection and demodulation in the case of an intelligent receiver such as in a CR. Obviously, with no knowledge of the transmitted data and many unknown parameters at the receiver, such as the signal power, carrier frequency and phase offsets, timing information, etc., blind identification of the modulation is a difficult task. This becomes even more challenging in real-world scenarios with multipath fading, frequency-selective and time-varying channels.

Thus, this chapter highlights existing standards, benchmarks and methods in the spectrum sensing literature, and the limitations associated with them. It elucidates the motivation for an advancement of the research in these fields. The main objectives of the work presented in this thesis are to develop robust spectrum sensing and automatic modulation classification techniques for CR. Thus, the work presented in the following chapters, is focused on robust and accurate spectrum sensing and modulation classification methodologies for cognitive radios.

Chapter 3

Data Models and Experiment Setup

With the aim of developing robust sensing and classification algorithms, likelihood-based techniques are adopted in some cases, since they minimize the probability of error. In these techniques, the problem at hand is formulated as a hypothesis testing problem. Following a composite hypothesis testing procedure, the unknown state of the fading process and the noise distribution parameters are estimated, and a likelihood ratio test is then used to choose the appropriate hypothesis. Thus, there is a need to understand the signal and noise models used in various chapters of this thesis.

In this thesis, the signals of interest are assumed to be digital, amplitude or phase modulated i.e., the modulation schemes considered are phase shift keying (PSK) and quadrature-amplitude modulation (QAM) schemes, which are used in a variety of wireless communication systems. The data models used are elucidated in the simulations sections of each chapter. Additionally, various statistical-physical models for the additive non-Gaussian noise are considered. This chapter describes the physical and mathematical model of the noise that is used in the work presented in the later chapters. The symbols used will be consistent throughout the thesis unless otherwise mentioned. The second part of this chapter is wholly dedicated to a discussion on the experimental setup for data acquisition using universal software radio peripheral2 (USRP2).

3.1. Data and Noise Models

In realistic environments, most of the radio scenarios coexist with a variety of sources of electromagnetic radiation that cause interference to the radio. These sources, which introduce additive noise into the system, can include atmospheric noise, co-channel interference in wireless networks, and incidental radiation from various man-made devices, such as automobile ignitions, elevators, microwave ovens, clocks and busses of computers, and LCD monitors, among many others. Various measurement campaigns conducted in a variety of environments concur that this additive noise is well modeled by non-Gaussian processes and in most cases exhibits impulsive characteristics [109]. In this chapter, one of the most popular models for noise distribution, the symmetric- α -stable ($S\alpha S$) model is presented.

3.1.1. Symmetric-alpha stable model

A strong justification for the use of Gaussian distribution in modeling additive noise is the central limit theorem (CLT) which states that the sum of independent and identically distributed (i.i.d) random processes with finite variances converges to a Gaussian random process. The more powerful generalized central limit theorem states that the limiting distribution of a sum of i.i.d random processes is a stable distribution [110]. Stable distributions have tails heavier than a Gaussian distribution and have infinite variance. These two characteristics of the stable distribution make it a popular model to represent the non-Gaussian noise, which exists in realistic environments and exhibits impulsive behavior. In this section, the focus is on symmetric stable distributions, which are a subclass of stable distributions with skewness parameter equal to zero. Under appropriate assumptions about the spatial distribution of the noise sources, their emission characteristics and the propagation conditions in a physical environment, it has been shown in [111] that the $\mathrm{S}_\alpha\mathrm{S}$ distribution can be used to model the noise. A detailed analysis of the derivation and the features of this statistical physical model are presented in [111]. Gaussian distribution is a special case of the $\mathrm{S}_\alpha\mathrm{S}$ distribution when $\alpha = 2$. Gaussian noise model is used in Chapters 4 and 6 of this thesis, while some specific models that are used in the work are explained in Chapter 5 of this thesis.

In the next section, the experimental setup for data acquisition is explained in detail.

3.2. Data Acquisition using USRP2

In the work in this thesis, USRP2 [112] and GNURadio [113] are used to obtain data from real environment or that is transmitted from a signal generator. In order to capture and analyze the signals, a USRP2 board with a wide bandwidth transceiver (WBX) daughter board has been used. The relevant features of the USRP2 board are

1. Two 14-bit 100MS/s Analog to Digital Converters.
2. Two 16-bit 400MS/s Digital to Analog Converters.
3. Gigabit Ethernet Interface.
4. Capability to process signals as wide as 50MHz in bandwidth.
5. The RF range varies from 0 to 5.9GHz and limited by the antenna module used

The WBX daughter board can operate from 50 MHz to 2.2 GHz band and hence offers an excellent choice for testing wide range of signals. In the USRP2, high sample rate processing, like digital up- and down conversion takes place in the Field Programmable Gate Array (FPGA). The data is transferred to the host PC over the gigabit Ethernet interface and the low sample rate operations are performed on the host computer. Alternatively, the FPGA can be used to do some amount of user desired processing for which there is free space available in the FPGA to insert custom modules. The USRP2 contains a Xilinx Spartan 3-2000 FPGA that can be used for storing data as well as running user-defined intellectual property (IP) cores. In the work presented in this thesis, the free space in the FPGA is used for storing and buffering the input samples after RF to IF conversion, and for sensing purpose. The details of the usage of USRP2 for sensing in specific application scenarios are provided in Chapters four, five and six. This flexibility due to the increased size of FPGA allows the USRP2 to be used as a standalone system. To make the programming easier, the configurations and firmware of the USRP2 are stored in a secure digital (SD) flash card. In the setup used for capturing signals in the lab, the antenna module fetches the RF signal from sensing environment and shifts the signals to an intermediate frequency (IF) in the USRP2 daughterboard. The down shifted IF signal is passed to the USRP2 motherboard where the ADC operation is performed.

Digital down converters (DDC) can be implemented in the FPGA depending on the application scenario to convert the digitized data to baseband. The DDC also performs the decimation of the incoming data to moderate the data rate at which signal passes through the gigabit Ethernet interface without causing any loss of information.

Figures 3.1 and 3.2 provide the front view and the top view of the USRP2 board respectively. The top view gives a sectional image of the FPGA and the daughter RF board.

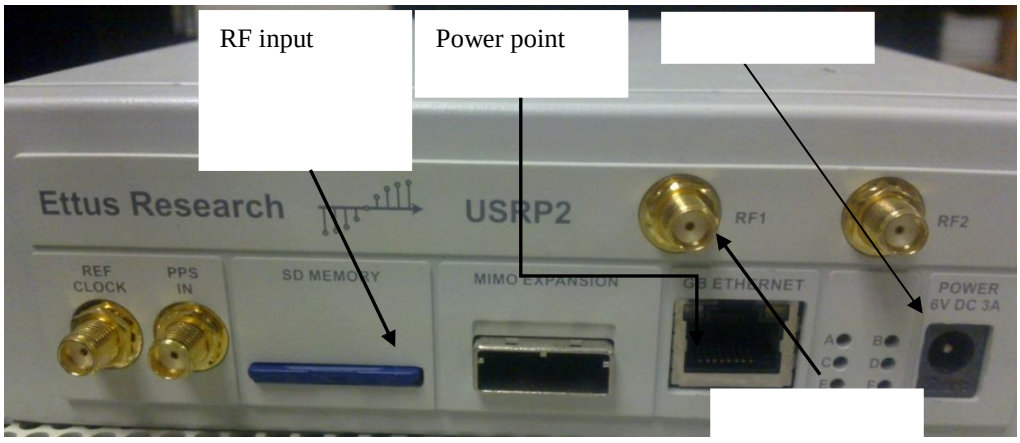

Figure 3.1. USRP2 front view.

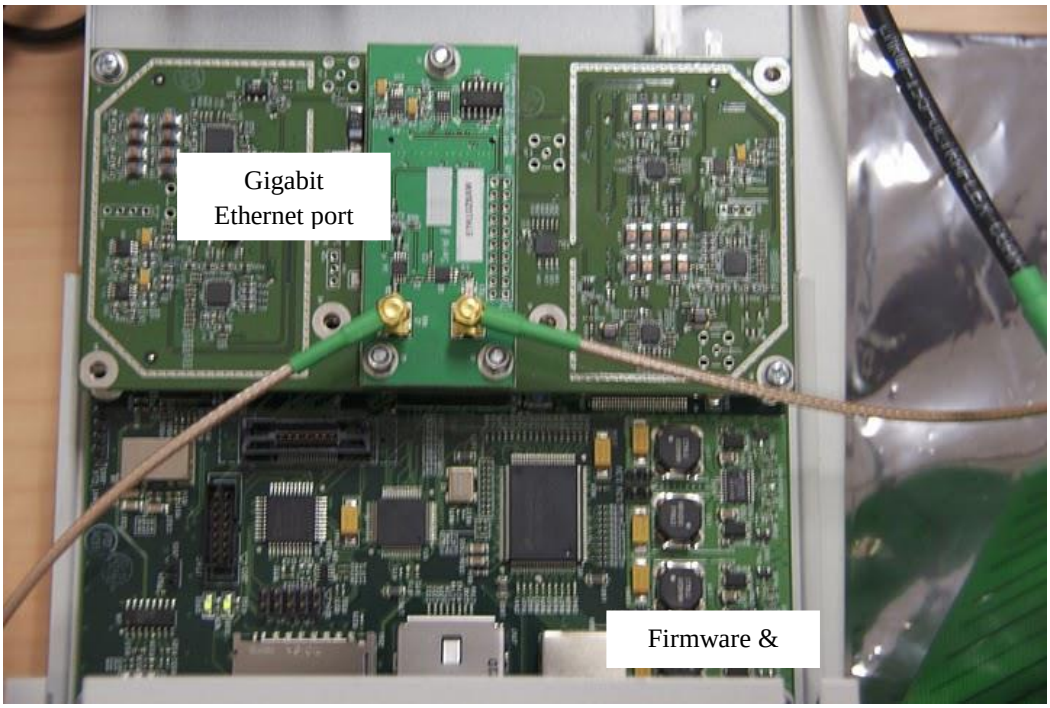

Figure 3.2. USRP2 top view.

The digital output from the ADC is mixed with a digitized sine and cosine component to obtain the Q channel and I channel respectively which will produce the sum and the difference components. The unwanted components are filtered by passing through digital filters. The post processed data (complex I and Q) is then transferred by the FPGA module to the host computer via the gigabit Ethernet controller.

The FPGA present in the USRP2 board performs the complex signal processing tasks that involve high level of computation and throughput. Operations such as digital up conversion, digital down conversion, decimation and interpolation are thus handled by the FPGA residing in the USRP2. The control of the various analog components present in the USRP2 board is also done by the FPGA. It uses a gigabit Ethernet interface to communicate with the host machine. This allows a higher data rate for data transfer purposes. The gigabit Ethernet interface is used for exchanging the configuration as well as signal data and it is capable of handling simultaneously up to 50 MHz of RF bandwidth in and out of the USRP2. The configuration data for setting the required parameters such as RF frequency, decimation and interpolation rates, ADC and DAC configuration is provided by the host machine to the USRP2 module. In addition, to enable precise synchronization operations, an output to an external reference is provided. The important aspect of the USRP2 is that the FPGA code cannot be altered; however, the user can set the configuration parameters, as mentioned previously.

The task of managing the RF front end is dedicated to daughter boards which can be mounted on the USRP2. A variety of daughterboards are available which operate across a wide range of frequencies ranging from around DC to 6 GHz to support a wide range of applications. Figure 3.2 shows the USRP2 motherboard with a WBX daughterboard attached to it. The daughterboards usually are equipped with an electrically erasable programmable read-only memory (EEPROM) that allows the host software to setup the USRP2 according to the daughterboard connected. An error is reported in case this EEPROM is not programmed. The daughterboard consists of the antenna along with the synthesizer, mixer and local oscillators. The USRP2 has two daughterboard slots which can be used in receive-only, transmit-only and transceiver type daughterboards. The receive-only and transmit-only daughter boards take up only one slot whereas the transceiver type daughterboards take up two slots. Thus both transmit and

receive can be performed using one USRP2 module [112]. For the antenna, a Thomson ANTD120 indoor DVB-T antenna with RF connector was used as shown in Figure 3.3.

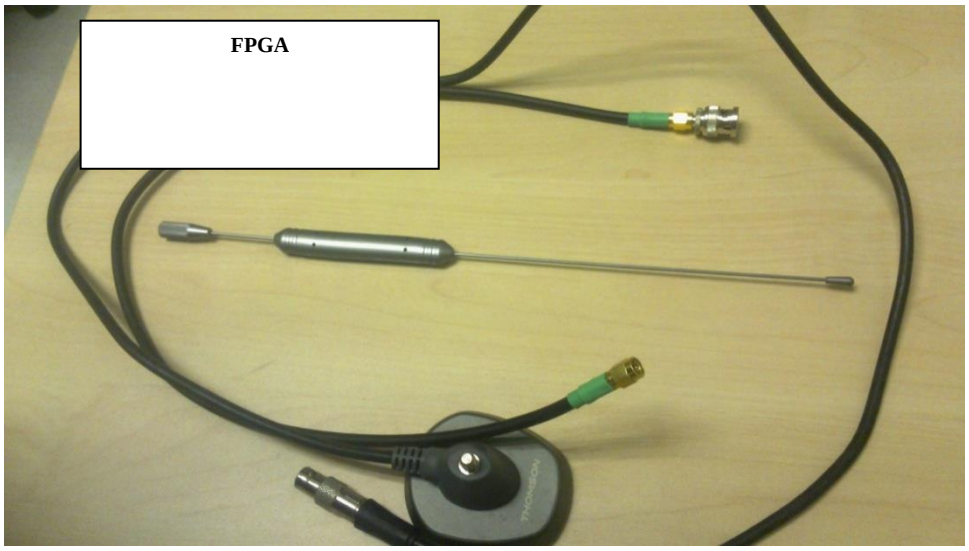

Figure 3.3. RF antenna front view.

In the next section, integration of USRP2 and GNU Radio is explained in detail.

3.3. GNU Radio Framework

GNU Radio is a free & open-source software development toolkit that provides signal processing blocks to implement software radios. It can be used with readily-available low-cost external RF hardware to create software-defined radios, or without hardware in a simulation-like environment. It is widely used in hobbyist, academic and commercial environments to support both wireless communications research and real-world radio systems. GNU Radio project is utilized to integrate the USRP2 board with the host computer.

As seen from the Figure 3.4 [112], the high sample rate operations are carried out in the FPGA by the USRP2 board and then the data is passed over to the host via the Gigabit Ethernet. The GNU radio framework has built in modules to perform many of the signal processing tasks that are required for our purposes. The GNU Radio tool kit provides an all-encompassing framework to use software modules to realize radio functionalities.

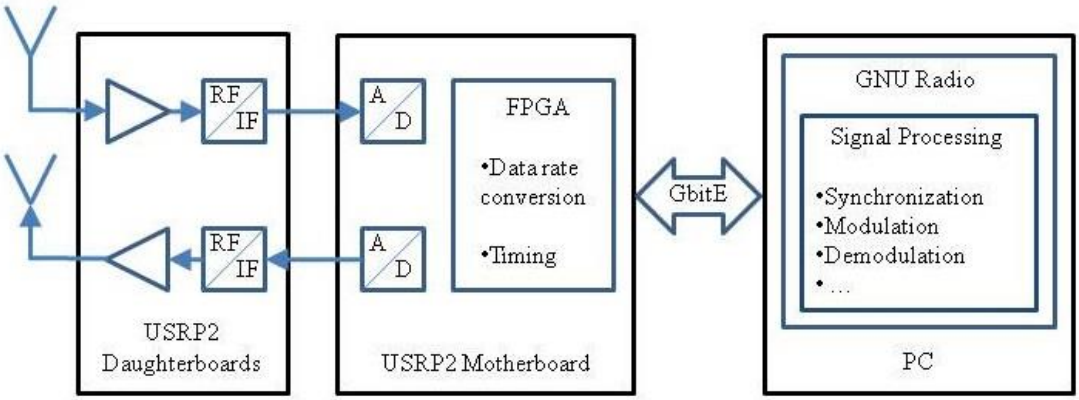

Figure 3.4. Block diagram of a USRP2 operating in GNU Radio framework.

The framework of GNU Radio provides the necessary libraries of signal processing blocks like modulators, demodulators, filters, etc which can be used to construct an SDR. The structure of the GNU Radio's software is organized in a two layered architecture. The blocks used for signal processing, being performance critical, are implemented in C++, while the task of connecting and gluing the signal blocks together is done using Python at the top layer. Figure 3.5 shows the clear linkage between the various layers in a GNU Radio platform. Python language is used to create the flow graph of the blocks that are configured with the correct parameters. The signal source blocks are connected to the sinks via the processing blocks. The signal processing blocks are used to process the streams of data from their input port to their output port.

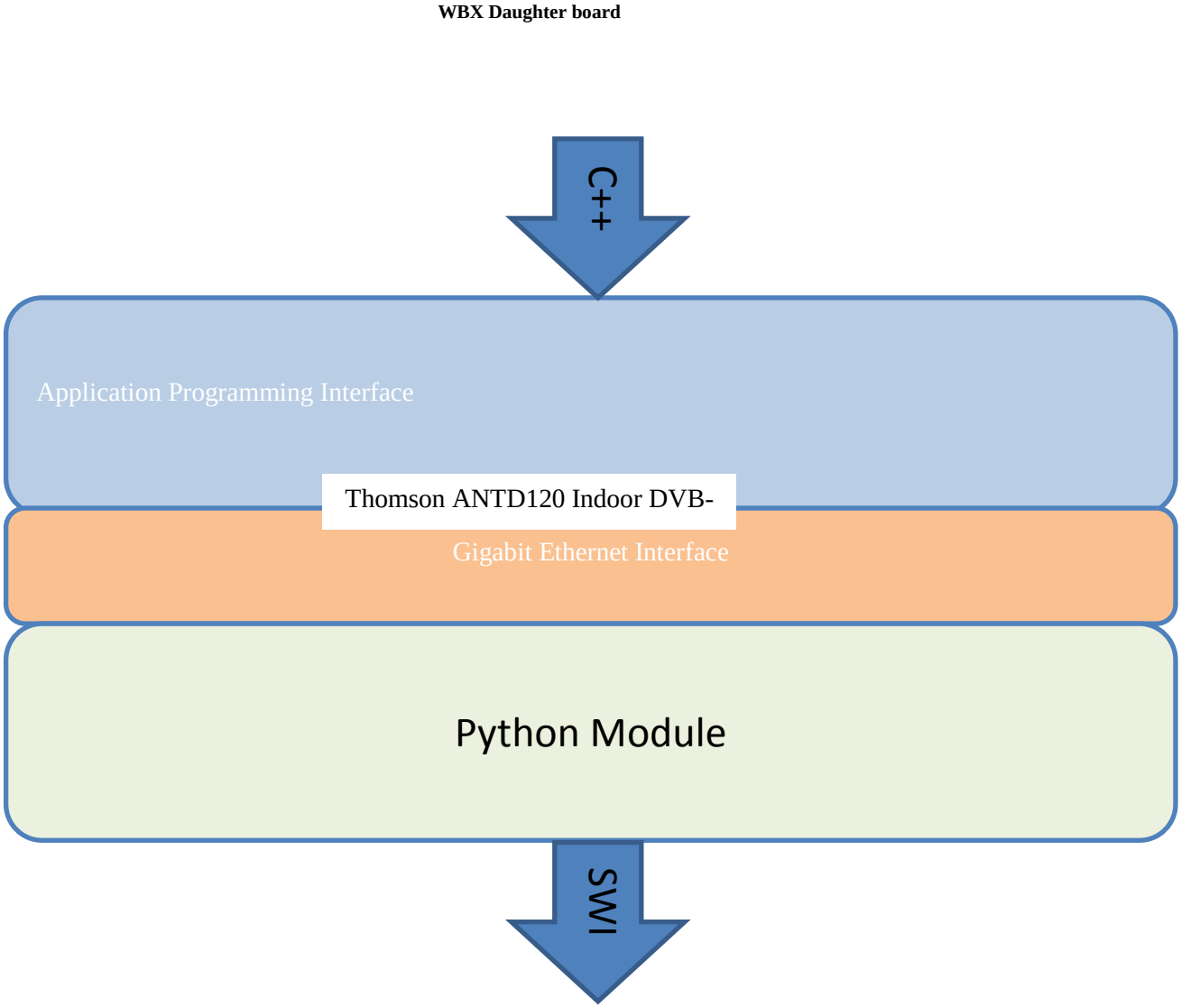

Figure 3.5. Software architecture of GNU Radio.

The input and output ports of a signal processing block can be configured. Therefore, a block can have multiple outputs and multiple inputs. The signal processing blocks are written in C++. Python and C++ are interfaced together using the Simple Wrapper and Interface Generator (SWIG). SWIG is the wrapper for the C++ modules and generates the corresponding Python code and library so that these classes and functions can be called from Python. The GNU Radio project has already created a large repository of signal processing blocks very similar to the blocks available in Matlab/Simulink. GNU Radio is a free and open-source software development toolkit that provides signal

processing blocks to implement software radios. It can be used with readily available low-cost external RF hardware to create software-defined radios, or without hardware in a simulation-like environment. If necessary, customized signal processing blocks written in C++ can be created and integrated to the framework [113]. There is also a graphical environment available to create a custom radio called GNU Radio Companion (GRC). This helps in building the flow graph with ease. The GRC generates the python script required to execute the data flow graph. In this chapter, the use of GRC is mentioned briefly since no predefined blocks were available in the literature for data acquisition for sensing purposes. Existing python scripts were modified to get I and Q values. The hardware setup required to capture the signal is summarized in Table 3.1.

TABLE 3.1. HARDWARE CONFIGURATION OF DATA ACQUISITION

Processor	Intel Pentium 3.17 GHz (Core 2 Duo) Intel Pentium 2.26 GHz(Core 2 Duo)
OS	Ubuntu 10.04 or later
GNU Radio	3.3 or higher

Data Acquisition Equipment

SDR RF hardware	USRP2
USRP Daughterboards	WBX with Thomson Antenna

Test Measurement Equipments

Signal generators	Agilent E4438C
Spectrum analyzer	Rohde & Schwarz signal analyzer
Mobile Device	Nokia, Samsung mobile phones

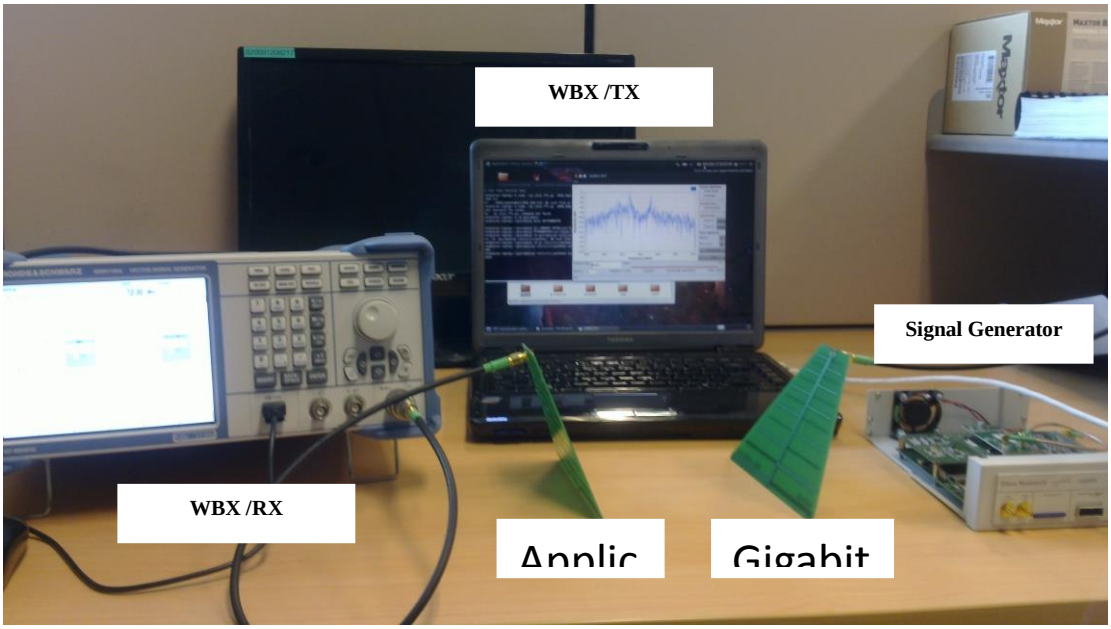

Figure 3.6(a). Setup to capture signals using WBX antennae and USRP2.

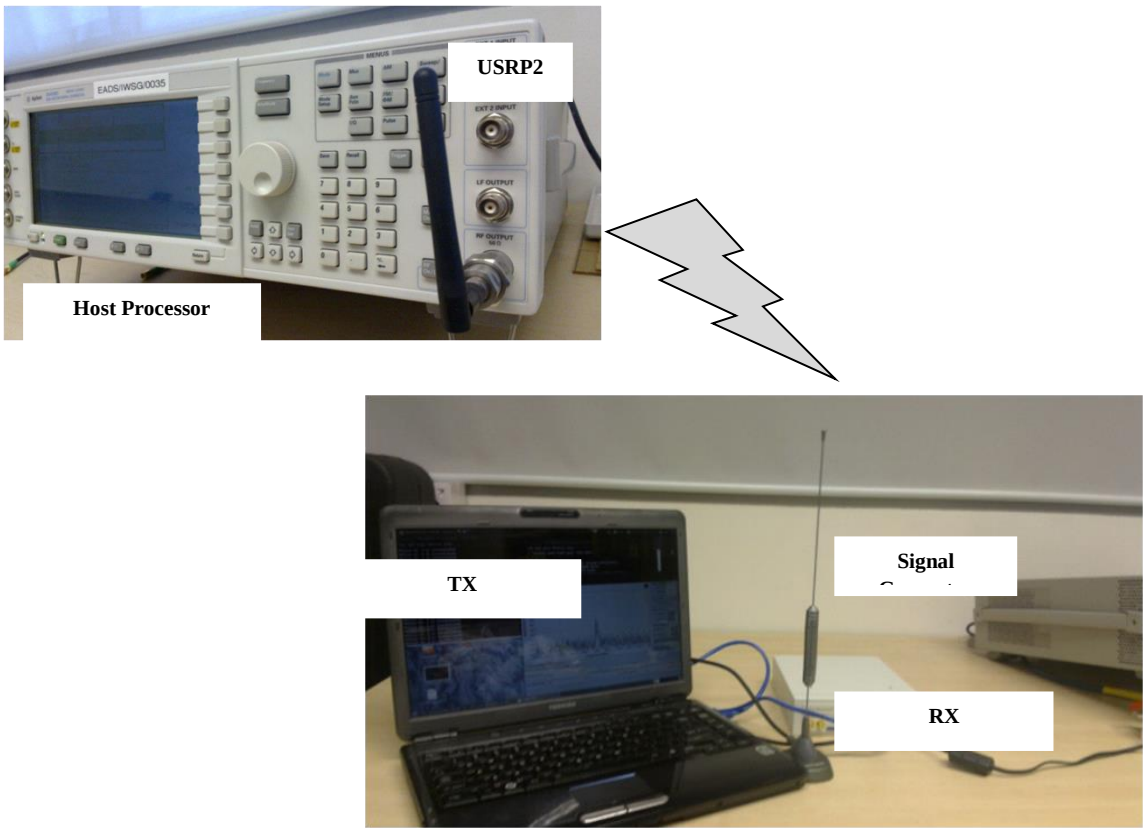

Figure 3.6(b). Alternate setup for testing algorithms using Thomson DVB-T antenna and USRP2.

Figure 3.6 (a, b) show the setups to generate and capture signals for various modulation formats like QPSK, QAM, BPSK, etc using WBX and Thomson antenna. A signal generator is used to generate the modulated signal with AWGN added to it. This is passed to the USRP2 board where I & Q values are demodulated and decoded and written to a text file. The steps involved in setting up USRP2 and GNURadio for experimental purposes (over-the air tests) are addressed in each chapter of this thesis, depending on the application scenario.

3.4. Summary

In this chapter, the noise and data models used in the work presented in this thesis are described. Additionally, a discussion on the experimental setup for data acquisition using universal software radio peripheral2 (USRP2) and GNU Radio is also presented. Implementation details of GNU Radio are discussed extensively. The experiment setup and the data models presented in this chapter are used for all the work presented in this thesis. In the next chapter, filter bank based spectrum sensing algorithms are proposed.

Chapter 4

Spectrum Sensing based on Filter Banks and Energy Detection

4.1. Introduction

In Chapter 2, the three main techniques for spectrum sensing: matched filtering, energy detection and feature detection were discussed in detail. It has been established in the literature that energy detection is the best solution for blind or random signal detection, as it does not require any assumption or prior knowledge about the signal. Most of the literature on spectrum sensing for a CR is focused mainly on the various detection methods available. These detection methods focus mainly on detecting the presence of occupied or unoccupied channels. In an ideal scenario, the CR must be able to locate vacant bands over a wideband signal dynamically, with low overhead in terms of computational complexity. For this purpose, the CR must be able to locate the PU signal accurately, by estimating their center/edge frequencies.

The spectral edge estimation for determining the exact locations of waveforms in a wideband spectrum also forms an important component in the latest mobile wireless communication systems. The concept of CR allows the user equipment (UE) to scan the spectral environment with respect to instantaneous spectrum allocation. In the original context of CR, this information is used for efficient spectrum usage by different UEs using various radio access technologies. However, in the case of Long Term Evolution (LTE) functionality, knowledge about the environmental spectral composition is extremely valuable for the designs of both transmit and receive paths [114, 115]. If the

UE detects significant interference to the wanted signal, then both the analog frontend and the digital frontend (AFE/DFE) of the receive path provide full performance, i.e. highly linear amplifiers, filters of high order, etc. This full performance mode, in turn, results in high power consumption by the UE. On the other hand, if there are only few blockers present, which contain little energy, the receive path does not have to run in full performance mode, resulting in relaxing the desired specifications and consequently saving power consumption. A system concept handling this task for the Universal Mobile Telecommunications System (UMTS) test case has been described in [116]. All existing methods are based on highly efficient filter bank chains of different kinds depending on the application.

Most of the applications in signal processing and communications use both analysis and synthesis filter banks. This is because they are primarily used for reconstructing the signal corrupted with noise as the systems have prior knowledge of the received signal. However, in the above-mentioned scenario, analysis filter banks are used to split the wideband spectrum into subbands that can be processed to obtain the required information and synthesis filter banks are not employed. The classical filter banks that are present in the literature give perfect reconstruction performance only when the analysis and synthesis filters are ideal. In a practical scenario, aliasing will result from the downsampling/upsampling operation and corrupt the output signal. Since aliasing distortion is inherently non-linear, it may be very undesirable in certain applications. Thus, higher order analysis/synthesis filters would be required to reduce aliasing distortion within tolerable levels. The higher the filter order (i.e., the greater the number of filter taps), the better the filter's response. However, higher filter order require larger number of coefficient multiplications (computational complexity) and hence increased power consumption. This increased cost (due to the requirement of high order analysis/synthesis filters) can be offset by utilizing the efficient polyphase implementation of the FIR filter [50]. The main objective of the work in this chapter is to develop reliable detection methods for spectrum sensing. These algorithms must be able to function over a wide bandwidth with little prior knowledge about the received signals and yet be robust with low computational complexity. They must also be able to detect multiple channels simultaneously. In a typical CR scenario, this will enable the CR to

quickly select the best available (vacant) channel for communication. In the blocker detection case of LTE, as mentioned previously, it would help in detecting multiple blockers at the same time.

Therefore, in this chapter, the goal is to realize a multi-rate signal processing solution for spectrum sensing, detection and subsequent identification of the exact location of channels. The most common filter banks available in the literature for multicarrier communications in CR are the polyphase discrete Fourier transform filter bank (DFTFB) and tree structured quadrature mirror filter bank (TQMFB). In multicarrier communications, filter banks are employed for channelization. In such a case, spectrum sensing can be performed with virtually no extra cost. In addition to detection, a novel multiple frequency edge estimation algorithm is proposed in this chapter.

Limited work on wideband spectrum sensing for edge frequency estimation have been documented. In [117], a wideband dual-stage spectrum sensing technique using Discrete Wavelet Transform (DWT) is proposed. It provides a Multi-Resolution Spectrum Sensing (MRSS) feature. In [57], multiscale wavelet analysis is employed to detect the spectral edges for wideband spectrum sensing. Multiband joint detection was proposed in [118]. However, all of these methods deploy wavelets on the power spectral density (PSD) of the received signal to obtain details about the spectral edges. These methods are discussed in detail and compared with the proposed method later in Section 4.6.

Wavelets are usually realized using TQMFB in most cases. This requires high sampling rates in order to characterize the entire bandwidth of the received signal. On the other hand, a polyphase DFTFB is advantageous over wavelets method as the FFT is computed at a lower sampling rate in the case of a DFTFB [50]. The main motivation of the work in this thesis is to enable spectrum sensing in CR networks, using filter banks and energy detection to aid in accurate spectrum opportunity detection.

The chapter is organized as follows. The limitations of the conventional filter bank based spectrum sensor is discussed in Section 4.2. Section 4.3 elucidates the proposed spectrum sensing scheme. Sections 4.4 and 4.5 are dedicated for design of the frequency edge estimation algorithm along with extensive simulations. The proposed

spectrum sensing scheme is compared with wavelets in Section 4.6. Synthesis results and simulation results are explained in the last sections of this chapter.

4.2. Limitations of Filter Bank based Spectrum Sensor

Spectrum sensor based on filter banks consists of an *M*-channel uniform DFTFB to split the wideband signal $r(n)$ into *M* subbands of uniform bandwidths as shown in Figure 4.1. $P_0(z)$ to $P_{M-1}(z)$ represent the polyphase components of the prototype lowpass filter (LPF). The other frequency bands are realized through modulation of the prototype filter using an *M*-point IDFT. The subbands are fed to energy detectors which consist of a power estimator that compares the estimated power with a threshold value to decide on the PU's presence in the respective band [50]. In most cases, the same DFTFB is used as the channelizer (to extract individual channels from wideband input) if the input signal channels fall into the subbands of the DFTFB. The focus in this work is on spectrum sensing and therefore channelization is not considered within the scope. A comprehensive literature survey on channelization is available in [10, 11].

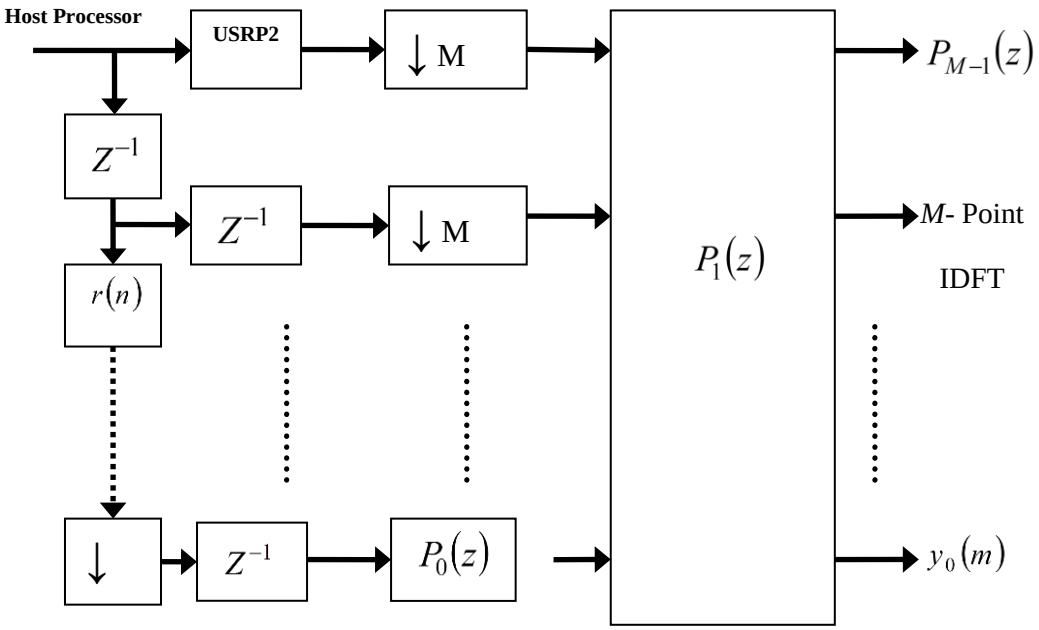

Figure 4.1. *M* -Channel DFTFB.

DFTFBs yield subbands of equal bandwidths at the output of the filter. However, in most of the communication scenarios, the channels can be of different bandwidths and

need not fit into the subband bandwidth. Figure 4.2. illustrates such a spectral scenario. The spectrum sensing resolution (width of subband) is uniform in a DFTFB, which is fixed by the passband width of the prototype LPF, and therefore, the signal channel bandwidth need not coincide with this resolution.

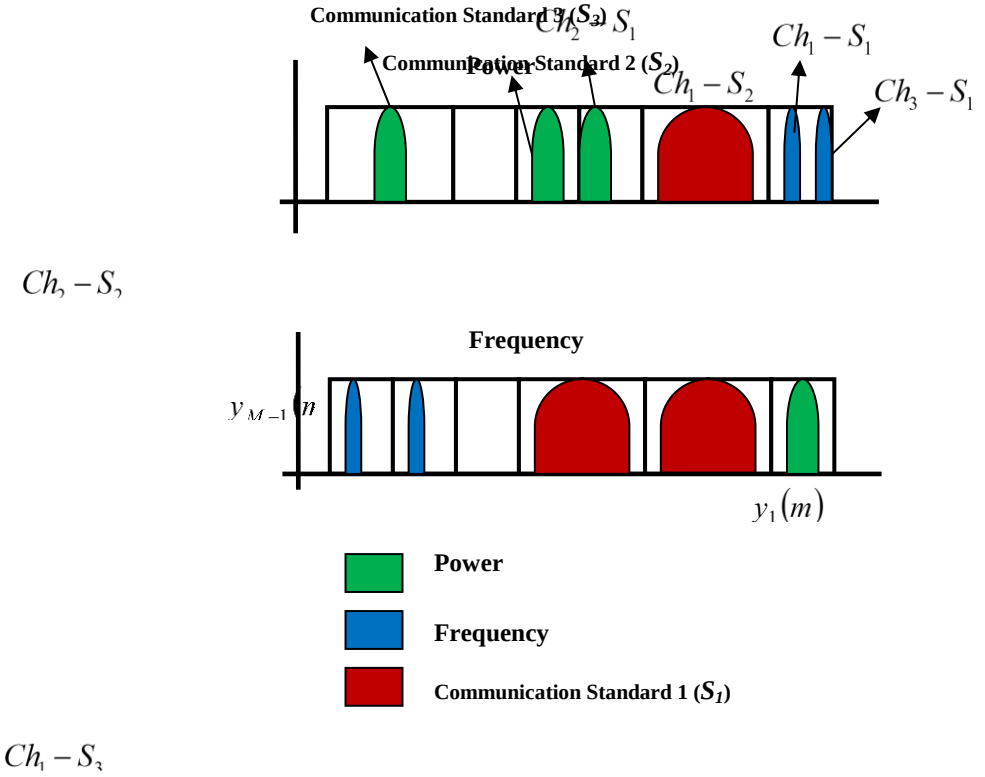

Figure 4.2. Spectral Scenario depicting the limitation of DFTFB spectrum sensor. (a) Input spectrum to a DFTFB. (b) Output spectrum as deciphered by a conventional DFTFB.

The input spectrum shown in the illustrative example of Figure 4.2(a) consists of signals of three communication standards, $S_1, S_2,$ S_3 of distinct channel bandwidths. In Figure 4.2 (a), '$Ch_x - S_y$' denotes x^{th} channel of communication standard 'y', where $y \in \{S_1, S_2, S_3\}$. Conventional single-stage DFTFB has the following limitations when it is employed for sensing the spectrum of a wideband signal that has several channels of distinct bandwidths. The first channel of S_1 (labeled as $Ch_1 - S_1$) is split into two subbands by the DFTFB, the next two channels of S_1 ($Ch_2 - S_1$ and $Ch_3 - S_1$) are spread over two adjacent subbands. Two channels of S_2 ($Ch_1 - S_2$ and $Ch_2 - S_2$) are contained inside a single subband of the DFTFB and a single channel $Ch_1 - S_3$ of the wideband

standard S_3 is divided into two parts by the DFTFB spectrum sensor. In such a case, when energy detection is done on the input spectrum, to detect the location of the channels, it errs in determining the position of channels as shown in the output spectrum of Figure 4.2(b). This results in $Ch_1 - S_1$ being mistaken as $Ch_1 - S_2$ and $Ch_2 - S_2$. In the same way, $Ch_2 - S_1$ and $Ch_3 - S_1$ maybe mistaken as $Ch_1 - S_3$ and finally $Ch_1 - S_2$ and $Ch_2 - S_2$ maybe mistaken as $Ch_1 - S_1$. One obvious way to tackle this problem is to keep the resolution of the DFTFB equal to the bandwidth of the signal channel that has the least bandwidth. However, if the output subband width of a single stage DFTFB filter is designed to match the smallest channel bandwidth, the prototype filter should be designed with a very narrow band, which in turn requires a substantially higher order filter and consequently higher complexity. In the same way, increasing the resolution in order to increase granularity will in turn increase the computational complexity, as the filter has to be designed with higher order and many subbands have to be processed in parallel.

A multi-stage DFTFB spectrum sensor can overcome these limitations and can be used to locate the spectrum holes accurately. In this context, a tree-structured discrete Fourier transform filter bank (TDFTFB) detection technique that is able to accurately estimate the channel edge frequencies of the wideband signal is proposed. In this chapter, a detailed analysis of the TDFTFB-based detection method with simulation results and over-the-air tests is presented. It is also compared with the conventional wavelets based methods [8, 9, 13, 14] for hardware complexity and detection performance. All these methods are synthesized in the field programmable gate array (FPGA) to obtain the hardware resource and power consumptions. The details of this approach are discussed in the next section.

4.3. Proposed Filter Bank based Sensing

4.3.1. Problem Formulation

The problem of detection is formulated as a binary hypothesis test as explained in Chapter 2. The propagation of the PU signal over a frequency band is assumed to be

corrupted by additive white Gaussian noise added to the symbols, which are faded. This continuous time signal is denoted as

$$r_c(t) = \alpha(t)s(t) + w(t) \tag{4.1}$$

where $r_c(t)$ is the received signal, $s(t)$ is the transmitted signal, $\alpha(t)$ represents the attenuation and phase offset to the transmitted signal due to multipath fading effects and $w(t)$ is the AWGN. Assume that the frequency band of interest BW_{in} is sampled at a sampling rate f_s, where the sampling period $T_s = 1/f_s$. The received discrete-time signal is then $r_c(n)$. According to the sensing (detection) problem, there are two hypotheses involved,

$$H_0 : r_c(n) = w(n) \tag{4.2}$$

$$H_1 : r_c(n) = \tilde{s}(n) + w(n) \tag{4.3}$$

where H_0 testifies the presence of noise alone, and H_1 testifies the presence of a signal immersed in noise. $\tilde{s}(n)$ denotes the signal samples including the effect of multipath fading effects on the transmitted signal $s(n)$, $w(n)$ is the discrete-time AWGN with zero mean and variance σ_g^2 and $\tilde{s}(n)$ can be a superposition of multiple primary user signals under fading over the specified bandwidth. It is assumed that the noise and signal are uncorrelated with each other. Therefore, the spectrum sensing hypothesis is to detect the presence of a signal against the alternative that, there is no signal present. In the proposed scheme, the received signal is processed through a multi-stage DFTFB that is specifically designed based on a few initial working conditions that are described later in this section. The tree-structured *M*-channel DFTFB (called TDFTFB) based sensing scheme is shown in Figure 4.3. Each stage of the proposed scheme consists of p_i number of *M*-channel DFTFBs where

$$p_i = M^{i-1} \tag{4.4}$$

M is a power of 2 and *i* correspond to the i^{th} stage of the analysis. At each stage, energy detection is performed on the subbands and the detection information is passed on to the next stage along with the subbands that follow the binary hypothesis test. The subbands that show the presence of a signal in the first stage are passed onto the next stage and further processing is done. The progressive nature of tree structure gives multi resolution analysis of the input spectrum as it divides the input in a dyadic manner into two or more parts.

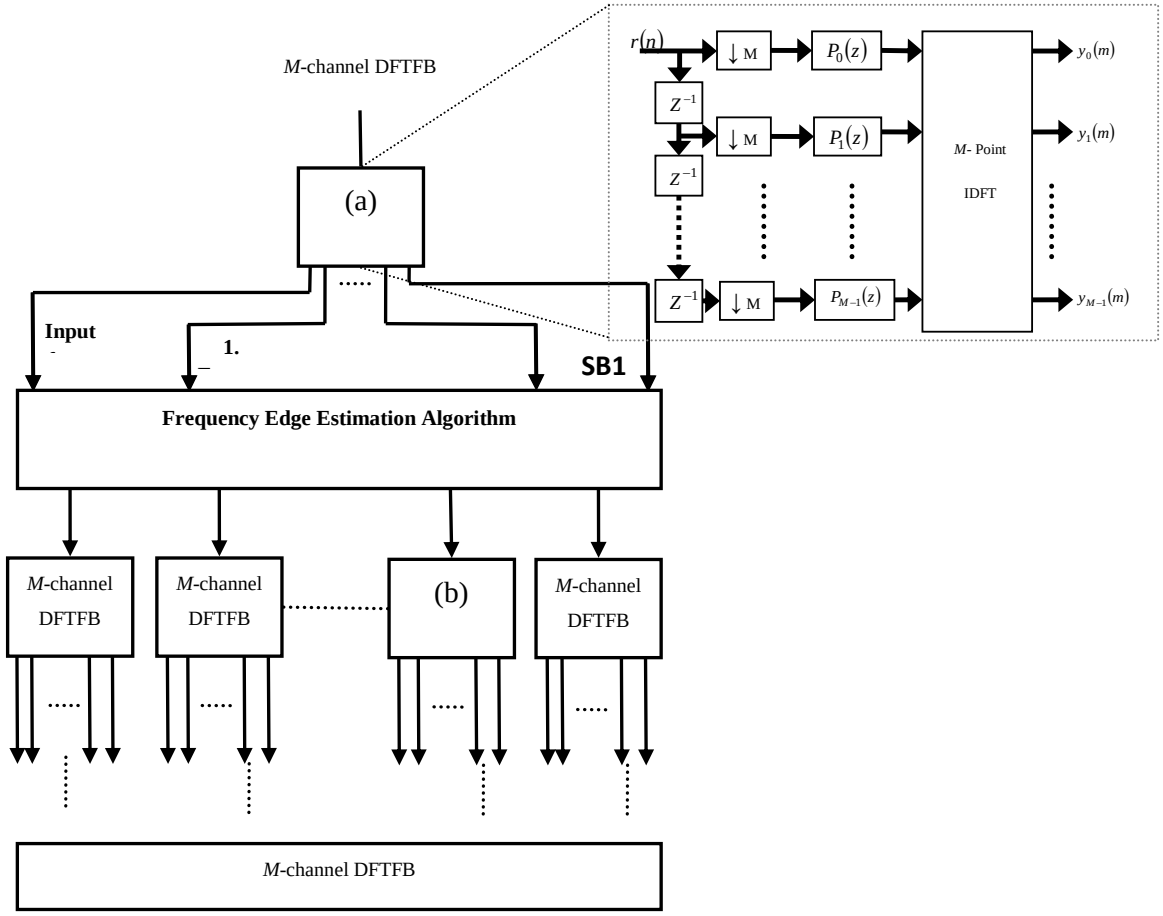

Figure 4.3. Proposed TDFTFB based sensing scheme.

The sensing granularity increases with the number of stages in the tree-structure. The detection accuracy is directly affected by the parameter *M*, which is the number of subbands of the filter bank. In order to obtain higher detection accuracy, the value of *M* must be large, which in turn will increase the computational complexity. By using a multi-stage filter bank, the computational complexity incurred in using a narrow

transition bandwidth prototype filter in the case of a conventional single stage filter bank can be reduced while the detection accuracy is increased.

The following assumptions about the signal spectrum are necessary to formulate the detection and frequency edge estimation algorithm.

1. The radio channels are of distinct bandwidths and the bandwidths of all the channels that can be present in the signal spectrum are known apriori to the receiver. However, the channel locations (center frequencies) are not known.
2. The maximum number of channels present in the signal spectrum is known.
3. The noise variance of the communication channel is known.

Thus, the objective is to determine the location of the channels by determining the edge frequencies of the channels. Conventional single-stage DFTFB based energy detector has severe constraints in achieving these tasks due to the limitations described in Section 4.2. The working conditions are derived based on the assumptions about the signal spectrum, which are used to calculate the number of subbands M in each stage and the minimum number of stages, n. The steps to determine the number of stages required for the TDFTFB are as follows:

1. Let f_{pass} and f_{stop} be the passband and stop band edges of the prototype LPF respectively. f_{pass} of the LPF is chosen such that it corresponds to the bandwidth of the widest channel among all the signals existing in the input spectrum. The rationale behind choosing this is that, the output of the first stage will directly provide channels of the signal with the largest bandwidth in the wideband spectrum. These subbands can be further processed separately, to obtain channels of smaller bandwidths.

2. The minimum number of stages, n, is chosen such that, the output subbands of the n^{th} stage of the DFTFB, have same channel bandwidth as that of the least channel bandwidth among the bandwidths of all the channels that exist in the input signal. Thus, a relation between the maximum bandwidth, the minimum bandwidth and n can be established.

3. The TDFTFB is designed such that the output of the first stage using a single DFTFB gives subbands, each of bandwidth equal to the maximum bandwidth channel existing in the input signal. Hence, for an n-stage TDFTFB, the remaining $n-1$ stages correspond to

splitting BW_{max} into finer subbands, to yield output subbands with bandwidth equal to the minimum channel bandwidth signal available in the input spectrum. An M-point DFTFB is used at all stages, which reduces the implementation complexity involved in designing different point DFTFBs.

$$\frac{BW_{\max}}{BW_{\min}} = M^{n-1} \tag{4.5}$$

The minimum number of stages, n, of M-channel TDFTFB required to obtain subbands of bandwidth BW_{min} can be obtained from equation (4.5) as follows,

$$n = 1 + \frac{\log_{10}\left(\frac{BW_{\max}}{BW_{\min}}\right)}{\log_{10}(M)} \tag{4.6}$$

The relation between the ratios of BW_{max} to BW_{min} versus n, for different values of M is shown in the Figure 4.4.

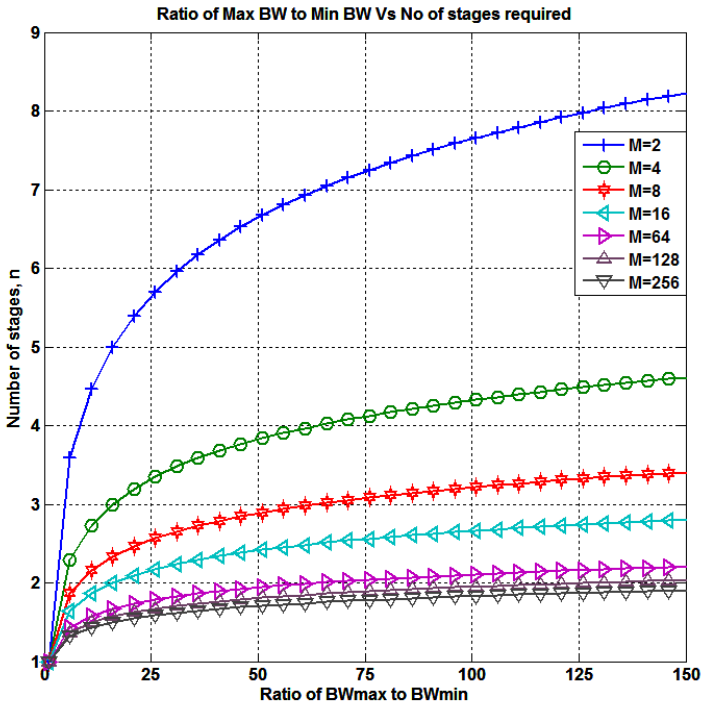

Figure 4.4. Ratios of BW_{max} to BW_{min} vs number of stages.

It can be noted that the minimum number of stages, n from equation (4.6) happens to be a real number. However, in real implementation scenario of a multi-stage filter

bank, the number of stages has to be an integer. For this purpose, $\lceil n \rceil$ is used in the proposed design, where $\lceil \ \rceil$ denotes the ceiling operation. For e.g., if $I_1 < n \leq I_2, \{I_1, I_2 \in Integers\}$, then $\lceil n \rceil = I_2$ is chosen. Furthermore, the following observations are made from Figure 4.4:

1. For a given ratio of BW_{max} to $BW_{min,}$ the number of stages required is fewer for larger values of M.

2. For larger values of M, a large change in ratio of BW_{max} to BW_{min} gives a small change in the number of stages required.

3. The slope of the plot for all the values of M is almost a straight line parallel to the "Ratio of BW_{max} to BW_{min}" axis, for higher values of ratio of BW_{max} to BW_{min} , and the increase in number of stages, is less from M=8 onwards. In some cases, the increase in number of stages is almost zero. For example, for $M > 64$, the number of stages required for a ratio of BW_{max} to BW_{min} from 100 to 125, is 2.

By having a prior knowledge about the number of PU channels, and their bandwidths, the number of stages in the filter bank can be derived using the equation (4.6). The minimum number of stages, n and resolution M can be chosen such that the complexity of the filter bank is reduced. For the same ratio of BW_{max} to BW_{min} , and number of stages, choosing a higher value of M will increase the complexity as the filter has to be designed for more parallel operations and a higher order FFT. The number of stages of the filter bank can also be kept low in order to reduce the delay in sensing. For example, consider an input signal with three channels consisting of a Personal Digital Cellular (PDC) signal (channel bandwidth 25 KHz), a WCDMA channel (5 MHz) and a GSM channel (200 KHz). Then BW_{max} is given by WCDMA signal of 5 MHz, and BW_{min} is given by the minimum bandwidth i.e. PDC channel bandwidth of 25 KHz.

The process involved in the proposed filter bank is as follows: in Stage 1, an M band DFTFB is employed to sense the spectrum. The first stage gives the output that corresponds to the signal with BW_{max}. The subbands that do not show any presence of signal are not processed further. This reduces some computations involved in not using the corresponding subbranches of the filter bank. If there are narrower band users in the

spectrum, then the detection is not precise and it is further processed in the next stage. At every stage, the values needed for estimating the spectral edge is calculated. In order to understand the working of the proposed scheme, design details and simulation results for a specific input spectral scenario are explained in the next section.

4.4. Design and Simulation Results

For simulation purposes, a spectral scenario where the input signal consists of three channels: CH1: 1.53 MHz – 3.03 MHz, CH2: 5.55 MHz - 6.12 MHz and CH3: 8.55 MHz - 11.25 MHz is considered and simulated in MATLAB/SIMULINK. The TDFTFB is simulated in MATLAB SIMULINK. The spectral power of the subbands obtained from the first stage TDFTFB is computed, and the power values are compared with a threshold to decide the presence of a channel in MATLAB. The proposed method is based on energy detection because it is simple and easy to implement. As done in conventional energy detection method, the threshold, λ, is determined based on the noise variance of the communication channel, which is assumed to be known to the receiver. The subbands with energy greater than the threshold are further processed using the next stage of the TDFTFB.

For the above example spectral scenario, BW_{max} = 2.7 MHz, and BW_{min} = 570 KHz. Therefore, the ratio of BW_{max} to BW_{min} is approximately 5. For this ratio, the value of M is decided from the plot given in Figure 4.4. The number of stages required is 2, and M =8. Thus, M is chosen as 8 as the complexity of a 2-stage 8-point DFTFB is much lower than that of a 2-stage 64-point DFTFB. The prototype filter required for the DFTFB is designed with passband edge frequency f_{pass} and the stopband edge frequency f_{stop} (normalized to 1) 0.125 and 0.127 respectively. The sampling frequency is chosen as 30 MHz. The peak pass band ripple, ∂_p and the minimum stopband attenuation, ∂_s are fixed as 0.1 dB and -60 dB respectively. The prototype filter length, L, obtained using Bellanger's formula [12] is 1312, which is substantially large because of the narrow transition bandwidth (given by f_{stop}–f_{pass}=0.002) of the prototype filter.

The bandwidth of interest is BW_{in} and the input is sampled at a sampling rate f_s such that, $f_s = 2BW_{in}$. In this specific example, f_s =30 MHz. In general, a polyphase DFTFB splits the wideband spectrum $\{0, f_s\}$ into eight subbands of uniform bandwidth as shown in Figure 4.5 where f_s is normalized to 2π. The resolution of the DFTFB is uniform throughout the wideband spectrum. In order to analyze these subbands, they are downsampled to baseband by a factor *M*. With the knowledge of the location of the original frequency of the subband analyzed and the normalized frequency of the subband analyzed at the baseband, an equation for the edge frequencies of a possible signal in the spectral region is proposed. Before the details of edge detection algorithm are presented, a detailed understanding of the working of the filter bank is elucidated here.

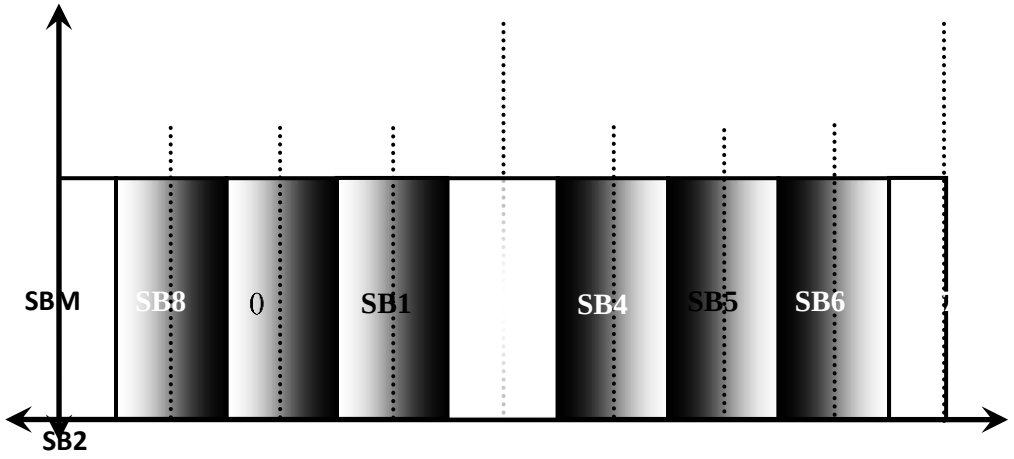

Figure 4.5. Subband splitting of a DFTFB.

In real life communications, modulation is a key component that converts the digitized data into I and Q components based on a modulation constellation. These I and Q values are complex valued for most of the modulation schemes like QAM, PSK in theory. This plays a major role in the spectrum of the transmitted signal. When the signal is transmitted, it is filtered using a pulse shaping filter and then upconverted to the desired frequency using a carrier frequency. The final transmission is performed only on the real samples of the input signal. Thus, according to the imaging property of Fourier transform, the input signal has a mirror image in the negative frequency side of the spectrum. Thus, the spectrum in the negative input frequency range of the input spectrum,

$\left\{-\frac{f_s}{2},0\right\} or \{-\pi,0\}$ and the positive input frequency range, $\left\{0,\frac{f_s}{2}\right\} or \{0,\pi\}$ are mirror images. It is evident that, in Figure 4.5, the spectrum in the region $\left\{0,\frac{f_s}{2}\right\} or \{0,\pi\}$ corresponds to the positive input frequency range and $\left\{\frac{f_s}{2}, f_s\right\} or \{\pi,2\pi\}$ corresponds to the negative input frequency range of the input spectrum and they are mirror images of each other (as it is 2π periodic). However, only the real parts of the subbands can be realized using real filters. This corresponds to the regions in $\left\{0,\frac{f_s}{2}\right\} or \{0,\pi\}$. The DFTFB performs a polyphase splitting of the subbands and an IDFT performs the shifting of prototype filters to the desired spectral regions. These spectral regions are downsampled so that the detection algorithm can be processed at the baseband. Hence, the regions of SB2, SB3, SB4 in Figure 4.5., when brought to baseband produces both a real and imaginary part, out of which only the real part can be realized. SB1 and SB5 are real valued while the remaining subbands produce complex-valued outputs based on the property of IDFT. Moreover, as a multi stage DFTFB is used; the input to the next stage of the filter bank has to be real in nature. If it is complex, additional filters have to be implemented for the imaginary portion of the signal and that would increase the number of computations exponentially. Thus, in subbands where the output is complex, only the real portion is realized and used. However, the imaginary portions are not lost and are, in essence, the real portions of the spectral regions of SB8, SB7 and SB6 respectively due to the imaging property of FFT.

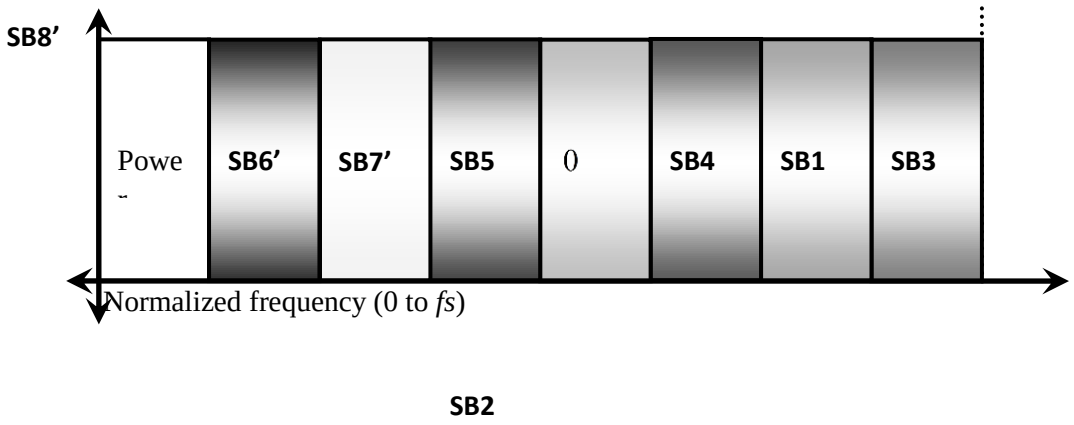

Figure 4.6. Realizable spectral region using all the subbands.

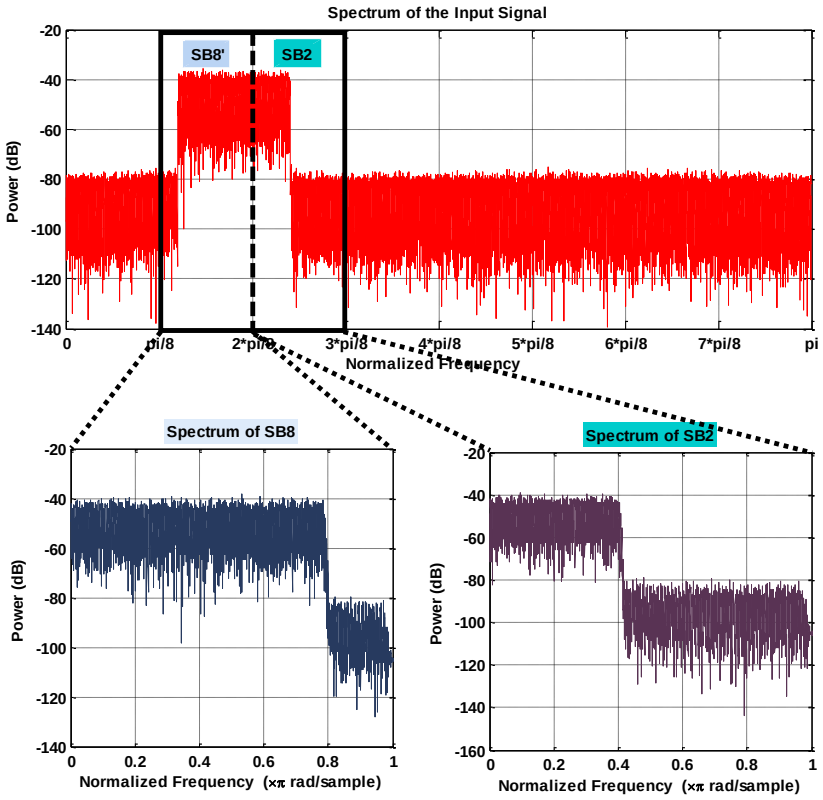

Figure 4.7. Example subband splitting using DFTFB

This is illustrated in Figure 4.6 and explained using an example spectrum in Figure 4.7. A channel exists in the region between $\left\{\frac{\pi}{8},\frac{3\pi}{8}\right\}$ as shown in Figure 4.7. This input spectrum is subjected to an 8- channel DFTFB, and the subbands SB2 and SB8 are plotted below the input spectrum graph. The realizable part of SB2 is from the region $\left\{\frac{2\pi}{8},\frac{3\pi}{8}\right\}$ of the input spectrum $\{0,\pi\}$. It is evident that the output spectrum of subband SB8 is actually the mirror image of the spectrum in the region $\left\{\frac{\pi}{8},\frac{2\pi}{8}\right\}$. In essence, a falling edge becomes a rising edge and vice-versa in the case of two-sided spectrum. An algorithm that utilizes this imaging property of FFT is proposed as an edge detection algorithm along with the multi-stage DFTFB architecture. In the spectral scenario considered for edge detection in Section 4.4., the subbands are split as shown in Figure 4.8. Thus, the real part of all the subbands are used to span the full input spectral region

as explained in the Figure 4.6. The mirrored regions are shown as SB8', SB7', SB6', and SB5' in Figure 4.8 which illustrates the concept for a test case as shown below.

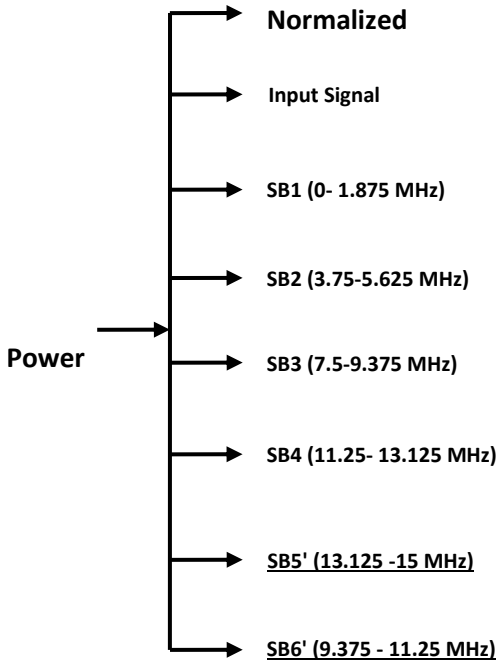

Figure 4.8. Subband splitting by the first-stage of TDFTFB.

In the next subsection, the frequency edge estimation algorithm, using the energy detection information obtained at different stages of the filter bank, is elucidated in detail.

4.5. Frequency Edge Estimation Algorithm

In order to determine the frequency edges, all the subbands undergo binary hypothesis testing based on energy detection. If the subband shows power value greater than the threshold, it is processed further to yield finer details about the subband signal in the next stage. The coarse information obtained about the energy of the subbands is used to determine the edge frequencies of the channels present in the subbands. An iterative formula to determine the edge frequencies of channels in the input spectrum is proposed in this section. At any stage, for subbands from 1 to $\frac{M}{2}$ (in this case SB1 , SB2, SB3 and SB4), due to the splitting of the input channels by the filter bank, the subband might contain either a rising edge of a channel, a falling edge of a channel or a full channel inside the subband. These values can be calculated in a blind fashion using the proposed

algorithm. The rising edge and falling edge frequencies can be easily calculated by determining the edge frequency at each stage and iterating it over the number of stages. As mentioned previously in section 4.3.1, the number of channel waveforms present in the input spectrum is assumed to be known to the receiver. A channel spanning over two or more subbands can be determined by analyzing the power spectral distribution. For the subbands from $\frac{M}{2}+1$ to M, this corresponds to the negative frequency spectrum i.e., the mirror images of the spectrum in the first four subbands. Thus, the rising edge of a channel in this spectral region is actually a falling edge in the original spectrum. Keeping in mind that this is a mirror image of the original spectrum, the equations to determine the edge frequencies are provided here. This anti-symmetry is evident from the formula for both rising edge and falling edge frequencies, ${f_{rising}}^{sb}$ and ${f_{falling}}^{sb}$ respectively.

$$\begin{aligned} {f_{rising}}^{sb} &= \sum_{i=1}^{n} \frac{f_s\left(P_i - 1\right)}{M^i} \text{ for } s_b \in \left[1, \frac{M}{2}\right] \\ &= f_s - \sum_{i=1}^{n} \frac{f_s\left(Q_i - 1\right)}{M^i} \text{ for } s_b \in \left[\frac{M}{2}+1, M\right] \end{aligned} \tag{4.7}$$

$$\begin{aligned} {f_{falling}}^{sb} &= \sum_{i=1}^{n} \frac{f_s\left(Q_i - 1\right)}{M^i} \text{ for } s_b \in \left[1, \frac{M}{2}\right] \\ &= f_s - \sum_{i=1}^{n} \frac{f_s\left(P_i - 1\right)}{M^i} \text{ for } s_b \in \left[\frac{M}{2}+1, M\right] \end{aligned} \tag{4.8}$$

where P_i is the number of all the subbands from the set {SB1, SB8, SB2, SB7, SB3, SB6, SB4, SB5} in the stage *i*, which is estimated to contain the PU signal based on the binary hypothesis. (i.e. there is at least one subband prior to this subband number, that satisfies the null hypothesis criterion in the given order); Q_i is the last number of all the subbands from the set {SB1, SB8, SB2, SB7, SB3, SB6, SB4, SB5} in the stage *i*, which is estimated to contain the PU signal (i.e., there is at least one subband after this subband number, that satisfies the null hypothesis criterion in the given order)*;* *n* is the number of stages*;* s_b is the number of subband; *M* is the number of DFTFB channels (in this case,

M=8). The algorithm to determine the edge frequency is shown in the Figure 4.9. The received signal is split into subbands and energy detection is performed. The subbands are put to binary hypothesis test and based on the likelihood of a signal, the subsequent stage is activated.

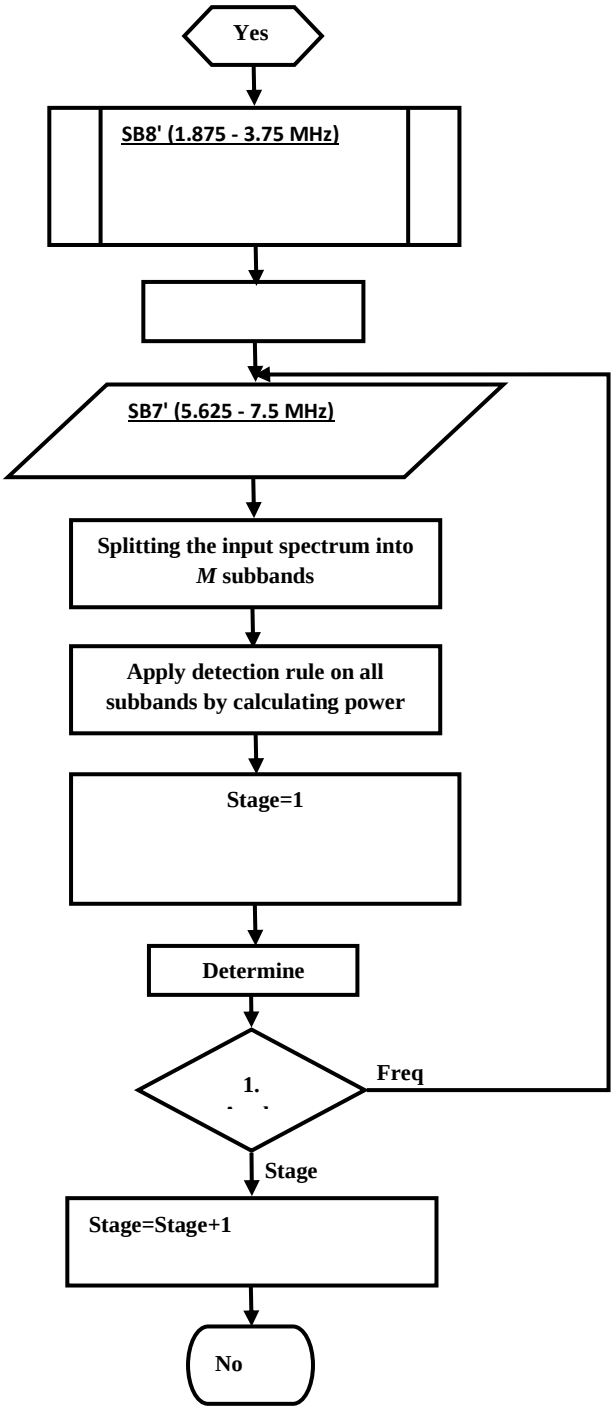

Figure 4.9. Algorithm for the edge detection process.

The values of estimated edge frequency is calculated at each stage. Using these information, after all the iterations are over, the overall estimated edge frequencies are calculated using equations (4.7) and (4.8).

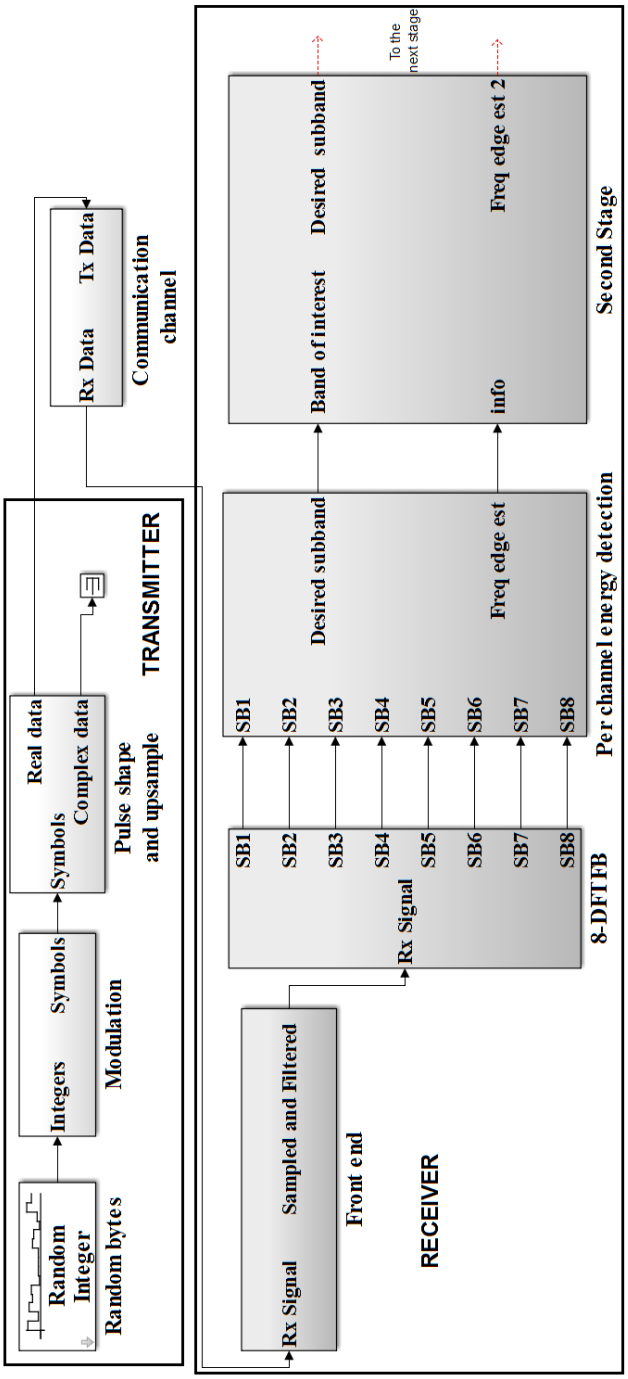

Figure 4.10. Simulation schematic of the proposed edge detection method.

The proposed scheme for edge detection, for the specific scenario considered in this work, is illustrated in Figure 4.10., which shows both the transmitter and the receiver

side. The transmitter side consists of random byte generation followed by modulation. The modulated signal is then pulse-shaped, upconverted and transmitted using a carrier signal over a communication channel. The receiver side consists of the proposed multi-stage tree structured filter bank. It consists of a receive path with an ADC sampler and a filter and the proposed TDFTFB with energy detection block at each stage. Depending on the detection information at each stage, the next stage is processed.

The simulation of the proposed system from the transmit side to the receiver side is provided in Figure 4.10. Figure 4.11 gives the underlying hardware architecture used for energy detection in this work. Energy detection is carried out by taking a mean of the magnitude-squared values of the input samples, for a specific frame length, and comparing it with a known threshold to determine the presence or absence of a channel. The input spectrum of the three channels considered for simulation in Section 4.4 is plotted in Figure 4.12.

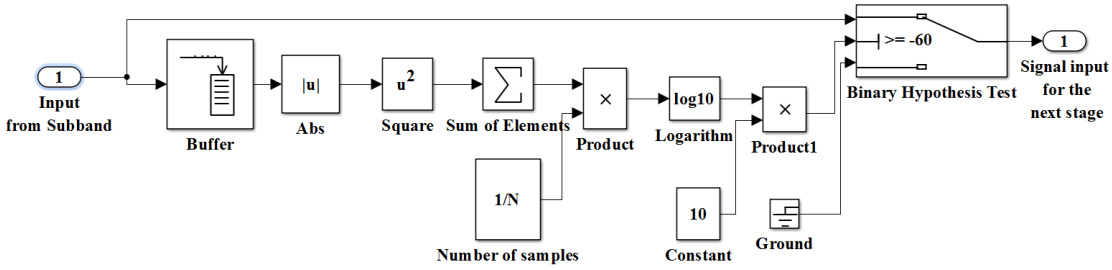

Figure 4.11. Architecture for energy detection in the edge detection process.

For simulation purposes, a spectral scenario where the input signal consists of three channels: CH1 with frequency band 1.53 MHz – 3.03 MHz, CH2: 5.55 MHz - 6.12 MHz and CH3: 8.55 MHz - 11.25 MHz is considered. The procedure to determine the edge frequency using the proposed algorithm for the input spectrum scenario considered is as follows. In the first stage of the TDFTFB, the first subband, SB1, shows power value greater than the threshold. This shows presence of a channel in this subband. In the second stage, SB1 is further split into eight subbands where the subbands 4 and 5 fail the null hypothesis test. The values of P_i*'s* and Q_i*'s* for this channel can be found out as Q_1=1, P_1=1 and Q_2=5, P_2=4. Using these values, the edge frequencies are estimated at each stage and accumulated.

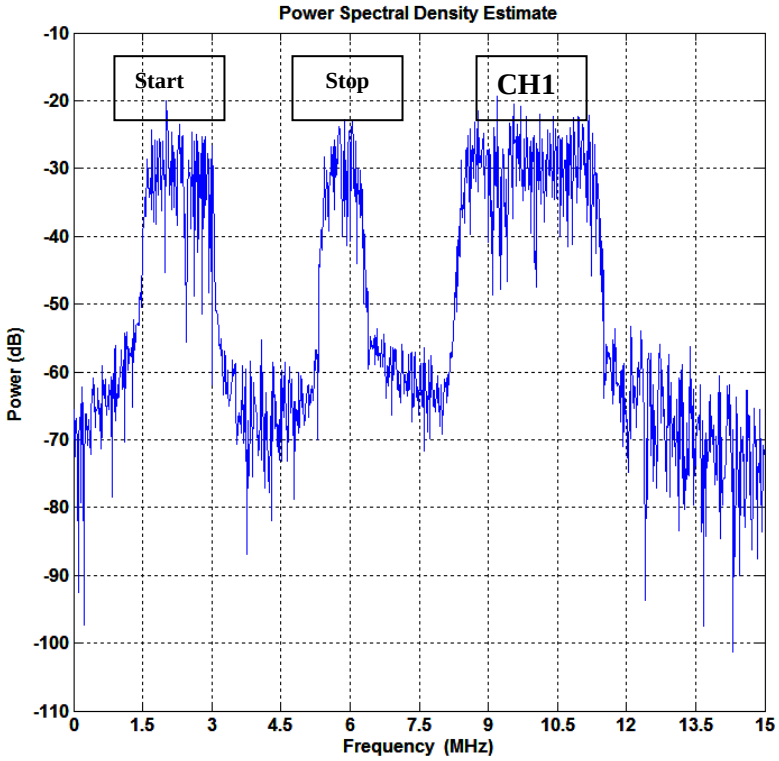

Figure 4.12. PSD of Input Spectrum showing CH1, CH2 and CH3.

The accuracy of edge estimation is dependent on the number of stages in the filter bank, *n* and the number of subbands, *M*. Figure 4.13 shows the average percentage error in calculating the edge frequencies of all the channels considered in this example, using the proposed method versus the number of stages, represented by $\log_{10}\left(\frac{BW_{\max}}{BW_{\min}}\right)$ as given in equation (4.6) for an SNR of 3 dB, for various values of *M*. SNR of 3 dB is chosen randomly.

Figure 4.13 illustrates the working of the proposed method based on its parameters, namely, the number of stages and the number of subbands in the filter bank. For a given *M*, the error in edge estimation decreases as the number of stages increases. For a given number of stages, the TDFTFB with larger *M* has lower error in frequency edge estimation.

In the next sub-section, the performance of the proposed algorithm is compared with the conventional wavelets based edge detection.

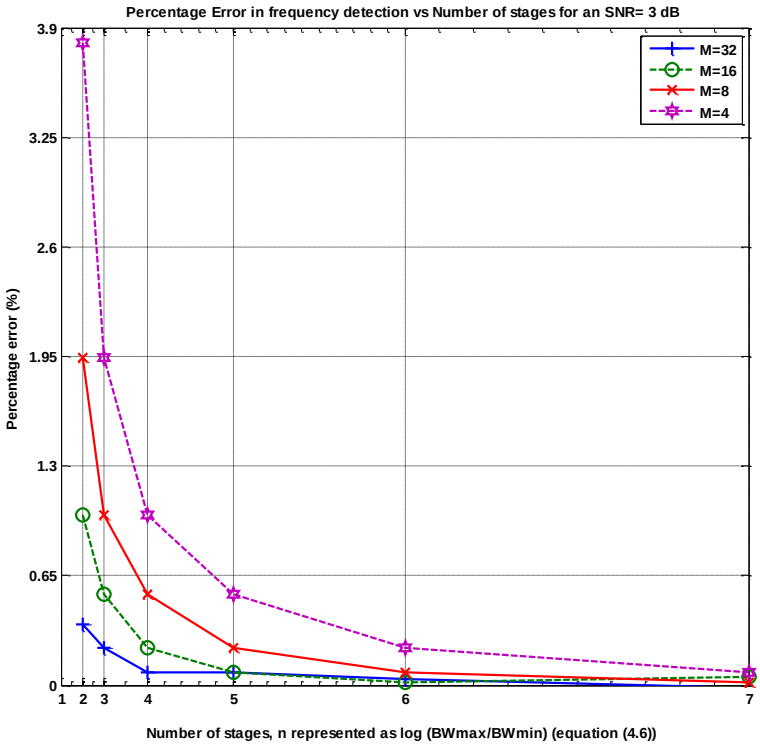

Figure 4.13. Percentage error versus number of stages, *n*, determined by $\log\left(\frac{BW_{\max}}{BW_{\min}}\right)$

4.6. Comparison with Wavelets based Edge Detection

4.6.1. Wavelets based Edge Detection

Wavelet analysis employs the approach of multi-resolution analysis, by which different frequencies are analyzed with different resolutions. The signal that needs to be analyzed is multiplied with a wavelet function to compute the transform at each segment and resolution. The wavelet functions are scaled and translated versions of the original mother wavelet function. This section presents a brief review of wavelets based edge detection [57] followed by the presented work.

Discrete Wavelet Transform (DWT) is designed for the multi-resolution analysis that decomposes the given signal space in the frequency domain into an approximate space, *V*, and detail space, *W*, as shown in equation (4.9) [57]

$$V_{j+1} = W_j \oplus V_j = W_j \oplus W_{j-1} \oplus V_{j-1} \tag{4.9}$$

where W_j is the orthogonal complement of V_j in V_{j+1} space and $\oplus$ represents the orthogonal sum of two subspaces. These two subspaces, V_j and W_j are constructed by orthonormal scaling functions, $\phi_{j,k}$, and orthonormal wavelet functions, $\psi_{j,k}$, respectively. Scaling function, $\phi_{j,k}$, and wavelet function, $\psi_{j,k}$, are obtained as

$$\phi_{j,k}(x) = 2^{j/2}\phi\left(2^j x - k\right) = \sum_l h_{l-2k}\phi_{j+1,k}(x) \tag{4.10}$$

$$\psi_{j,k}(x) = 2^{j/2}\psi\left(2^j x - k\right) = \sum_l g_{l-2k}\psi_{j+1,k}(x) \tag{4.11}$$

where $j,k = 0,\pm1,\pm2...$, j corresponds to the decomposition level of wavelet [57]. g_{l-2k} and h_{l-2k} are two sequences (filter coefficients) needed to decompose the signal. Thus, wavelet decomposition involves calculating the approximate coefficients, c, and detail coefficients, d, at the jth level and kth time, as given below

$$c_{j,k} = \sum_l h^*_{l-2k} c_{j+1,l} \tag{4.12}$$

$$d_{j,k} = \sum_l g^*_{l-2k} d_{j+1,l} \tag{4.13}$$

DWT decomposes the received signal spectrum into dyadic scale components but decomposes only the approximation space. In order to split the input spectrum into subbands of uniform bandwidth, discrete wavelets packet transform (DWPT) is used. DWPT splits both the approximation and detail space, thereby giving subbands with equal bandwidths at the output stage. In the input frequency spectrum, a frequency edge is a point where a sudden change occurs in the signal spectrum. This has an effect on the detail coefficients of the wavelets, as the details are high at an edge. However, noise can be mistakenly interpreted as a detail. The operations done at each scale of the wavelets analysis is used for detection of the edges. The working of wavelet-based spectrum sensing using multiscale products (products of the detail coefficients at different scales) and the multiscale sums method (sums of the detail coefficients at different scales) is explained in detail in next subsection.

4.6.2. Multiscale Wavelet Product and Wavelet Sums Method

In [57], a multiscale product wavelet edge detection based spectrum sensing method was proposed. The method uses wavelet-based techniques for detecting irregular edges or steps in the signal PSD as opposed to irregularities in time series. Dynamic sensing solutions are formulated based on the maxima of waveform transform modulus [119] and the peaks of multiscale products [120], which result in detection and estimation of the locations of spectral irregularities. Similarly, multiscale sums method [21, 121] were proposed as an alternative to multiscale products method. In this section, the salient features of these methods in the literature are discussed and compared with the performance of edge estimation algorithm presented in this chapter.

The multiscale wavelet product method involves, carrying out the discrete wavelet transform on the signal PSD of interest. In the PSD, the steps and irregularities at scale *j* are defined as local sharp variations. These local sharp variations form the local maxima of the wavelet modulus. These local maxima can be used to determine the edge frequencies of the channels. The desired local maxima of wavelet modulus are tracked by their propagation to multiple coarser scales, with the goal of de-noising. Such an idea of exploiting the multiscale correlation can be carried out in a direct way, giving rise to multiscale analysis techniques. Applying the method in [57] to the spectral scenario in Figure 4.12, the multiscale wavelet products can be obtained. The whole wideband signal is taken and DWPT is applied to the PSD of the input signal. A 5-level wavelet decomposition is chosen randomly to decompose the PSD of the input signal into different scales. The bandwidth of the subbands at the output stage is the same for both TDFTFB and wavelets, when five scales are considered for DWPT. Daubechies first order wavelet function is chosen as the wavelet base function [57]. The product of wavelet coefficients at various scales are taken in order to determine the edge frequencies.

The multiscale products reveal the edges and irregularities in the spectrum as shown in Figure 4.14. The multiscale wavelet product of scales 1 to 4 is denoted as P1234 and multiscale sums of scales 1 to 4 is denoted as H1234. Although Figure 4.14 shows a few edges and irregularities, not all the edges were detected.

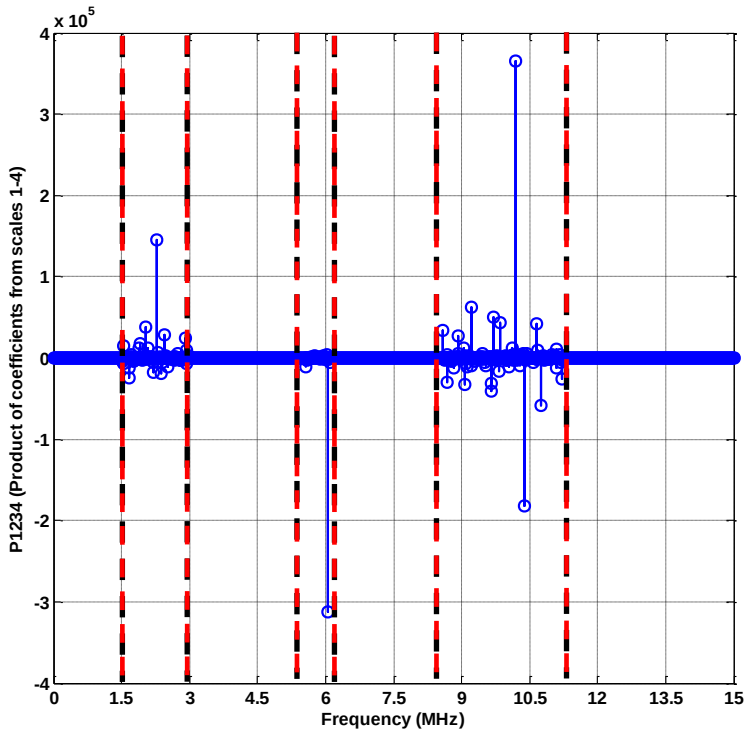

Figure 4.14. Multiscale wavelet products for scales 1 to 4 showing edges and irregularities.

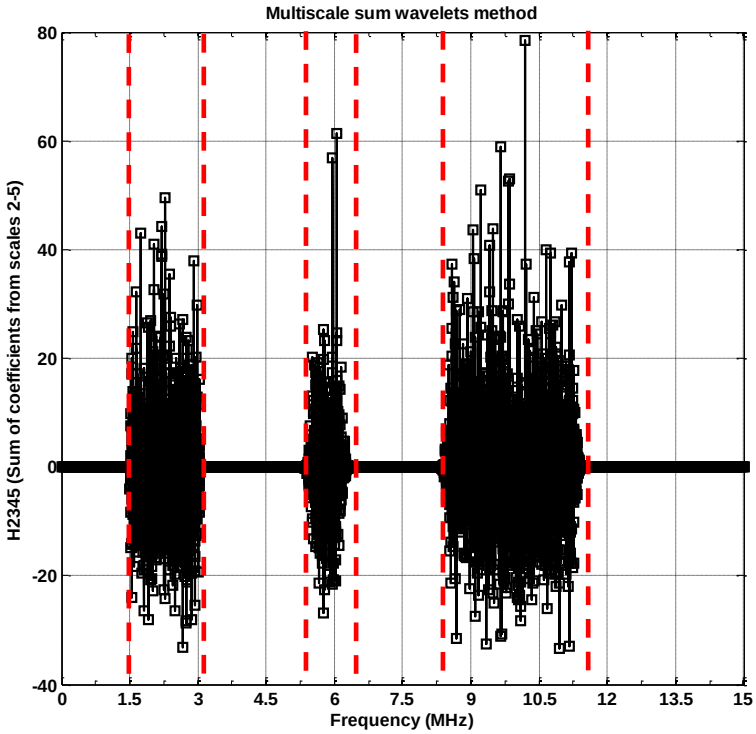

Figure 4.15. Multiscale wavelet sums for scales 2 to 5 showing edges and irregularities.

Figure 4.15 shows the plot for sum of scales method. The spectral regions that do not have any input signal, provides a sum of scales value of zero as compared to the edges. From Figure 4.14 and 4.15, it is evident that the sum of scales method is better in determining the edges in both the low and high frequency ranges when compared to the product of scales method.

The product of scales method relies on the product of the detail coefficients of all levels of the DWPT. If there is only noise present in the signal, there are no detail coefficients available for that spectral region at all levels of the dyadic analysis. Therefore, the product and sum values are zero. This is shown in Figures 4.14 and 4.15, in the regions of spectrum where there is no signal. However, when there is a mixture of noise and signal, the sum of scales method has an advantage over the product method because of its cumulative nature, at the frequency edges. Wavelet transform can be considered as the correlation between shifted and scaled versions of the mother wavelet with the signal in hand. In other words, it measures the similarity between the mother wavelet and the signal, at different spatial resolutions. Due to noise uncertainty, there are scales at which, edges at certain regions of spectrum has low value of detail coefficients. This low value is manifested when product of the scales are performed at the end of all levels, whereas it is accumulated in the sums method. Therefore, the product of scales method produces clear edges for certain portions of the spectrum (in this case, higher frequencies), whereas the sum of scales method produces clear edges for all the regions of spectrum.

The edge frequencies of the input signal using the method proposed in this chapter are estimated using the equations (4.7 and 4.8). Table 4.1 provides the comparison of the error in edge estimation for the proposed method and wavelets products and sums method for the specific spectral scenario considered. The estimation of edge frequencies is performed for 500 versions of noise added to the signal and average of the errors is calculated. The error is computed as the percentage difference in estimated edge frequency to the real edge frequency of the channel for each simulation.

TABLE 4.1. ABSOLUTE AVERAGE ERROR IN THE ESTIMATION OF EDGE FREQUENCIES OF ALL THE CHANNELS IN THE INPUT SIGNAL USING THE PROPOSED AND WAVELETS METHOD (500 SIMULATIONS).

Input channels	Multiscale wavelets Product (P2345) [57]	Multiscale wavelets Sum (H2345) [21, 121]	Proposed method (2-stage, 8 point DFTFB)
CH1	Rising edge error: 0.56% Falling edge error: 2.81%	Rising edge error: 1.23% Falling edge error: 0.73%	Rising edge error: 1.95% Falling edge error: 0.97%
CH2	Rising edge error: 1.32% Falling edge error: 0.06 %	Rising edge error: 1.78% Falling edge error: 2.23 %	Rising edge error: 1.97% Falling edge error: 1.85%
CH3	Rising edge error: 0.915% Falling edge error: 0.52%	Rising edge error: 1.25% Falling edge error: 0.38 %	Rising edge error: 1.62% Falling edge error: 0.55%
Absolute Average Error	**1.0823%**	**1.2416%**	**1.63%**

The absolute average error (average of accuracy for all 3 channels over all the edges) in detecting the edge frequencies of all the channels are calculated by finding the sharp variations in the multiscale products P1234 for the multiscale product method [61] and in H2345 for the multiscale sums method [125, 126]. It is found that the wavelets product method has an average accuracy of 98.9% for frequency edge estimation, while the wavelets multiscale sums method has an accuracy of 98.76% for the three channels considered in the design example. However, the detection accuracy is slightly less at 98.37% using the proposed method. Although the edge detection accuracy of wavelets method is slightly higher than that of the proposed method, wavelets method has following drawbacks as compared to proposed method:

1. Since the wavelet approach targets wideband spectrum sensing, it requires high sampling rate (f_s) in order to characterize the entire wide bandwidth. However, the DFTFB has the option of downsampling the signal prior to filtering as shown in Figure 4.1, which reduces the rate at which input samples are processed. Moreover, the proposed method performs FFT at a reduced rate, thereby reducing the number of computations. If $\frac{f_s}{2}$ is the rate of wavelets based methods (if it is

realized using a TQMFB), the corresponding rate for the proposed method is $\frac{f_s}{M}$, where $M > 2$ in most cases.

2. Wavelet method involves application of DWT or DWPT to the PSD of a signal. The process of obtaining PSD of a wideband spectrum alone is a computationally intensive task if the whole wideband is considered. By performing DWPT on the PSD, further inreases the complexity. In addition to this, the method exploits the idea of multiscale correlation that involves product or sum of the wavelet coefficients obtained at different scales. This is a highly intensive operation as it involves calculating the product of all the coefficients at different scales/levels of the wavelet. This requires complex multiplications in hardware.

3. Although wavelets have the advantage of obtaining multi-resolution in the spectrum, a wavelet function needs to be designed according to the signals that are to be detected, which is not feasible in real time sensing.

4.7. Over-the-Air Tests

In order to evaluate the sensing performance of the proposed scheme in a real world scenario, over-the-air tests were conducted. To capture and analyze the signals, a USRP2 board with a WBX daughter board, as explained in Chapter 3, is used. The hardware setup required to capture the signal is summarized in Table 4.2.

TABLE 4.2. HARDWARE CONFIGURATION FOR OVER-THE-AIR TESTS

Processor	Intel Pentium 2.26 GHz (Core 2 Duo), 4 GB RAM
OS	Ubuntu 10.04 LTS
GNU Radio	3.3
SDR RF hardware	USRP2
USRP Daughter boards	WBX (50 MHz to 2.2 GHz)

In the over-the-air tests, signals were sent using the signal generator with an antenna connected to its RF output and received by the USRP2 board that is connected to

the MATLAB/SIMULINK interface, where the detection is performed. The signal generator transmits the signal at known signal power level. The receiving antenna, which is connected to the USRP2, is positioned at a distance of 1-3m from the transmitting antenna. This is to ensure there is a clear line of sight for the transmitted signal to mitigate the effects of fading. This setup is shown in the Figure 4.16.

A signal with three channels consisting of a PDC, TETRA and a GSM channel is sent. The number of stages, *n* and number of subbands, *M* were calculated based on equation (4.6). The signal power was fixed at -50 dBm. In over-the-air tests, there is no control over the noise channel. The noise need not be purely AWGN and there is the effect of multipath on the transmitted signal. Although the distance between the transmitter and receiver is only 3m in the prototype, the other equipments in the room could cause interference to the receiver. Moreover, the neighboring walls and ceiling could provide multipath ways of the transmitted signal. In order to perform energy detection in such a case, there is a need for the receiver to know the noise characteristics such as variance, and noise power. These noise characteristics were estimated when no signal was sent in the desired channel and the threshold for energy detection was set. The frequency of operation chosen was 465 MHz in the TV white space region. The power spectral density of one frame of the transmitted signal is plotted in the Figure 4.17.

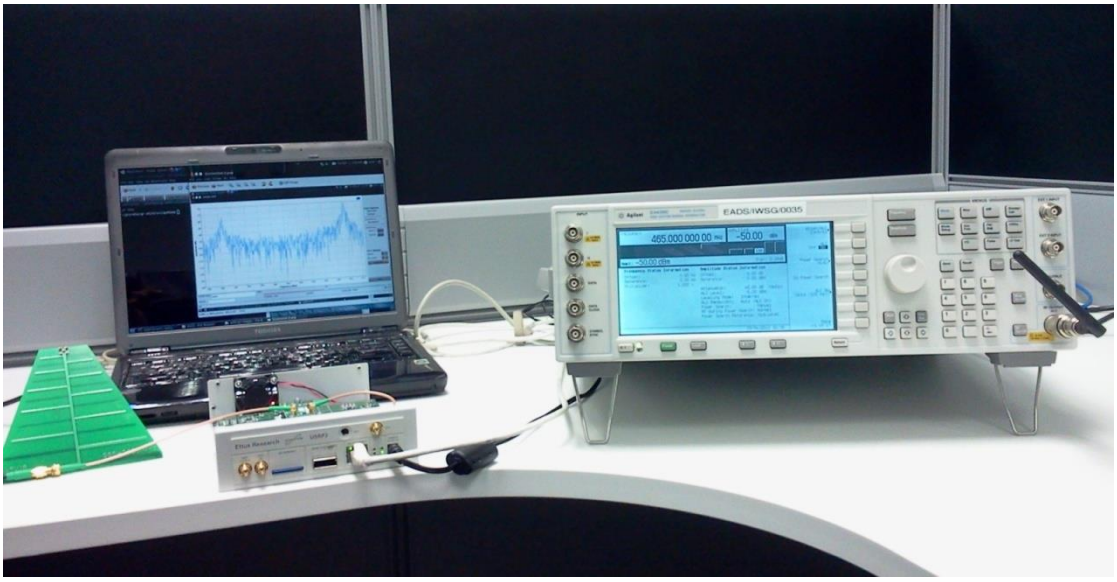

Figure 4.16. Over-the-air test setup.

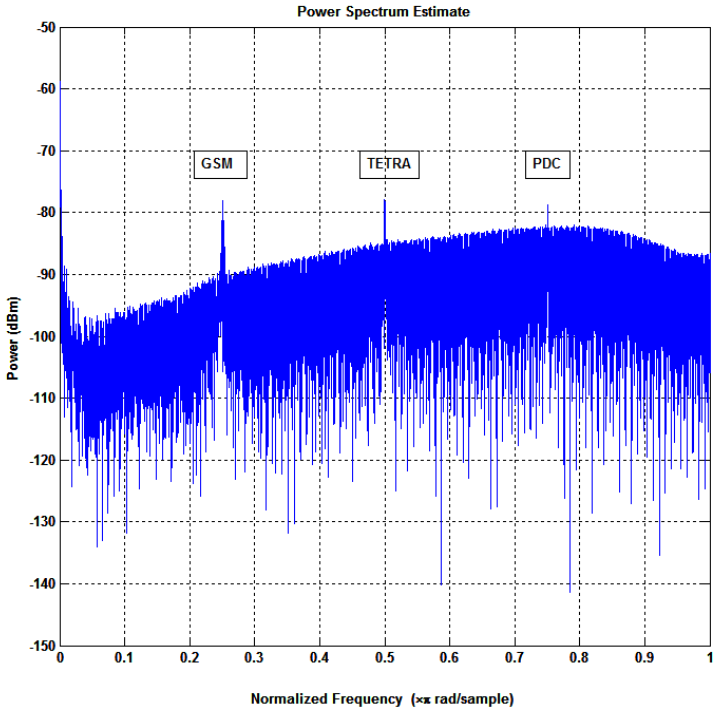

Figure 4.17. A single frame of the PSD of the signal transmitted.

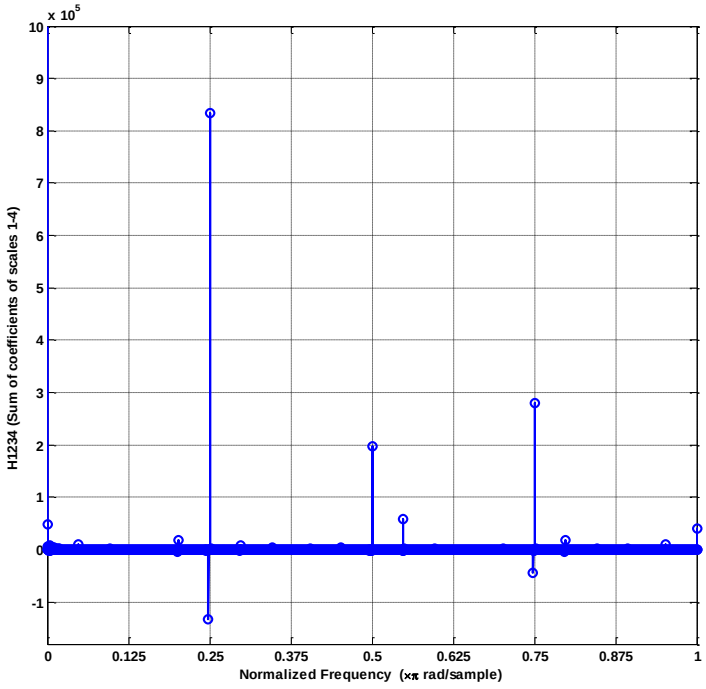

Figure 4.18. A frame of multiscale wavelet sums for scales 1 to 4.

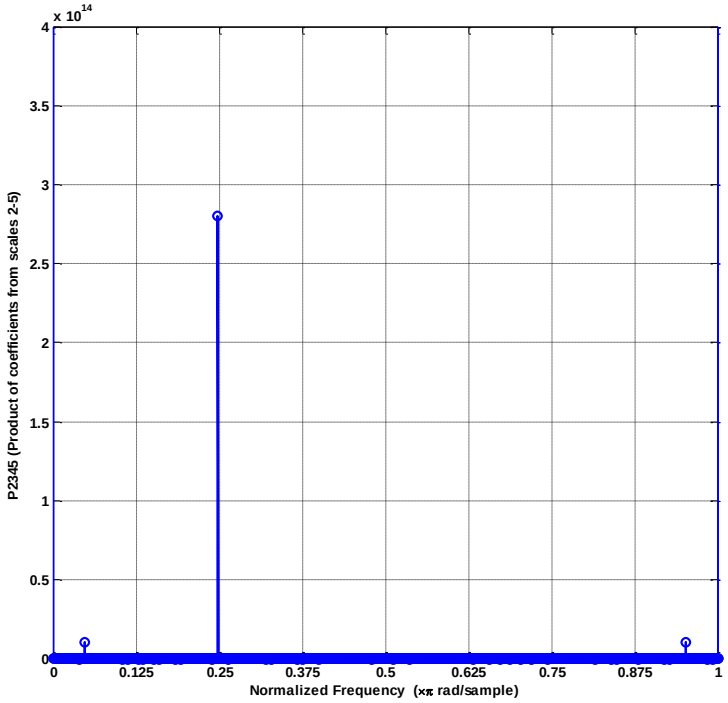

Figure 4.19. A frame of multiscale wavelet products for scales 2 to 5.

Figures 4.18 and 4.19 illustrate the working of multiscale wavelet sums method and multiscale wavelets product method applied for the input signal shown in Figure 4.17. The multiscale wavelet sums method provide a better illustration of the edges present in the input spectrum when compared to multiscale product method. This is because; the number of scales chosen for multiscale product and multiscale sum is random. Depending on the location of certain frequency bands, the irregularities shown gives an accurate match. For e.g. The P2345 in Figure 4.19 performs better for signals in low frequency range, but fails to detect the edges in the intermediate and high frequency range. The multiscale product method fails to detect edges of two other channels completely. This is mainly because of the mother wavelet chosen, which localizes only certain regions of the spectrum while providing less localization to other regions. The number of scales taken for multiscale sum and products also play a crucial role. Moreover, if the signals being analyzed are similar in pulse shape to the mother wavelet, the wavelet transform will characterize the salient properties of the signal efficiently and hence a better illustration of the estimation of frequency edges in the spectrum.

Ten versions of the same signal were transmitted and received using the USRP2 board. The proposed method determined the edges of the channels with an average accuracy of 93.83% over all the channels and simulations. The wavelets product method performed poorly, with an average accuracy of 87.67%, whereas the wavelets sums method gave a very high detection accuracy of 96.34%. This difference in accuracy mainly stems from the fact that, the wavelet scales chosen for multiscale product and multiscale sums are different. There is no clear empirical solution to select the number of scales for the wavelets method in the literature. If same scale set is used for both the methods, the performance of the products and sums method are dependent on the similarity between the mother wavelets chosen and how close the input spectrum resembles the mother wavelet function. This has been shown in [61, 125, 126].

4.8. Complexity Comparison with Wavelet Edge Detection

Multiplication is the most power consuming operation in digital filter banks. The number of real multiplications required for the proposed TDFTFB is compared with the number of multiplications required for conventional wavelets method. The complexity involved in computing the spectral energy is not accounted for in our comparison as energy detection is common for both the systems.

The complexity of a conventional single-stage DFTFB is the sum of the complexities of coefficient multiplications in the prototype filter of length L and that of the M-point DFT operation. One of the advantages of using a polyphase structure/FFT operation is that the number of samples can be reduced at the first stage to N/M. The filtering operation on the N samples of input, require $2LN$ multiplications for both the real and complex part of the signal. The DFT can be implemented using FFT algorithms and by using polyphase implementation the number of complex multiplications is $M\log(M)/2$. Thus, for a single stage DFTFB the number of multiplications, $Nmult_{DFTFB}$, is given as follows

$$Nmult_{DFTFB} = 2\left(L + \frac{M}{2}\log_2 M \right)\frac{N}{M} \tag{4.14}$$

The complexity of the proposed TDFTFB is the sum of complexities of *n* stages of DFTFB and that of the FFT operations, which can be derived as

$$Nmult_{propTDFTFB} = 2\left(L + \frac{M}{2}\log_2 M \right)N\sum_{i=1}^{n}\frac{1}{M^{i-1}} \tag{4.15}$$

The complexity of wavelets in terms of multiplications can also be calculated similarly by assuming that the length of filter and number of input samples are *L* and *N* respectively. The number of decomposition levels, *Q*, determines the complexity of the wavelets method. Assuming that a DWPT is performed, an equal subband splitting for fair comparison between the two is facilitated. The number of multiplications of the wavelets filter bank can be calculated as

$$Nmult_{wavelets} = 4L\left(N + \frac{N}{2} + ... + \frac{N}{2^Q} \right) \tag{4.16}$$

For a fair comparison between the two methods, the ratio of BW_{max} to BW_{min} is assumed to be the same. This is because, the number of stages in the proposed filter bank and the wavelets method are determined based on this factor. By controlling this parameter in both the TDFTFB and wavelets, the bandwidth of the subband in the final stage are made equal to BW_{min}. The comparison of the two methods in terms of real multiplications is presented below in the Table 4.3.

In the multiscale product method, there are extra computations in terms of real multiplications of coefficients at various scales. This is not considered while calculating the number of real multiplications for the wavelets method. Moreover, wavelet decomposition is performed on the received PSD and not on the received time samples. The real multiplications involved in calculating the PSD of the received input are also not accounted in this analysis.

TABLE 4.3. COMPARISON OF NUMBER OF REAL MULTIPLICATIONS OF THE PROPOSED METHOD AND WAVELETS BASED METHOD FOR INPUT SEQUENCE LENGTH=2048, FILTER LENGTH=40 BY VARYING THE RATIO OF BW_{MAX} TO BW_{MIN}

Ratio of BW_{max} to BW_{min}	Proposed TDFTFB	Wavelets filter bank	Percentage savings in real multiplications for the proposed TDFTFB
1	244224	503808	51.5%
3	248040	629760	60.61%
8	248100	670432	63%
13	248101	671703	63.06%

In order to obtain the complexity incurred in realizing the filter bank architecture and edge estimation alone, the above two factors were not featured in the calculations. The complexity of the wavelets filter bank alone is compared in the Table 4.3 for various scales obtained by changing the ratio of BW_{max} to BW_{min}. For a given input sample length of 2048 samples, and filter length L=40, the proposed method is 63% less complex compared to the wavelets based method for the ratio of BW_{max} to BW_{min} =13. It is established in equation (4.6) that as the ratio of the of BW_{max} to BW_{min} increases, the number of stages increases in a logarithmic fashion. Thus, for a higher increase in the ratio, there is very small increase in the number of stages. This, in turn, is reflected in the number of real multiplication savings. The complexity analysis of the proposed method and wavelets method for the given scenario, for various numbers of input samples is plotted in the Figure 4.20.

It can be noted that as the number of input samples increases, the number of real multiplications for the wavelets method increases at a faster rate than the proposed method. This is mainly because of the scaling property of the wavelets. At a given level, the filtering operation is dyadic in nature, whereas the proposed method has $M > 2$. Thus, the rate of increase of the number of multiplications with an increase in sample number is more for wavelets based method.

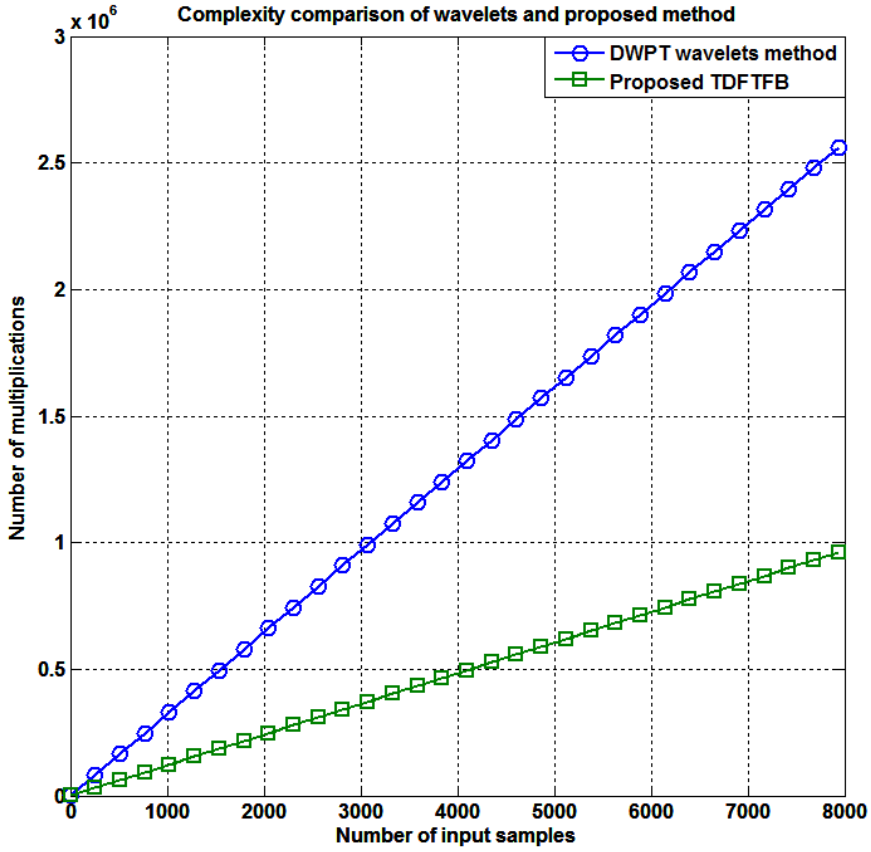

Figure 4.20. Complexity comparison of the proposed and wavelets methods (DWPT) for a ratio of BW_{max} to BW_{min} =5, for different length of input sequences, using a 40-tap filter.

4.9. Synthesis Results

The proposed filter bank and the wavelets method were synthesized on Xilinx's Virtex-5 FPGA to compare both methods in terms of hardware area occupied and power consumed. A model based design using MATLAB Simulink and Xilinx System Generator (Sys Gen) was employed for this purpose. A 2-stage 8-point TDFTFB was realized for the proposed TDFTFB method, with a 42-tap filter of coefficient word length 12 bits. For a fair comparison, a DWPT decomposition of four levels was considered. This is because, a wavelet transform splits the input frequency range (one-sided frequency range) into two subbands at each level, whereas a DFTFB splits the two-sided spectral frequency into many subbands. The implementation results are shown in the Table 4.4. The power dissipation was obtained using Xilinx XPower estimator available for calculating the power consumption of a Sys Gen implementation using Xilinx.

TABLE 4.4. COMPARISON OF HARDWARE COMPLEXITY IN TERMS OF POWER CONSUMPTION FOR THE PROPOSED METHOD AND WAVELETS METHOD WITH 42 TAPS USING A COEFFICIENT WORDLENGTH OF 12 BITS.

Parameter	Proposed TDFTFB (2-stage)	Wavelets method (4-level)
Gate Count	18517	24003
Number of Slice Registers	7979	10147
Power Dissipation (mW)	298	591

The key factor in the implementation complexity is the number of filter taps and the number of stages of the filter bank. However, as discussed earlier, the main aspect of the proposed method is to determine the edge frequencies of the PU channel, which is vital for detecting spectrum holes in cognitive radios. Therefore, for a fair comparison between wavelets and proposed method, the implementation in FPGA was verified functionally by comparing the outputs at a specific channel for both methods. It can be seen that, the power consumption of wavelets method is approximately twice that of the proposed method. The proposed method occupies 22.9% less number of slices as compared to the wavelets based method. The wavelets method is also required to operate at a higher sampling rate in order to compensate for the incoming signal at higher rate which is reduced in the proposed method due to the usage of polyphase DFTFB. This is the reason for low power consumption as compared to the wavelets method.

4.10. Summary

Spectrum sensing for cognitive radio receivers requires dynamic determination of the locations of the channels present in the input signal. In the work presented in this chapter, a computationally efficient signal processing scheme based on a tree-structured discrete Fourier transform filter bank (TDFTFB) for multiple channel spectrum sensing in cognitive radios was proposed. It finds application in latest wireless communication scenario such as LTE blocker detection and also for determining jammers in military communication. However, it performs slightly inferior for lower SNR cases, which is an

inherent limitation of energy detection. The complexity analysis showed the proposed method achieves 63% reduction in the number of computations (real multiplications) when compared with the wavelets based method for detecting the frequency edges. The design example and the simulation results showed that the proposed filter bank solves the issues due to subbands of uniform bandwidth associated with the conventional DFTFB. In addition, the proposed method is shown to determine the edge frequencies of the channels with an error of less than 2% for a specific spectral scenario with a 3 channel input using a 2 stage, 8 point TDFTFB that can be reduced further by using more stages. The percentage error plotted versus the number of stages showed that as the resolution and number of stages increases, the error decreases exponentially. The architecture was implemented on Xilinx Virtex-5 FPGA platform with a high coefficient precision of 12 bits. The design example and simulations show that the gate count resource utilization of our detection scheme is 22.9% lesser than the wavelets method at the cost of a slight degradation of 0.5% in detection accuracy. Over-the-air tests showed that the performance of the wavelets method is highly input specific, as it localizes the spectrum based on the wavelet function assumed. In our method, since energy detection is performed, the disadvantages in detection accuracy due to uncertainty in noise have to be mitigated which are handled in the next chapter.

In the next chapter, a scheme for spectrum sensing and automatic modulation classification in cognitive radios is proposed. In the present chapter, the spectrum sensing was done using energy detection which fails due to noise uncertainty and under fading. To mitigate this, spectrum sensing is done using the proposed cumulants derived using fractional lower order statistics in the next chapter. The performance of the proposed method is compared with the conventional method based on higher order statistics (HOS) for various noise conditions. It will be shown through simulations that the proposed method would perform well in both Gaussian and non-Gaussian conditions as compared to the conventional method.

Chapter 5

Fractional Lower Order and Higher Order Statistics based Signal Detection and Classification

5.1. Introduction

Signal detection and modulation classification are becoming increasingly important in a variety of wireless communication systems. One of the fields in which these algorithms are being extensively employed is that of cognitive radio networks (CRN). CRN are employed in military and public safety communications applications such as those involving dynamic spectrum management, electronic warfare and surveillance [2]. For example, in the military communications scenario, there is a need to detect intruder signals, which try to interrupt military signals. The military communication signals are often masked by a high level of chaotic environmental noise, and there is no prior information at the receiver about these intruder signals. An even more challenging scenario in military communications is that of electronic warfare; where the receiver needs to identify the modulation format employed in the signal in order to prevent further pervasive action by the intruder. In the commercial applications using CRN, the input signal consists of various communication standards and multiple channels

(frequency bands) of different bandwidths corresponding to the PUs, and it is required to identify these input signals and PUs.

In Chapter 4, the problem of detection was investigated in detail. This involved using filter banks and the method of energy detection. The objective was to determine the presence of a vacant band by detecting the frequency edges of the PU channels accurately. Several detection algorithms were formulated for detecting the frequency edges of the channels under the assumption that the channel noise is Gaussian in nature. This assumption, combined with a second-order statistics based energy detector, allowed us to derive mathematically tractable expressions for estimates of the frequency edges. However, in reality, the assumption that noise has a Gaussian distribution is not always valid. The noise present in a real communication scenario is often non-Gaussian owing to contributions from synthetic and natural electromagnetic sources, devices and equipment. Moreover, the detectors presented in Chapter 4 deteriorate in performance when faced with noise uncertainty and interference. These detectors perform poorly under highly noisy and fading conditions and cannot provide appreciable detection performance if the noise is non-Gaussian. Hence, it becomes necessary to modify the detectors in order to tackle a non-Gaussian noise environment. One of the major challenges involved in doing this, is that the radio needs to operate with limited or no prior knowledge of the signal, the fading experienced by the signal, and the distribution of the noise added in the channel.

The work in this chapter aims to develop a general solution for the problem of detection and automatic modulation classification (AMC). It develops new techniques for estimating the parameters that characterize the non-Gaussian noise process for corrupted signals under fading conditions. This chapter consists of two major parts: (i) detection of wideband spectral signals, and (ii) modulation classification of these detected signals.

In sections 5.2 and 5.3, the communication system is described, and the signal and noise models used to describe it are elaborated. The problem formulation is then laid out and some efficient existing spectrum sensing and AMC methods are elucidated. An integrated scheme for spectrum sensing and modulation classification for cognitive radios is then presented in the section 5.4. It consists of two major component blocks: a

spectrum-sensing block and an automatic modulation classification block. A test statistic for detection and classification based on (i) fractional lower order statistics (FLOS) and (ii) fourth-order cumulants, which are based on higher-order statistics is proposed. An important aspect of the design of detection and classification methods involves the selection of the detection/comparison thresholds required in the algorithm, to optimize the detection/classification method. The calculation of these thresholds are discussed and presented in detail.

In sections 5.6.2 and 5.6.3, the performance of the integrated sensing-classification scheme is evaluated using Monte Carlo simulations. The experimental details of a data acquisition system, which was set up to receive real time signals for use in this evaluation is also explained. An analysis of the characteristics of noise in the collected data is used to validate our algorithm. A channel correction algorithm to mitigate the effects of fading and improve the detection performance is presented. A feature based method for AMC of signals corrupted by non-Gaussian noise and under fading using a GLRT method is investigated in detail.

5.2. Problem Formulation

The communication channel is assumed to be corrupted by non-Gaussian noises added to the PU symbols that undergo fading. This can be described as

$$r(n) = \sum_{k=0}^{L-1} h(k) s_i(n-k) + w(n) \qquad 1 \le i \le N_M \tag{5.1}$$

where $r(n)$ is the received symbol sequence whose modulation type and symbol energy are unknown. $s_i(n)$ is the transmitted symbol sequence that corresponds to the modulation scheme m_i, among the N_M modulations to be classified which are denoted as $\{m_1, m_2, ..., m_{N_M-1}, m_{N_M}\}$. The average power of each modulation scheme is normalized to unity. $h(n)$ represents the channel coefficients corresponding to a multipath channel of

length *L*. The symbols $r(n)$ used in the equation (5.1) are of length *N* for each block of computation. $w(n)$ is the additive noise in the channel.

Most of the available literature on CR assumes the noise to be Gaussian in nature [50, 101, 122-128]. However, when the data sample size is not sufficiently large, it may not constitute a Gaussian process even in the presence of AWGN. The small sample size performance of the energy detector in AWGN is proposed in [129]. An expression to obtain the minimum number of samples required to achieve a desired probability of detection and false alarm is provided in [129]. The justification for assuming the noise to be Gaussian distributed is mainly due to the central limit theorem that states that normalized sum of any number of finite variance independent and identically distributed (i.i.d) random variables converges to a Gaussian distribution. However, CLT does not consider the addition of random variables of large variance, which are sometimes present in a real communication scenario due to interference from other equipments and devices. According to a more generalized form of CLT known as the generalized CLT, the convergence limit of a number of i.i.d random variables is a symmetric-alpha stable distribution [111, 130] and therefore it is more reasonable to use this class of distributions to model the additive noise in communication systems which can sometimes be more impulsive than the Gaussian noise. The impulsive nature of a non-Gaussian noise distribution is characterized by a statistic known as excess-Kurtosis [131]. The excess-Kurtosis for a Gaussian distribution is zero, and a distribution that has a positive excess-Kurtosis can be characterized as more impulsive than Gaussian. Due to its effectiveness in modeling systems that are corrupted by non-Gaussian impulsive noise, the class of α - stable distributions is considered. Gaussian noises are in fact, a special class of the larger class of α - stable distributions with the characteristic exponent, α=2. It is shown in [127, 132] that a complex $S\alpha S$ random variable *X* has a finite fractional lower order moment (FLOM) for $q < \alpha \leq 2$, and its fractional q^{th} order correlation sequence can be defined as

$$\langle X_n, X_m \rangle = E\left(X_n * X_m^{\,q-1}\right) \tag{5.2}$$

where $\langle X_n, X_m \rangle$ is the expression for autocorrelation of time shifted sequences of random variable X and $E(\ )$ is the statistical expectation, and * denotes the convolution operation. It can be seen that, for q = 2, equation (5.2) gives autocorrelation sequence of the random variable X. In the literature, the FLOS based algorithms have been proven to be robust for impulsive, as well as Gaussian noise [110, 130]. The FLOS based analysis can tackle a broader class of noise and handles interference robustly [111, 127]. For the noise models in our work, the PDF of two generalized noises are explained in the next subsections.

5.2.1. Generalized Gaussian (GG) distribution

The PDF of a generalized Gaussian (GG) random variable of unit variance, parameterized by the parameter ρ , is given by

$$q_{GG}(z) = \alpha(\rho)\exp\left\{-\beta(\rho)|z|^{\rho}\right\}, \rho > 0 \tag{5.3}$$

where $\alpha(\rho) = \frac{\rho\sqrt{\gamma(3/\rho)}}{2\sqrt{(\gamma(1/\rho))^3}}$, $\beta(\rho) = \rho\sqrt{\left(\frac{\gamma(3/\rho)}{\gamma(1/\rho)}\right)^{\rho}}$ and $\gamma(\ )$ the Gamma function. As the parameter ρ is decreased, the impulsiveness of the noise in GG distribution increases monotonically.

5.2.2. Cauchy-Gaussian Mixture (CGM) distribution

Though the *SαS* distributions can suitably be used to model the channel noise in our work, these distributions have a difficulty in terms of mathematical usability. This comes from the fact that there exist closed form expressions for the probability density functions (PDFs) of only two types of *SαS* noise - Cauchy noise and Gaussian noise. Hence, an ingenious way to model *SαS* involves using a mixture distribution of these two types of noise. This mixture distribution, called the CGM distribution, is a mixture of Cauchy and Gaussian noise PDFs. It is used as an approximation to the broader class of

symmetric alpha stable (*SαS*) processes as given in [111, 127]. The PDF consists of two parameters α and β and is given as

$$q_{CGM}(z) = \alpha \frac{\sqrt{2}\beta}{\pi\left(\beta^2 + 2z^2\right)} + (1-\alpha)\frac{1}{\beta\sqrt{2\pi}} e^{-\left(\frac{z^2}{2\beta^2}\right)}, 0 \le \alpha < 1, \beta > 0 \tag{5.4}$$

where α is the mixture parameter, and β corresponds to the scale parameter, which is a measure of dispersion of *SαS* distributions, equivalent to variance of Gaussian noise. As α is increased, the impulsiveness of the CGM distribution increases. However, CGM has a tail heavier than that of a GG PDF and decays algebraically [111]. Hence, the GG model is chosen for the simulations and analysis of the proposed detector and classifier.

5.3. Problem Definition and Previous Works

The sensing (detection) problem involves testing between the two hypotheses:

$$H_0 : r(n) = w(n) \tag{5.5}$$

$$H_1 : r(n) = s_i(n) + w(n) \tag{5.6}$$

where H_0 testifies the presence of noise alone, and H_1 testifies the presence of a signal (among the N_M signal modulations considered) immersed in noise. The decision on presence of a signal is carried out using a test based on a statistic. In this thesis work, FLOS based cumulants are proposed as the decision statistic for both detection and classification. In the next subsection, automatic modulation classification methods are discussed.

5.3.1. Automatic Modulation Classification Methods

Based on the classification theory, there are *M* modulations to be classified, which are denoted as $\{m_1, m_2, ..., m_{N_M-1}, m_{N_M}\}$. The probability of correct classification is formulated as

$$P_{cc} = \sum_{i=1}^{N_M} P\left(m_i \middle| m_i\right) P_{m_i} \tag{5.7}$$

where P_{m_i} is the probability of modulation type m_i which is equal to $1/M$ since all modulation types are equally likely. A confusion matrix is used for quantifying the performance of the classifier in this thesis work. AMC is broadly classified into two major methods- decision-theoretic methods and pattern recognition methods [133-136]. Decision-theoretic approach generally uses likelihood based detectors (LBD) [124], whereas pattern recognition methods use feature based detectors (FBD) [125]. According to LBD methods, AMC is considered as a multiple hypothesis problem. LBD methods are based on the idea that all the information required for classification is present in the PDF of the received waveform.

Depending on the mathematical model for the unknown quantities, the major techniques which have been presented in the literature to tackle the problem are: (i) average likelihood ratio test (ALRT), (ii) generalized likelihood ratio test (GLRT), (iii) hybrid likelihood ratio test (HLRT), (iv) quasi ALRT and (v) quasi HLRT [133-136]. ALRT based methods are those which treat the unknown quantities as random variables with certain PDFs. If the chosen PDF is the same as the true PDF, the ALRT results in an optimal classifier in the Bayesian sense. On the other hand, the GLRT based approach deals with the unknown parameters by treating them as deterministic unknowns. This approach uses ML to estimate the unknown parameters (in the case when an optimal detector does not exist). Both these methods have some relative advantages and disadvantages. ALRT involves a multidimensional integration, whereas GLRT involves a multidimensional maximization. ALRT is rendered impractical because of the difficulty in performing a multidimensional integration for a large number of unknown quantities and the need for prior knowledge about the PDFs. Alternatively, in GLRT, maximization over the various data symbols might lead to incorrect classification, as the determined value of the likelihood function might be same for the case of nested signal constellations, for example 16-QAM and 32-QAM. However, averaging over the unknown data symbols in HLRT has been shown to mitigate this problem of GLRT [128]. On the other hand, in

the FBD approach, the AMC extracts key features necessary for classification from the received signal and determines the modulation type of the transmitted signal based on those features extracted, using a decision rule. In the literature, available examples of features that are used for classification include the variance of the centered normalized signal amplitude, phase and frequency [102], the variance of the zero-crossing interval [137], the variance of the magnitude of the signal wavelet transform after peak removal [138], and cyclic cumulants, based on HOS up to eighth-order [125]. FBD based methods are non-optimal but very easy to implement and can achieve higher performance than LBD methods. In order to utilize the advantages of both these methods, a feature-based generalized likelihood test for detection and classification is proposed in this chapter. The proposed scheme along with the algorithms is described in detail in the next section.

5.4. Proposed Scheme for Spectrum Sensing and Automatic Modulation Classification

The proposed scheme for spectrum sensing and automatic modulation classification in cognitive radio is shown in the Figure 5.1.

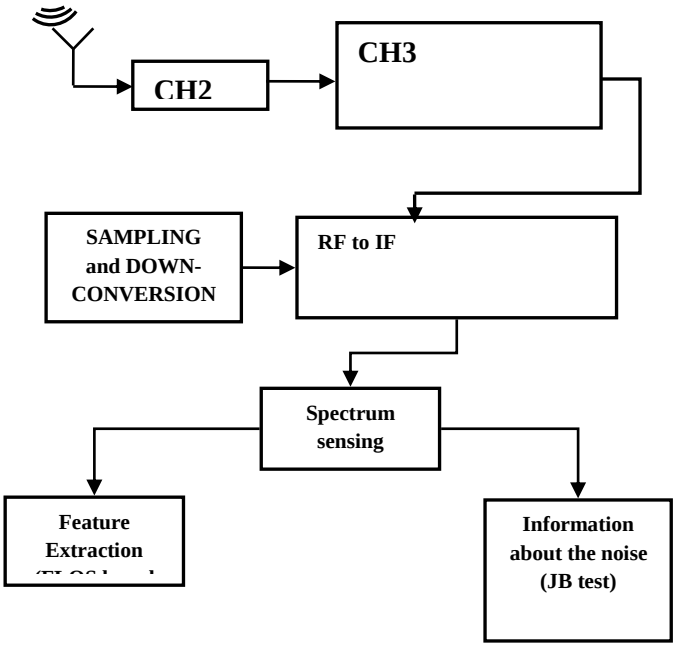

Figure 5.1. Proposed scheme for spectrum sensing and modulation classification in a typical CR scenario.

The CR scans a wideband signal and the desired band is down converted and digitized to the baseband for processing. The proposed method assumes that the CR has prior knowledge of the frequency band of interest and the bandwidth. The unknown parameters are the presence/absence of the signal and the modulation scheme. The required features are extracted from the received signal in the feature extraction block using the proposed algorithm based on FLOS and cumulants. The feature extraction block obtains information about the noise characteristics from another block which performs a Jarque-Bera (JB) test [139] frequently (for example, the analysis of noise can be done every time the CR detects the presence of a vacant band). Depending on the application of the CR, the band of interest is then detected for presence of a signal or detected for a specific modulation using the automatic modulation classification (AMC) block. This AMC block performs classification of the received signal into a known modulation type. This aspect of the proposed scheme can be used for applications where there is an absolute necessity to determine the modulation scheme of the received signal. The proposed method for detecting FLOS based cumulants is discussed in the following subsection.

5.4.1. Estimation of FLOS based Cumulants for the Received Signal

The proposed method is based on fourth order cumulants as a test statistic for detection and a key feature for classification. Cumulants are used as HOS features to describe the characteristics of a signal, defined in [140]. According to the properties of higher order statistics [126], a typical zero-lag, 4^{th} order, 2^{nd} conjugate cumulant and a 2^{nd} order, 1^{st} conjugate of a sequence s are denoted as $C_{42}(s)$ and $C_{21}(s)$ respectively. The original normalized fourth order cumulants is defined as [126] [140]

$$C_{n42}(s)=\frac{C_{42}(s)}{\left(C_{21}(s)\right)^2}=\frac{\frac{\sum_{n=1}^{N}|s(n)|^4}{N}-\frac{\left|\sum_{n=1}^{N}s^2(n)\right|^2}{N^2}-2\left\{\frac{\sum_{n=1}^{N}|s(n)|^2}{N}\right\}^2}{\left\{\frac{\sum_{n=1}^{N}|s(n)|^2}{N}\right\}^2} \tag{5.8}$$

In this work, a modification to the original fourth order cumulants is proposed by combining FLOS and HOS (equations (5.2) and (5.8) respectively denote the statistical expression for FLOS and HOS). In the proposed method, each integer order moment in the cumulant expression (for e.g., $C_{21}(x)\equiv cum\left(x,x^*\right)=E\left(|x|^2\right)$) is replaced by its FLOM. For a zero-lag system, the expression for q^{th} order FLOM can be derived from equation (5.2) as $E\left(|X|^q\right)$. Hence, $C_{21_p}(x)\equiv cum\left(x^p,x^{p*}\right)=E\left(|x|^{2p}\right)$. This method is applied for all the integer higher order moments and the final test statistic is derived as shown below

$$\hat{C}_{n42_p}(s)=\frac{C_{42}(s)_{FLOS}}{\left(C_{21}(s)_{FLOS}\right)^2}=\frac{\frac{\sum_{n=1}^{N}|s(n)|^{4p}}{N}-\frac{\left|\sum_{n=1}^{N}s^2(n)\right|^{2p}}{N^2}-2\left\{\frac{\sum_{n=1}^{N}|s(n)|^{2p}}{N}\right\}^2}{\left\{\frac{\sum_{n=1}^{N}|s(n)|^{2p}}{N}\right\}^2} \tag{5.9}$$

where p is the fractional component. A good estimate of equation (5.9) is the cumulant value of the received signal (given in equation (5.1)), which is given by

$$\hat{C}_{n42_p}(r)=\frac{\frac{\sum_{n=1}^{N}|r(n)|^{4p}}{N}-\frac{\left|\sum_{n=1}^{N}r^2(n)\right|^{2p}}{N^2}-2\left\{\frac{\sum_{n=1}^{N}|r(n)|^{2p}}{N}\right\}^2}{\left\{\frac{\sum_{n=1}^{N}|r(n)|^{2p}}{N}\right\}^2} \tag{5.10}$$

Equation (5.10) is used as the test statistic for spectrum sensing in order to determine the presence of a PU signal. The justification for combining FLOS in cumulants is with the objective to make the sensing method more robust to different noise conditions. It is already shown in the literature that the estimation variances of FLOS moments are small compared to the variances of the higher order moments [141]. Moreover, by incorporating FLOS, the proposed method can handle noises that are additive non-Gaussian in nature. This motivated us to develop the spectrum sensing algorithm and the AMC using the proposed FLOS based cumulants. In the next sub-section, the method to calculate the threshold for the proposed method is discussed.

5.4.2. Threshold Analysis

The theoretical values of normalized cumulants based on FLOS (given in equation 5.10) are calculated for various values of *p* for different modulations and simulated in Figure 5.2.

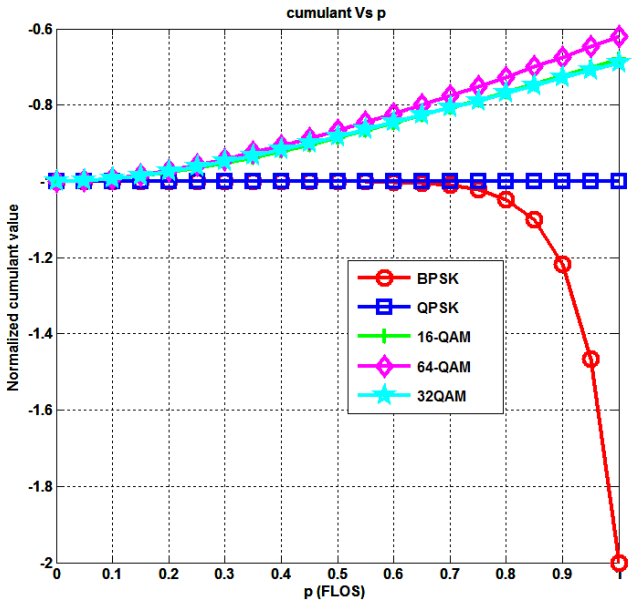

Figure 5.2. Normalized theoretical cumulant value vs p for various modulation schemes.

In this thesis, the theoretical values of FLOS based cumulant for Gaussian and impulsive noises are plotted in Figure 5.3. A large sample set of 75000 was taken in order to reduce the error due to smaller sample size (thereby forcing the simulated value as

close to the theoretical value as possible). The impulsive noises were generated using the GG distribution based on equation (5.3). From Figure 5.2, it can be deduced that the 16-QAM, 32-QAM and 64-QAM have similar fourth order cumulants and hence will not be distinguishable in extremely noisy and fading conditions. This can affect the performance of the classifier. By comparing Figure 5.2 and Figure 5.3, it is noted that the proposed cumulant value for some known modulation schemes is negative, whereas, the noise has positive value. This difference is used to sense the spectrum to determine the presence of signals. Moreover, as the impulsiveness of the noise increases, the value of cumulants increases exponentially. This property of FLOS improves the performance of the proposed method in non-Gaussian scenarios, as compared to other methods. The histogram of a typical non-Gaussian noise used (p=0.9) is plotted in Figure 5.4.

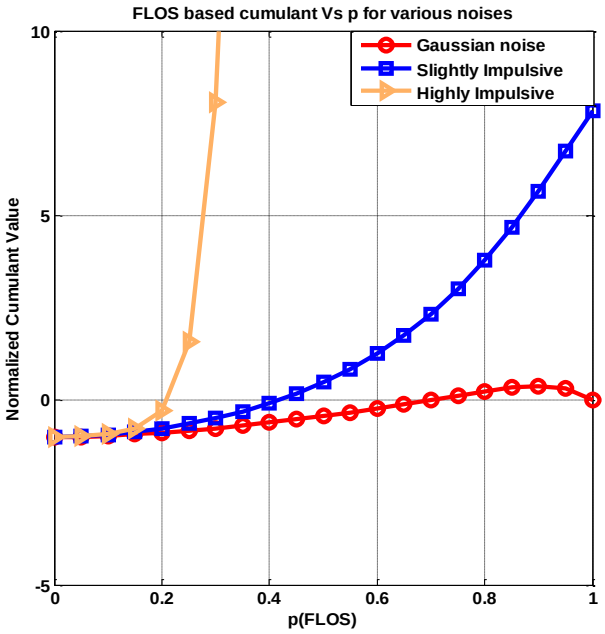

Figure 5.3. Normalized theoretical cumulant value vs p for various noises.

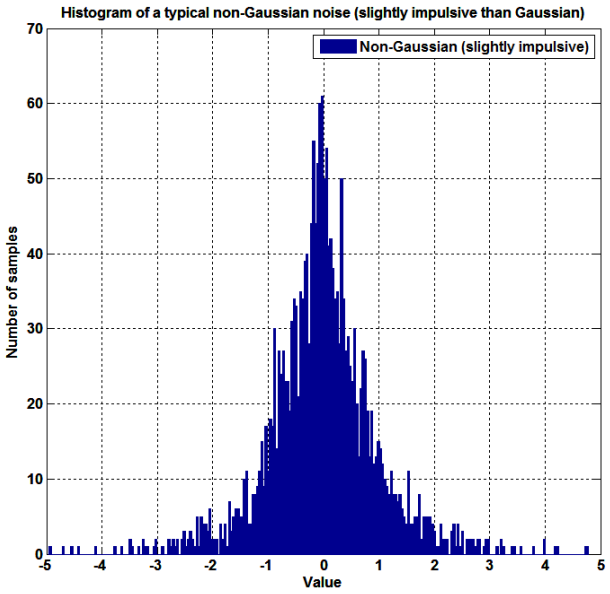

Figure 5.4. Histogram of a typical non-Gaussian noise (slightly impulsive than Gaussian with p=0.9).

In addition to the noise being non-Gaussian in nature, in real world communications, the transmitted signal is also deteriorated by fading. The effect of fading on the cumulant estimate must be considered in order to provide better classification probability in the case of fading conditions. Rayleigh multipath fading is considered as a reasonable model for fading in mobile environment when there is no clear line of sight between source and receiver. In this method, the signal is assumed to be affected by Rayleigh multipath fading.

Rayleigh fading is based on a Rayleigh distribution which is composed of complex random numbers whose real and imaginary parts (R_r and R_i respectively) are i.i.d zero mean Gaussian variables. The Rayleigh PDF is given by

$$f\left(R;\sigma_R\right)=\frac{R}{{\sigma_R}^2}\exp\left(\frac{-R^2}{2{\sigma_R}^2}\right) \tag{5.11}$$

where $R\in[0,\infty)$ is the rayleigh fading component, $R=\sqrt{{R_r}^2+{R_i}^2}$ and σ_R is the mode of the distribution. For Rayleigh fading, the raw moments are given by [23]:

$$E\left(|R|^k\right) = 2^{\frac{k}{2}} {\sigma_R}^k \gamma\left(k + \frac{1}{2}\right) \tag{5.12}$$

When the signal is affected by fading, all the moments estimated for the signal are multiplied with a degrading factor, which severely affects the classification probability. Hence, by calculating the sample moments for Rayleigh fading and using that as a compensating factor in the estimated cumulants of the receiver, the performance of classifier can be greatly improved which is shown later in this chapter. The channel filter coefficients consist of values from the distribution *R*. Since the signal and fading are independent of each other, all the fractional order moments of the received signal $r(n)$ can be written as

$$E\left(|r(n)|^k\right) = E\left(|s(n) * h(n)|^k\right) = E\left(|s(n)|^k\right) * E\left(|R|^k\right) \tag{5.13}$$

By incorporating the effect of Rayleigh fading in the original test-statistic (equation (5.10)), an estimate of the moments of the transmitted signal can be obtained by calculating the moments on the received signal. Thus, the expression for the estimate of each of the moments calculated in the cumulant expression given in (5.9) can be obtained as

$$\hat{E}\left(|r(n)|^k\right) = \frac{E\left(|r(n)|^k\right)}{E\left(|R|^k\right)} \tag{5.14}$$

$E\left(|R|^k\right)$ is calculated numerically using the PDF for Rayleigh fading and used when channel correction has to be done.

5.5. Proposed scheme using FLOS based Cumulants

Spectrum sensing is done based on the two hypotheses as discussed in the Section 5.3. The FLOS based cumulant is applied for an estimated value of *p* and compared with the theoretical value. However, there is a need to determine the nature of the noise present in the communication channel. For this purpose, a goodness of fit test to determine

whether the received noise is Gaussian in nature, is incorporated. The Jarque-Bera (JB) test is a two-sided goodness-of-fit measure used to determine the deviation from normality [139]. It is a statistic based on the sample kurtosis and the sample skewness. The test statistic, γ_{JB} is defined as

$$\gamma_{JB} = \frac{n_s}{6}\left(S^2 + \frac{(K-3)^2}{4} \right) \tag{5.15}$$

where S is the sample skewness, K is the sample kurtosis and n_s is the number of observations. S and K are computed as

$$S \equiv \frac{\mu_3}{\sigma^3} = \frac{\frac{1}{n_s}\sum_{i=1}^{n_s}(X_i - \bar{X})^3}{\left(\frac{1}{n_s}\sum_{i=1}^{n_s}(X_i - \bar{X})^2 \right)^{3/2}} \tag{5.16}$$

$$K \equiv \frac{\mu_4}{\sigma^4} = \frac{\frac{1}{n_s}\sum_{i=1}^{n_s}(X_i - \bar{X})^4}{\left(\frac{1}{n_s}\sum_{i=1}^{n_s}(X_i - \bar{X})^2 \right)^{2}} \tag{5.17}$$

where μ_3 and μ_4 are the estimates of the third and fourth central moments, respectively; $X_i, i = 1, 2...n_s$ are the observations; $\bar{X}$ is the sample mean and σ^2 is the estimate of the second central moment or the variance. The JB test performs a binary hypothesis test. It tests the hypothesis that the samples of a distribution follow a normal distribution with unknown mean and variance, against the alternative hypothesis that the samples do not follow a normal distribution. This test is suitable when the parameters of an unknown distribution are to be estimated and the Gaussianity of the distribution needs to be determined. The value of the γ_{JB} increases as the impulsive nature of the noise increases. When the γ_{JB} in equation (5.15) is greater than a critical value, the null hypothesis is rejected at a given significance level. The critical values can be calculated from the chi-square distribution table with two degrees of freedom for a given significance level since the JB test statistic is a chi-square random variable with two degrees of freedom. The

performance of the proposed sensing scheme is shown later in the simulations section of this chapter.

An FBD based method to determine the modulation of the received signal is also proposed. The strategy of any modulation classification algorithm is to maximize the likelihood function among the multiple hypotheses created for the multiple modulation schemes. However, the likelihood functions are determined using the assumption that the noise is Gaussian. In this chapter, this is performed by calculating the minimum distance between the estimated cumulants and the normalized cumulants. This method is easy to implement and yields good results. The steps to perform the detection and classification using the proposed method are as follows.

1. Use the JB goodness of fit test to determine the type of noise present in the system. This can be done by frequently collecting large number of samples for testing in the required frequency band. The frequency of such an operation can be determined by the service provider, considering the confidence interval of the previous goodness of fit tests carried out. Depending on the application for which the CR is used, the frequency band of interest is known to the receiver. If the JB test concludes that noise is approximately Gaussian, use *p=1*. If not, use the JB statistic value and compare it with the critical value to determine whether the noise is slightly or highly impulsive than Gaussian. This gives a qualitative knowledge of the noise present in the signal spectrum. The parameter *p* can be estimated by the maximum likelihood estimation (MLE) method, described as follows. The PDF of a GG random variable of unit variance with parameter *p* is given in (5.3) as

$$q_{GG}\left(w(1)...w(N), p\right) = \alpha(p)\exp\left\{-\beta(p)\sum_{n=1}^{N}\left|w(n)\right|^{p}\right\}, p>0 \qquad (5.18)$$

where $\alpha(p)$ and $\beta(p)$ are defined already. Given the *N* noise samples *w*(1), *w*(2)…*w*(*N*), the maximum likelihood estimate of *p* is found by maximizing the likelihood function i.e.

$$p_{est} = \arg\max_p \left[\alpha(p) \exp\left\{ -\beta(p) \sum_{n=1}^{N} |w(n)|^p \right\} \right] \tag{5.19}$$

The expression in the brackets in (5.19) can be replaced by its logarithm, as logarithm is a monotonically increasing function

$$p_{est} = \arg\max_p \left[\log(\alpha(p)) - \beta(p) \sum_{n=1}^{N} |w(n)|^p \right] \tag{5.20}$$

2. Estimate the FLOS based cumulant of the received symbols using equation (5.10) alone and also by incorporating equation (5.14) in (5.10) for the estimated value of *p*. (Ideally *p* =1 for Gaussian noise and as the value of *p* decreases the impulsiveness of the noise increases).

3. Determine the threshold for spectrum sensing, λ, which is defined as the midpoint between the highest value of proposed FLOS based cumulants in the modulation set (in this case 64-QAM has the highest value) and the noise. The theoretical value of the proposed cumulants for noise can be obtained for the estimated value of *p* from the Figure 5.3.

4. Perform spectrum sensing by comparing the value of the estimated cumulant against λ. If $\hat{C}_{n42p}(r) > \lambda$, it is concluded that the spectrum contains only noise, else it is concluded that there is signal present in the system. (Note: Most of the known signals discussed in this chapter have a negative cumulant value, whereas the noises (impulsive and Gaussian) have positive value for the cumulants, which can be used for classification.)

5. Perform AMC, to classify the received data into known modulation schemes. This is done by computing the mean square distance between the estimated cumulant value and the theoretical cumulant value for the entire modulation scheme in the set and choosing the modulation scheme closest to the estimated cumulant value (i.e., has minimum Euclidian distance). It is represented as

$$\text{mod} = \arg\min_i d_i \tag{5.21}$$

where $d_i = \left|\hat{C}_{n42_p}(r) - C_{n42_p}(s)_i\right|^2$ represents the distance between the estimated cumulant value of the received signal and the normalized cumulant value of the i-th modulation scheme in the modulation set considered, $C_{n42_p}(s)_i$ is the proposed theoretical cumulant value of the i-th modulation scheme and 'mod' gives the modulation scheme from the modulation set, that has the minimum distance with the received signal based on the estimated distance.

In the following section, the experimental setup and simulation results along with performance comparisons of the proposed method in various noises are given. The experimental setup includes real time data acquisition which shows that the noise in a wireless communication system cannot be modeled purely as Gaussian, due to smaller sample size, interference from other equipments, and other factors such as the terrain and communication channel.

5.6. Simulations and Results

5.6.1. Setup for Data Acquisition

In order to capture and analyze the signals, a USRP2 board with a WBX daughter board as described in Chapter 3 has been used. The details of the experimental setup are summarized in Table 5.1 below.

TABLE 5.1 HARDWARE CONFIGURATION FOR LABORATORY SETUP

Processor	Intel Pentium 2.26 GHz (Core 2 Duo), 4 GB RAM
OS	Ubuntu 10.04 LTS
GNU Radio	3.3 or later
SDR RF hardware	USRP2
USRP Daughter boards	WBX

The test setup consists of a WBX daughter board antenna, connected to a USRP2 board, which is connected to a host computer through a high-speed Ethernet cable. The framework provided by the GNU Radio project is used to integrate the USRP2 board with the host computer. The signals are captured from the wireless environment and passed on to the host computer as I & Q values (In-phase and Quadrature). The signal data flow is shown in Figure 5.5 and the experimental setup is shown in Figure 5.6.

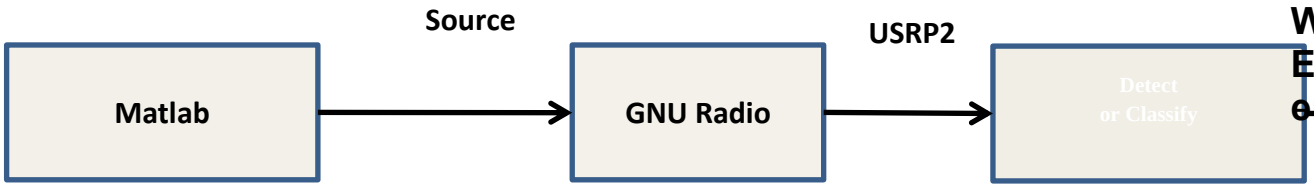

Figure 5.5. USRP2 Signal data flow.

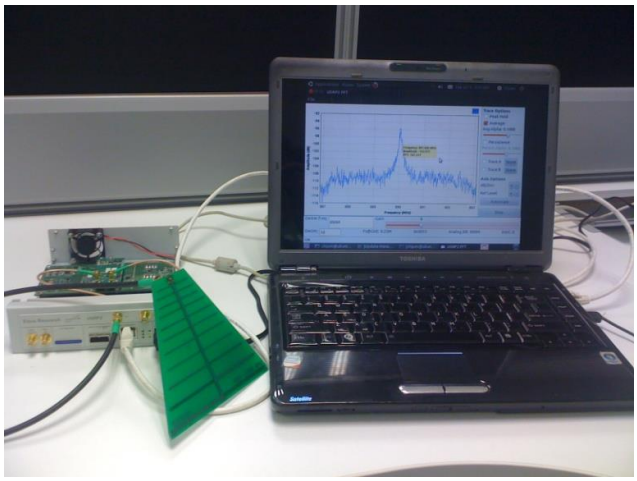

Figure 5.6. USRP2 Radio setup to capture signals.

The captured spectrum can be used to verify the assumption that the noise present in the real communication channel need not be purely Gaussian. This is performed using the JB test as discussed previously. It is also clear from the figures that the noise floor is different in different frequency bands, and this serves as a major challenge in sensing and classification methods. The laboratory setup was used to capture signals at various known frequency ranges to analyze the characteristics of the noise in the region. In order to determine the noise characteristics present in various frequency bands, JB test is performed on each of the signals received. Figure 5.7 shows the presence of non-Gaussian additive noise behavior in certain regions of signal

spectrum captured from the wireless environment. The results of the test are elucidated in Table 5.2.

TABLE 5.2 COMPARISON OF THE NOISE CHARACTERISTICS IN VARIOUS FREQUENCY BANDS

Center Frequency	Critical value (5% significance level) (N=2048)	JB test statistic	Type of noise estimated
891 MHz	5.9641	7.2551	Non Gaussian
1.5 GHz	5.9641	6.1568	Non Gaussian
1.6 GHz	5.9641	4.3380	Gaussian
1.8 GHz	5.9641	4.5441	Gaussian
2.1 GHz	5.9641	5.6884	Gaussian

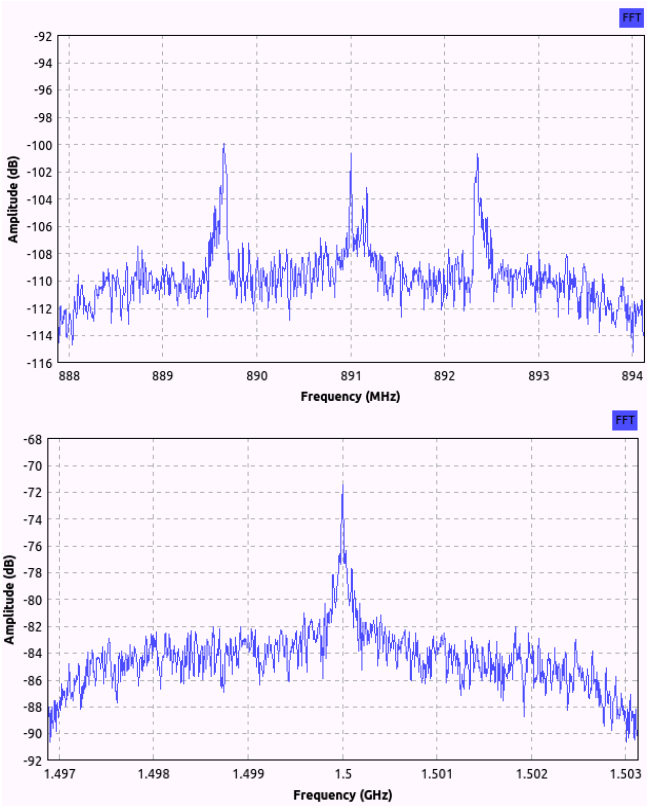

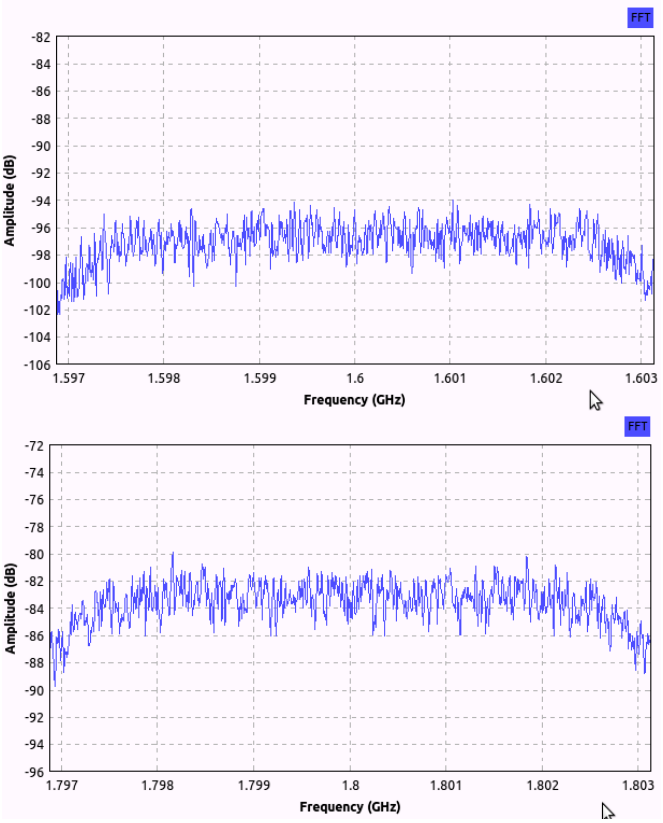

Figure 5.7. Received spectrum at different frequency bands.

Table 5.2 shows the instances where a specific band may contain the presence of an additive non-Gaussian noise. Since the value of JB test statistic is more than the critical value, the noise present in these bands are slightly impulsive than the Gaussian noise. These experiments justify the usage of a generalized Gaussian process and FLOS in our proposed method. The various noise samples collected can be used to calculate the impulsiveness parameter p in the communication channel using maximum likelihood estimation of p as described previously.

5.6.2. Performance Analysis of the Spectrum Sensing Method

In this subsection, the proposed spectrum sensing method is evaluated for performance comparison with the existing HOS method in different noise conditions. The threshold λ required for spectrum sensing is chosen as the midpoint of the value between the highest theoretical cumulant among the modulation set (64-QAM) and the cumulant value of noise. For example, if $p=0.9$, the threshold value is -0.1493. By performing sensing as suggested previously in this chapter, the performance characteristics of the

proposed sensing method in Gaussian and in non-Gaussian noise (which is more impulsive than AWGN) can be obtained. The performance of the detection algorithm can be measured with the probability of detection. P_d is the probability of detecting a signal on the required frequency when it is present in the data. Thus a large detection probability indicates better performance. In order to compute the P_d, the PDF of the decision statistic under both hypotheses in (5.5) and (5.6) needs to be determined. 3000 Monte Carlo simulations with 2048 received symbols in each trial are taken to calculate the detection probability.The proposed method is compared with the conventional HOS method for performance in the presence of AWGN and non-Gaussian (slightly impulsive and highly impulsive) noise based on the P_d as shown in Figure 5.8-5.10 respectively. In the AWGN case, the proposed method outperforms the conventional HOS method for a generalized SNR > -12 dB as shown below.

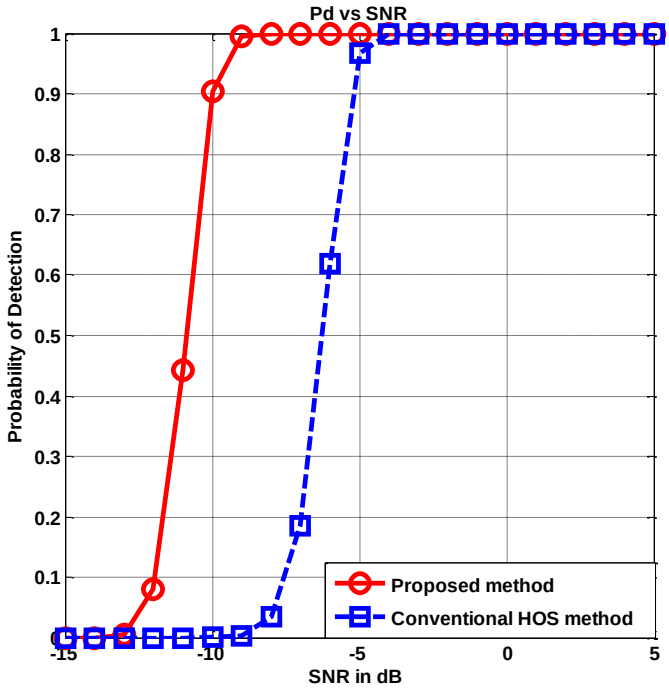

Figure 5.8. Comparison of probability of detection vs SNR in AWGN (p=1) for the proposed and conventional HOS method.

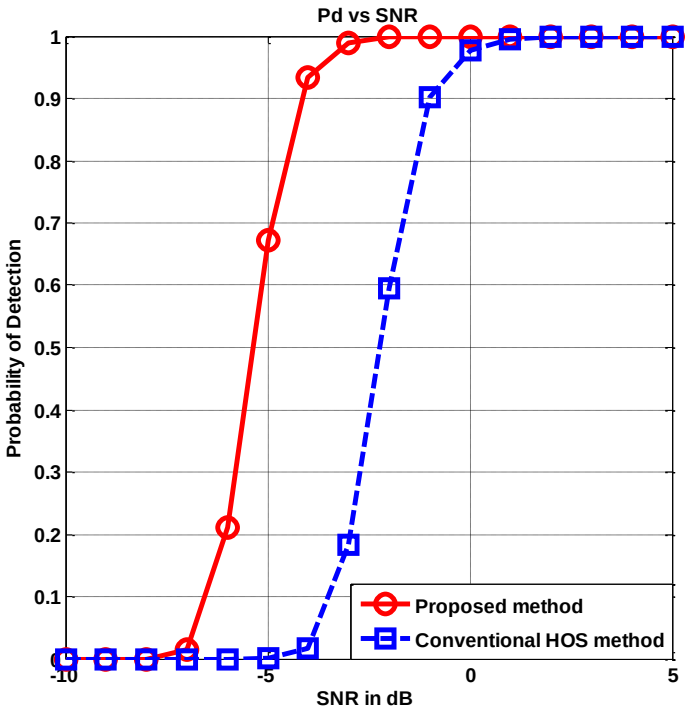

Figure 5.9. Comparison of probability of detection vs SNR in slightly impulsive noise (p=0.9) for the proposed and conventional HOS method.

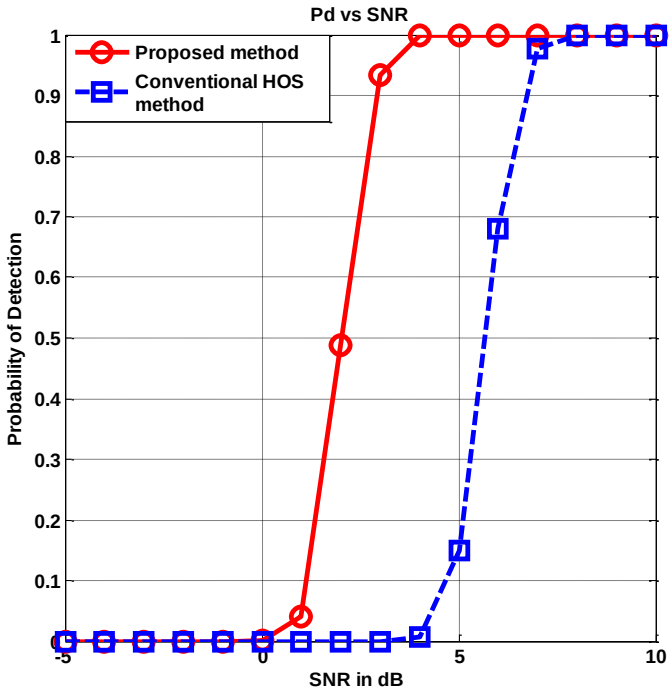

Figure 5.10. Comparison of probability of detection vs SNR in highly impulsive noise (p=0.7) for the proposed and conventional HOS method.

When the noise is non-Gaussian, the proposed method performs better than the conventional HOS method for SNR> -8 dB. But it is evident from these plots that the overall performance of both detectors deteriorate when the noise is more impulsive than Gaussian, as compared to the case when the noise is Gaussian. This is because impulsive noise affects the performance of any classifier due to the presence of spurious outlier values. These high variance variables add to the overall error in detection that is reflected as a poorer detection probability when compared with the Gaussian case. This deterioration is even more profound, as shown in the Figure 5.10, when the noise present is highly impulsive in nature. The performance of our sensing method is better than the conventional HOS method in various noise scenarios considered. The flooring of the detection curves in the plots is mainly because, under low SNR conditions, in order to get a clear detection probability, the number of symbols considered must be very large according to the CLT.

5.6.3. Performance Analysis of the AMC Method

In this subsection, the proposed AMC method is evaluated using Monte Carlo simulations for classification accuracy. P_{cc} is given in equation (5.7). Comparison of probability of classification versus SNR for the proposed and conventional HOS method in [126] in slightly impulsive noise (p=0.9) and highly impulsive noise (p=0.7) are shown in Figure 5.11 and 5.12 respectively. The proposed FLOS based cumulants method performs as well as the conventional HOS method [126] in the case of a noise slightly impulsive than Gaussian noise. The proposed method has a slightly higher P_{cc} for SNRs less than 14 dB and slightly lower for SNRs from 14 dB to 18 dB when compared with the conventional HOS method. It is illustrated through simulations that both the P_{cc} curves converge at an SNR of 20 dB in Figure 5.11.

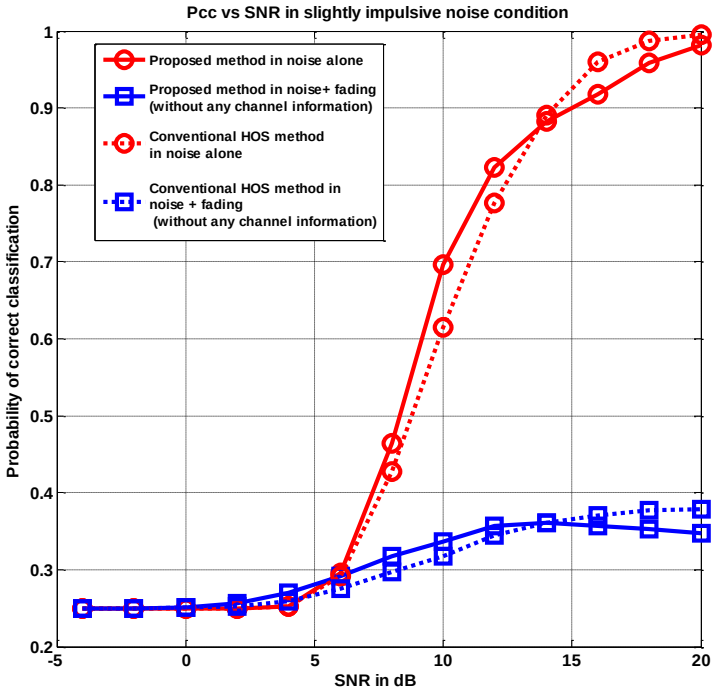

Figure 5.11. Comparison of probability of classification vs SNR in slightly impulsive noise (p=0.9) for the proposed and conventional HOS method in [126].

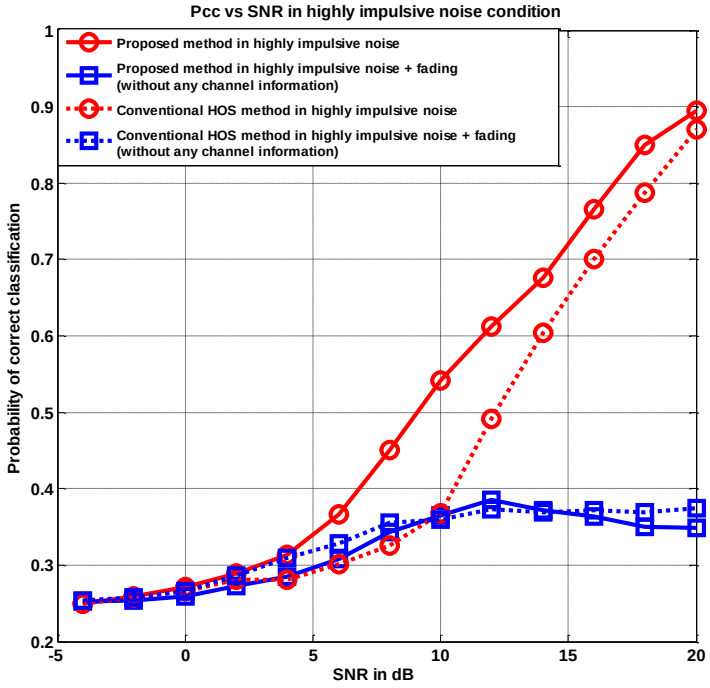

Figure 5.12. Comparison of probability of classification vs SNR in highly impulsive noise (p=0.7) for the proposed and conventional HOS method in [126].

Figure 5.12 shows that the performance of the FLOS based cumulant for highly impulsive noise is better than the conventional fourth-order cumulants [126] for SNRs ranging from 0 dB to 20 dB. This difference in the performance of the proposed method for slightly and highly impulsive noise conditions is mainly because the convergence of the proposed FLOS based cumulants method is different for different values of *p*, and depends on the value of the fractional order *p*. The convergence properties of functions involving fractional lower order moments are considered out of scope of this thesis work. The performance of the proposed method is identical to that of the conventional method in the case of a signal immersed in AWGN noise (*p*=1).

For analyzing the proposed AMC method in AWGN and fading, the confusion matrix is obtained in the presence of AWGN and fading. This is given by the conditional probability $P(m_i \mid m_i)$, where m_i is the i-th modulation scheme in the modulation candidate set. The selection of candidate set and the highest order modulation scheme puts a theoretical limit on the classification probability attainable.

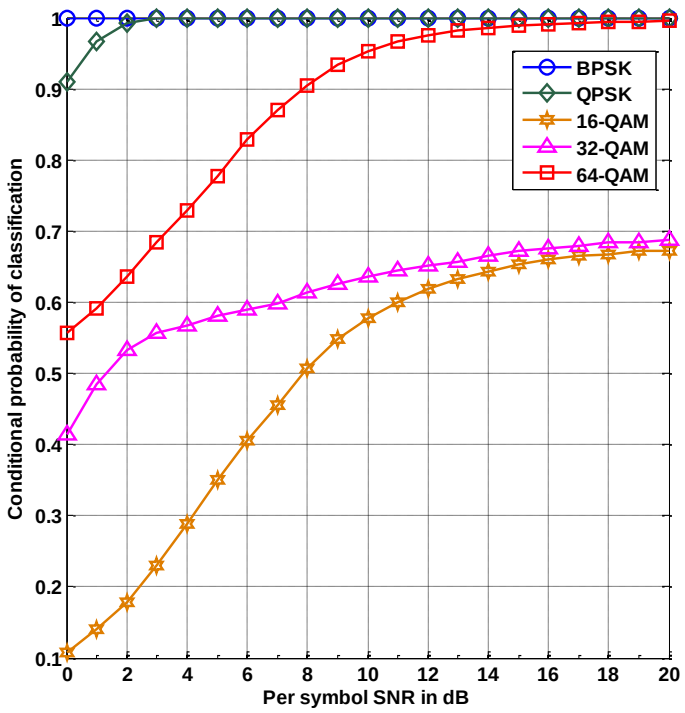

Figure 5.13. Conditional probability of classification vs SNR in AWGN (*p*=1) for the proposed AMC method.

A modulation set of {BPSK, QPSK, 16-QAM, 32-QAM, and 64-QAM} was taken. Monte Carlo simulations were conducted for 8000 noise profiles using 2048 symbols of received signal in each trial and the detection performance of a specific modulation is calculated.

The conditional probability of classification for the proposed AMC method is plotted for the assumed modulation set in Figure 5.13 and Figure 5.14 for the case of AWGN and Rayleigh multipath fading without channel information respectively. In Figure 5.13, it can be noticed that, {BPSK, QPSK} reaches higher probability of classification than {16-QAM, 32-QAM, 64-QAM}; because the theoretical values of the features are less distinguishable among the M-QAM constellations ({16-QAM= -0.68, 32-QAM= -0.68, 64-QAM= -0.619}) when compared to {BPSK= -2, QPSK= -1}. This difference in the cumulant value impacts the classification probability as given in the figures.

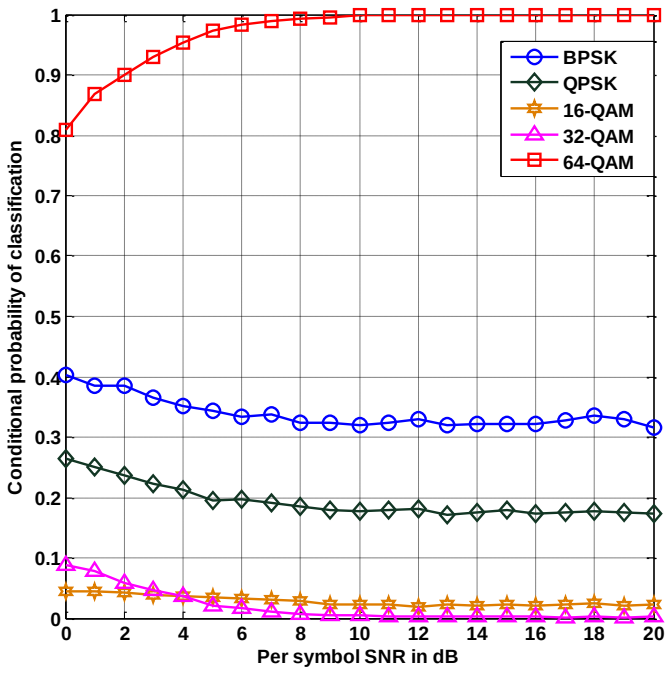

Figure 5.14. Conditional probability of classification vs SNR in AWGN (p=1) and multipath fading with L=4 without channel information for the proposed AMC method.

It is evident from Figure 5.14 that when there is fading and no channel information is available to the receiver; the performance of the proposed AMC is very

poor and highly dominated by the maximum constellation size considered in the modulation candidate set. This is because, although GLRT requires a multidimensional maximization that is computationally simple, it fails for a nested set of constellations (in this case {16-QAM, 32-QAM, 64-QAM}), and favors the constellation with the highest symbol density [133-136]. Therefore, the performance of the classifier is better for 64-QAM than 32-QAM and 16-QAM. However, for QPSK (also 4-QAM) the classifier performs better when compared to other QAMs because QPSK has a cumulant value that can be easily distinguished from BPSK and QAMs. Since all the transmissions are considered under the same average power condition, the constellation with more symbol density resembles noise, in the case of fading conditions. In addition, the constellation with more symbols for a given average power has shorter distance between their symbols and hence a high symbol error rate. Hence, even the noise in the channel can be classified as the constellation with highest symbol density. This justifies the high probability of classification for 64-QAM in Figure 5.14.

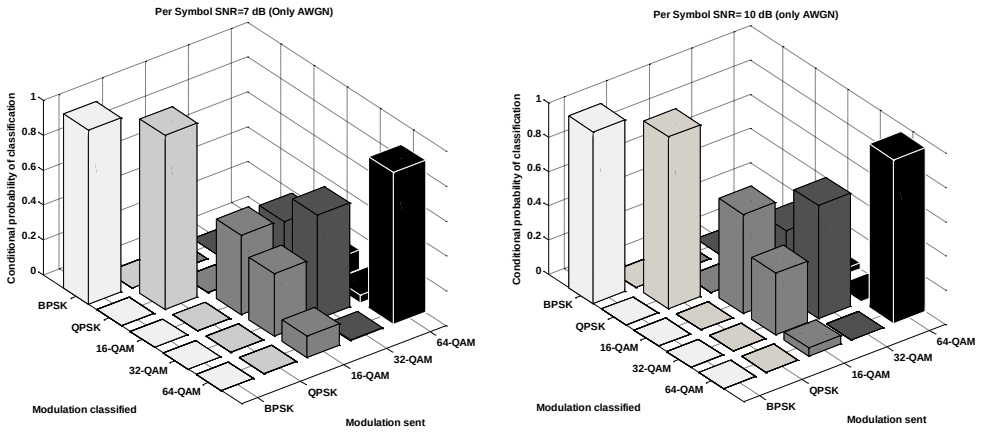

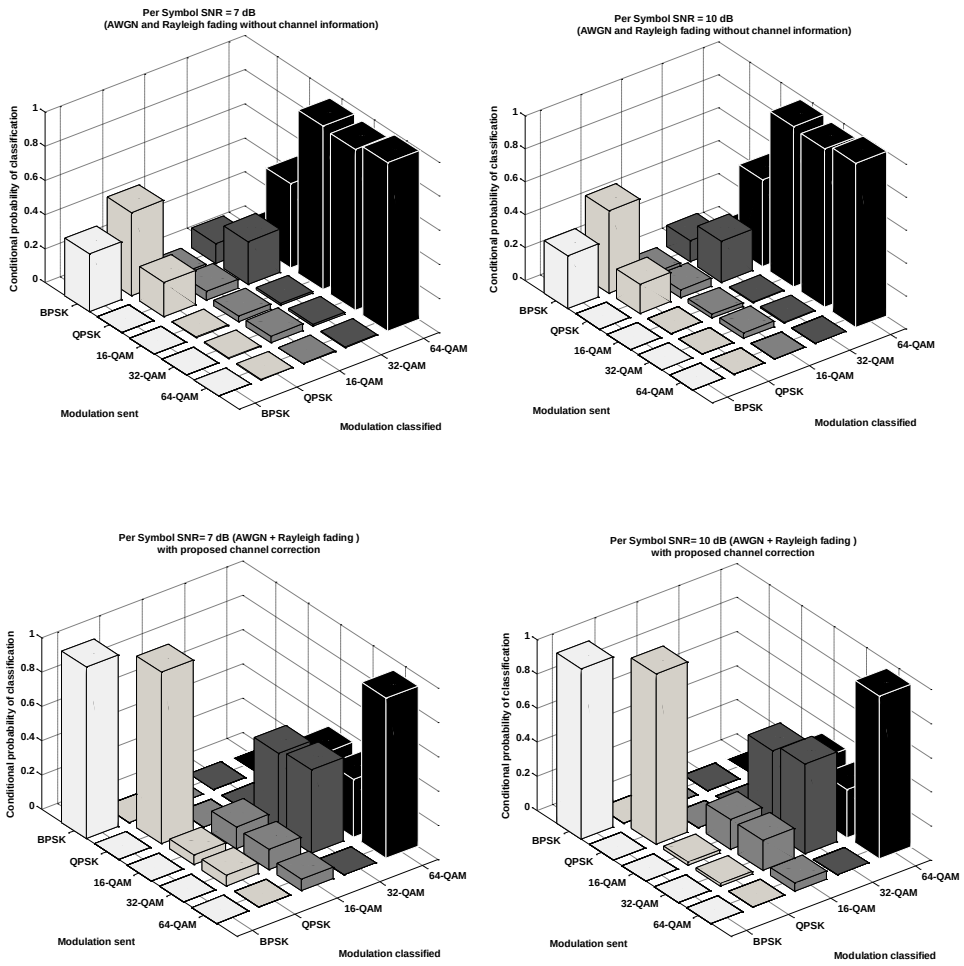

Figure 5.15. Confusion matrix as a bar plot showing probability of correct classification using the proposed AMC method for AWGN (p=1), multipath fading without channel information, and multipath fading with proposed channel correction for SNR= 7 dB and SNR= 10 dB.

The conditional probability of classification in a confusion matrix is given as a bar plot to illustrate the phenomenon mentioned above for two specific SNR values of 7 dB and 10 dB in the Figure 5.15. The performance of the classifier is very poor in the case of fading, which is seen as major misclassifications of all the modulation schemes into 64-QAM. Deploying the proposed channel correction by invoking equation (5.14), the classifier shows a significant improvement in the performance of {BPSK, QPSK} and only a marginal improvement for classification into the M-QAMs.

It is evident from the bar plot in Figure 5.15 that there is no misclassification among the PSKs and the proposed classifier provides high classification probability for the PSKs under fading conditions with the proposed channel correction method. A large

number of misclassifications are observed among the M-QAMs, especially between 16-QAM and 32-QAM.

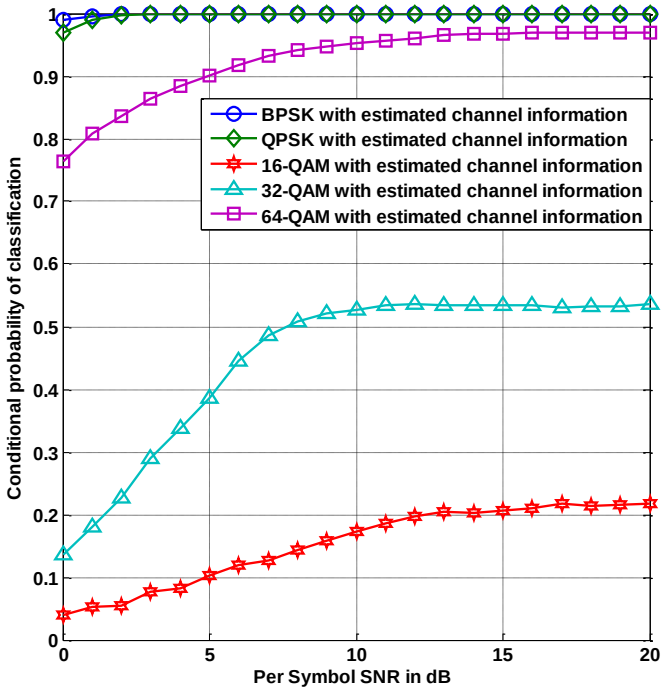

Figure 5.16. Conditional probability of classification vs SNR in AWGN (p=1), and multipath fading with $L=4$ with channel correction for the proposed AMC method showing improved performance.

This is mainly because the difference between the theoretical values of the features among 16-QAM and 32-QAM is very small. The plot in Figure 5.16 shows the overall improvement in the performance of the classifier for all the modulation schemes under fading with the proposed channel correction. However, the improvement is not equal among all modulations as mentioned previously. The improvement is higher for PSKs than for QAMs which is evident when Figure 5.16 is compared with Figure 5.14. There is a significant improvement in the classification ability of the classifier for BPSK and QPSK after the channel correction is employed, from 40% to 99% and 27% to 98% respectively, for an SNR of 0 dB. On the other hand, the improvement in the performance of the classifier for 16-QAM and 32-QAM is poor.

TABLE 5.3 COMPARISON OF THE PROBABILITY OF CORRECT CLASSIFICATION FOR THE PROPOSED MODULATION CLASSIFICATION METHOD AND THE CONVENTIONAL HOS METHOD IN THE PRESENCE OF AWGN AND RAYLEIGH MULTIPATH FADING (L=4)

P_{cc} for SNR= 10 dB	**Proposed AMC method (with channel correction)**	**Conventional HOS method with channel estimation [126]**
(*i*) **{BPSK, QPSK}** (*N=250)*	96.4%	90%
(*ii*) **{4QAM, 16QAM, 64QAM}** (*N=2048)*	84%	80%
(*iii*) **{BPSK, QPSK, 16QAM, 32QAM, 64QAM}** (*N=2048)*	73.1%	67.8%

Figures 5.13 to 5.16 illustrate the working of the classifier for various modulation schemes using the conditional probability of classification. In order to understand the overall performance of the classifier in the case of an unknown signal in AWGN and fading, P_{cc} is defined. Table 5.3 gives a comparison of the P_{cc} for the proposed and conventional HOS method for various modulation sets at an SNR of 10 dB. Table 3 gives a very high classification probability for the proposed method in the presence of fading using the proposed channel correction method when compared with the conventional HOS method for various modulation sets considered. The P_{cc} values were calculated for an SNR of 10 dB in the presence of AWGN and multipath fading with L=4. It can be noticed that, scenarios (*i*) {BPSK, QPSK} and (*ii*) {4QAM, 16QAM, 64QAM} are the sets considered in [126] for the performance of AMC. For a fair comparison, same scenarios were used to compare the performance of the proposed method and the conventional HOS based method. The proposed method outperforms the conventional HOS method in both the cases. The proposed AMC method also yielded a 5.3% improvement in the classification ability of signals in the presence of AWGN and fading for the modulation set (*iii*) {BPSK, QPSK, 16-QAM, 32-QAM, and 64-QAM} when compared with the conventional HOS based method. The simulation results in [126] show that conventional HOS based AMC method for fading channels achieves at least 20% improvement over other conventional AMC algorithms ([142], [143]) in terms of P_{cc} for SNR = 10 dB. Our method has been shown to perform better than the conventional HOS method in the same conditions as [126]. It can also be noticed from these results that set (*i*) requires fewer number of samples to reach higher classification probability than set

(*ii*). This is because the difference in the theoretical values of the features of the modulation schemes is high for set (*i*). It can also be noticed that as the number of modulation schemes increases in the modulation set, the classification ability decreases. It can be summarized from the analysis that the performance of AMC is highly dominated by the largest modulation to be classified in the candidate set, the type of noise, the amount of noise (determined by SNR) and the fading present in the signal spectrum. The proposed spectrum sensing method has been shown to perform better than the best conventional method for three types of noise scenarios. The proposed AMC method has been shown to perform as good as the conventional method in the case of Gaussian noise and more robust in case of a noise highly impulsive than Gaussian. It is also shown to perform better than the conventional method under fading conditions when there is no prior knowledge about the signal modulation and/or noise.

5.6.4. Complexity Analysis of the Proposed Method

The complexity analysis of the proposed FLOS based cumulants method is presented in this sub-section. The obvious difference between the proposed method and the conventional cumulants method is that, the proposed method has fractional order moments as compared to integer order moments. The implementation of a fractional order moment is complex in linear arithmetic due to the power operation and would vary according to the fractional order, *p*. This fractional power operation can be performed using off-line computation, which however would increase the load on host processor and the sensing time.

Another approach is to utilize logarithmic number system (LNS) for implementation of the proposed FLOS based cumulants. The FLOS based cumulants require the evaluation of x^p **,** where *p* is a fractional number. By replacing all the operands in the equation (5.10) with their logarithmic images, multiplications can be reduced to additions, while the operation of x^p, which is difficult to implement in linear arithmetic, is reduced to a simple multiplication. This can be elucidated as follows. Let *G* and *H* be such that $G = \log_b x$ and $H = \log_b p$, where *b* is the base of the logarithm. Then, $x^p = \left(b^{\log_b x}\right)^p = b^{p \log_b x} = b^{pG}$. Therefore, in such a case, a logarithmic

implementation simplifies a fractional power operation to a multiplication, a logarithmic and a look-up table (LUT) operation. It can be noted that, the complexity of such an implementation is dependent on the value of *b*, as the LUT contains the fractional, as well as integer power values for *b*.

For an input signal of *N* samples, the complexity in terms of real multiplications and additions for the conventional cumulants method and proposed FLOS based cumulants method is same if both the methods are implemented using the LNS method. However, for analysis sake, the complexity in terms of real multiplications and additions for the proposed cumulants method (implemented using LNS) and conventional cumulants method (implemented using linear arithmetic) are compared. The conventional cumulants method require $6N+1$ real multiplications and $3N$ real additions for calculating the value of cumulant as given in the equation (5.10) for an integer value of *p*. However, by applying the LNS method on the same equation for a fractional value of *p*, the complexity of the proposed method can be drastically reduced. The proposed method requires $3N$ real additions, $3N+3$ real multiplications, $2N+1$ logarithmic operations, and $2N+1$ LUT operations. Therefore, the number of real multiplications is drastically reduced from $6N+1$ to $3N+3$ in the proposed cumulants method when compared with the existing method. As real multiplications are computationally intensive, the complexity is reduced by almost 50%. However, there is a trade off, as the LUT and logarithmic operations compensate for this gain in complexity reduction. This section provided a brief analysis on the complexity of the proposed method. However, it should be noted that the complexity and convergence properties of FLOS are interdependent and this is considered out of scope of this work.

5.7. Summary

In this chapter, a scheme for spectrum sensing and automatic modulation classification in cognitive radios is proposed. Spectrum sensing is done using the proposed cumulants derived using fractional lower order statistics. The performance of the proposed method is compared with the conventional method based on higher order statistics (HOS) for various noise conditions. It is shown that the proposed method

performs well in both Gaussian and non-Gaussian conditions as compared to the conventional method. An experimental data acquisition setup was employed to obtain real time signals from the wideband spectrum to analyze the noise characteristics. A new pattern recognition based automatic modulation classification algorithm based on FLOS and cumulants, is proposed. The advantage of the proposed method is that the same statistic used for detection is used for classification. The challenge in designing a classifier is the lack of prior knowledge about the signal and channel information. Relevant features required for AMC are formulated using FLOS based cumulants, which are then compared with theoretical thresholds to perform classification. Monte Carlo simulations suggested that the proposed AMC algorithm outperforms the conventional cumulant based AMC when non-Gaussian (highly impulsive than Gaussian) noises were considered. In this chapter, the classifier is shown to be promising for fading conditions as well, by simply estimating the effect of fading factor on the cumulant estimates. By deploying the proposed channel correction in the classifier, it has shown improvement in the classification probability for {BPSK, QPSK} but only a marginal improvement for the classification of signal into the M-QAMs. However, the proposed method outperforms the conventional HOS method by 5.3% in terms of probability of correct classification under same conditions of AWGN and under fading.

After finding the vacant bands or spectrum holes, the CR is required to change its transceiver parameters to use the vacant band opportunistically, which is achieved using SDR technology. SDRs can be used to provide control over a variety of modulation schemes, transmission parameters and waveform requirements for various communication standards without changing the hardware. Spectrum sensing and DSA can be considered as a multi-layer problem involving a lot of parameters such as frequencies, bandwidths of operation, waveforms, power levels, noise scenarios, regulatory environments and application requirements. It is very difficult to develop optimal sensing algorithms that can consider most of these factors, in order to utilize the spectrum in a flexible manner. Instead, a flexible policy mechanism that supports spectrum sharing and usage of various waveforms according to the changes in policies has to be designed. All the radio devices are by definition policy-enabled devices, dealing with their own policies depending on the physical capabilities of the radio and the communication standard. CRs

and SDRs offer the ability to create policy-enabled devices that can help in utilizing under-utilized spectrum. Due to hardware constraints, a CR has to deploy a sensing policy that defines when and which frequency band needs to be sensed. Based on the sensing results, the CR decides which waveforms need to be loaded on to the radio. Sensing policies can be determined, in a dynamic fashion, either individually or collaboratively. They can determine which waveform standard need to be used based on a pre-determined rule and hence determine when the spectrum is to be considered available for opportunistic access. Some applications where such a policy-based radio can be used are public safety radios, emergencies and aerospace communications.

In the next chapter, a policy-based CR focusing on policy management by means of spectrum sensing is proposed. A separate channel known as the sensing policy channel (SPC) is allocated for this purpose. The CRs monitor the SPC frequently in order to sense signals at various frequency locations. Depending on these sensed signals, the CR determines which policies need to be loaded. These policies that can be loaded are already pre-defined in the CR. The motivation for a policy-based CR is to support dynamic adaptability of a CR which allows it to change policies without stopping or restarting the system. In addition, the authority to change policies resides with the CR and in order to provide improvement in the detection ability, a two-stage spectrum sensing model is proposed.

Chapter 6

Robust Two-stage Spectrum Sensing and Policy Management for Cognitive Radios

6.1. Introduction

The new class of radios, namely the SDRs, and CRs provide flexibility and agility that help in dynamic allocation of spectrum. In the previous chapter, the problem of spectrum sensing and automatic modulation classification was addressed using a novel method based on higher-order statistics and fractional lower-order statistics. However, after finding the vacant bands or spectrum holes, the CR is required to change its transceiver parameters to use the vacant band advantageously. This can be achieved using SDR technology. SDRs can be used to provide control over a variety of modulation schemes, transmission parameters and waveform requirements for various communication standards without changing the hardware.

The issue of spectrum sensing and dynamic spectrum access can be considered as a multi-layer problem involving many parameters such as frequencies, bandwidths of operation, waveforms, power levels, noise scenarios, regulatory environments and application requirements. It is difficult to develop optimal sensing algorithms that can take into consideration these factors in order to utilize the spectrum in a flexible manner. Instead, a flexible policy mechanism that supports spectrum sharing and usage of various waveforms according to the changes in policies needs to be designed [8]. All the radio

devices are, by definition, policy-enabled devices with their own specific policies, depending on the physical capabilities of the radio and the communication standard. CRs and SDRs offer the ability to create policy-enabled devices that can help in utilizing currently underutilized spectrum. Due to hardware constraints, a CR has to deploy a sensing policy that defines which frequency band needs to be sensed at a given time interval. Based on the sensing results, the CR determines which waveforms need to be loaded on to the radio. Sensing policies can be determined, in a dynamic fashion, either individually or collaboratively. They can determine which waveform standard needs to be used based on a pre-determined rule and hence, when the spectrum is to be considered available for opportunistic access. Some examples of applications where such a policy-based radio can be used are public safety radios, emergencies and aerospace communications [144].

Aerospace communications (during take-off and in-flight) and emergency radio communications (during emergencies such as earthquakes or tsunamis), can be considered as an application scenario for such a policy-based CR where sensing of a particular channel needs to determine which waveform has to be loaded. For e.g., in aerospace communications, when the aircraft is in the airport building, the users onboard can utilize WLAN allocated for their use and when the aircraft is in flight mode, WLAN or GSM can be utilized depending on the user's decision. Therefore, the SDR needs to determine which waveform to load (GSM or WLAN) depending on the location of the receiver node. For this purpose, the base station can communicate to the user, through a dedicated channel, and the SDR can reconfigure its configuration parameters accordingly. However, this communication should not interfere with the other flight –ground communication, hence there is an inherent necessity for the user to have cognitive abilities. The work in this chapter aims to develop a more general solution for the problem of detection by using the filter bank method proposed in Chapter 4 and the higher-order statistics based method. This chapter develops a new technique for estimating the spectral occupancy using a control channel that helps in changing the parameters of the radio. This chapter consists of two major parts: (i) detection of wideband spectral signals using the proposed method, and (ii) policy control for cognitive radios using the sensing information.

In the first part of the chapter, a policy-based CR focusing on policy management by means of spectrum sensing is proposed. A separate channel known as the sensing policy channel (SPC) is allocated for this purpose. In a scenario, where such a channel is not available, the service provider has to provide either the sensing information or the waveform to be used, and must be known to the CR beforehand. In such a case, the cognitive ability in a radio is not necessary, as there is an overload on the base station to allot the spectral resources efficiently to various CRs utilizing the spectrum. Therefore, there is an inherent need for a handshake between the service provider and the CR, for which a separate channel has to be allotted. SPC can be an additional feature in the handshake between the base station and the node. Ideal CR scenario or a military radio requires no dedicated channel to perform spectrum sensing [3, 4]. The CRs monitor the SPC frequently in order to sense signals at various frequency locations. Depending on these sensed signals, a CR determines which policies need to be loaded. The policies that can be loaded are already pre-defined in the CR. The motivation for a policy-based CR is to support dynamic adaptability that allows it to change policies without stopping or restarting the system. In addition, the authority to change policies resides with the CR and in order to provide improvement in the detection ability, a two-stage spectrum sensing model is proposed.

In the second part of this chapter, the performance of the integrated scheme is evaluated using Monte Carlo simulations. An experimental data acquisition system was set up to receive real time signals and perform noise analysis of the received signals that is used in the proposed algorithm. One of the key features of CR [1, 2] is the ability to sense a wideband spectrum in order to identify these holes. This requires the CR to change its receiver parameters in a dynamic fashion, which is achieved using SDR technology. SDRs can be used to provide control over a variety of modulation schemes, transmission parameters and waveform requirements for various communication standards without changing the hardware.

This chapter is organized as follows. Firstly, various policy management schemes in SDR and spectrum sensing technologies available in the literature are discussed. It also elucidates the need for a policy based CR followed by the proposed two-stage spectrum sensing method and the policy management describing the design insights used in our

method. In the later part of this chapter, various simulation results for the proposed spectrum sensing method and experimental analysis of the overall method is presented.

6.2. Policy Management in Radios

This section deals with policy management in SDR based CR technology in general, and to DSA in particular. In general, policy management in radios involves managing policies pertaining to the working configuration of a radio. This is performed by specifying certain objectives in the policies that can be interpreted and enforced by the radio. These policies are procedural statements expressing specific conventions like modulation scheme, carrier frequency, bandwidth etc., which are adopted by the communication standard. For example, in the conventional radio scenario, the usage of waveform channels is consolidated over time (say in the case of a GSM radio). Based on this information, decisions can be made to unload under-utilized channels or load more channels. If a channel has accepted more than a certain number of transactions during the last S minutes, then a new channel will be created to boost the QoS by the base station. On the other hand, if no activity is sensed over some period, then the base station will stop holding that channel. Such policies are controlled by the base station and the information is relayed to the end user when the user handshakes with the base station. However, in the context of a CR, there are sensing-based policies and refer to conventions that define when and which frequency band and standard have to be used for opportunistic access by the CR. A policy engine (PE) is defined as a program or process that can deploy these machine-readable policies [144]. The PE must be able to modify the run-time configuration of the CR based on the policies that get loaded. These policies are pre-defined in the PE, and get loaded onto the CR depending on the spectrum sensing unit.

The PE is an inference engine that initiates the change in resource configurations such as change in the operating frequency, the spectral band of interest, and other such device configurations in the case of a CR. The outputs of a PE are generally authorization commands that are specific to a standard. Much of the research in the area of policy-based CR has been focused on developing a formal language for expressing complex policies for various communication standards and network management problems [145-

150]. The Defense Advanced Research Projects Agency's (DARPA's) Next Generation (XG) radio communications program [8, 144-146] develops novel technologies and system concepts for DSA. The Phase III of the XG program focused on many technical issues, such as the processing power and signal sensing requirements. As part of the XG program, a policy-based network management system for controlling DSA was proposed in [146]. Most of the literature assumes that the CR can be implemented on an SDR platform. However, the CR architecture is one of the important issues in the deployment of a CR as it involves software interfaces and application-programming interface (API) that has to be provided by the services on the host platform. Apart from platform integration issues, the policy engine has to be integrated with the CR's software architecture. Software Communications Architecture (SCA) is one such layered architecture which provides APIs for control and information exchange as well as for integration with new applications that are supported by the core framework [151]. The Joint Tactical Radio System (JTRS) defines the SCA based on Common Object Request Broker Architecture (CORBA) middleware [152, 153]. The PE will be another component in this architecture that can interface with other components supported by the core framework. However, one of the most important architectural considerations is the definition of this interface of PE to the software environment of the radio.

In highly noisy scenarios, higher-order statistics (HOS)-based spectrum sensing using higher-order signal characteristics was proposed in [154]. It is a robust statistical approach, which can effectively sense the spectrum by calculating the relevant HOS features known as cumulants. They perform better at extremely low SNR environments but the disadvantage is that it requires a higher sample set to obtain the whole set of cumulants and better detection accuracies. This results in a longer sensing time. As a result, the HOS-based spectrum sensing methods cannot be directly applied to the wideband spectrum for real-time sensing. Many two-stage methods have been proposed in literature by combining the methods discussed above [107, 155-157]. For example, a two-stage sensing based on energy detection in both the stages with different sensing bandwidths was proposed in [155]. A CR first searches over a larger bandwidth in the coarse sensing stage using a simple method such as energy detection. Once the energy detector detects a spectrum hole, it goes to the fine sensing stage using a more robust

detector such as the cyclostationary detection. The fine sensing stage is activated to decide whether the channel is empty with confidence or the PU was present but missed in the detection during the coarse sensing stage. In a largely subscribed spectrum scenario such as the commercial mobile communications, the number of PUs is more. In such a case, determining spectrum holes becomes an even more difficult task because of out-of-band interference and spectral leakage that might lead to erroneous decisions on the spectrum usage. Using a two-stage sensing scheme for such a scenario will offer good detection accuracy. As mentioned above, in the coarse sensing stage, the spectrum is sensed over a large bandwidth consisting of many PU channels using energy detection. If the detection determines the presence of signal, the fine sensing stage is not activated. However, some vacant bands may have been missed because the coarse sensing stage operates on a larger bandwidth.

In order to find the spectrum holes, there is a need to perform sensing at the channel bandwidth in real-time. Fine sensing stage performs sensing at the channel bandwidth but only if coarse sensing fails to determine the presence of a PU. The CR not only has to sense the spectrum in real time but also move away from the band if there is any PU requesting channel access. This provides a bottleneck on the sensing time and poses a challenge in real-time spectrum sensing causing an inherent trade-off between sensing time and sensing accuracy. Therefore, the accuracy in sensing is affected when there is an upper bound on the sensing time. In order to reduce the overhead in performing spectrum sensing accurately and robustly at channel bandwidth, a separate sensing policy channel that has pre-defined policies regarding the spectrum usage is proposed. The sensing policy channel, proposed in this chapter, has to be sensed frequently in order to understand the utilization of a spectral region. The CRs check for specific signals in the sensing policy channel. Based on the signal sensed at various frequencies in the SPC, the corresponding policy is loaded. This policy contains the information on the waveform and the frequency band to be used for communication. The CR then loads the required waveform in the SDR without causing any interference in the specific band.

In order to facilitate the use of automatic policy management in CRs and to improve sensing performance, the present work investigates a two-stage spectrum sensing

method. The first stage is the filter bank based energy detector where the sensing policy channel is split into various subbands. The use of a filter bank helps in reducing the time taken for sensing the SPC when compared to serially sensing the spectral region. The power value of each subband is calculated in a parallel fashion. This power value is used as a normalization factor for the cumulants calculated in the next stage. The second stage consists of the cumulants operation on all the subbands based on HOS. Although the proposed scheme has two stages of operation, it differs from the conventional two-stage methods in [107, 155, 156] in two ways. Firstly, the methods in [107, 155, 156] perform sensing by attempting to detect the signals using binary hypotheses in both the first and second stage, whereas in this work, the hypothesis testing is performed only at the end of the second stage. Secondly, in this work the cumulant values calculated are normalized using the subband power values calculated in the first stage. This is performed to remove the effects of noise on the cumulant and improve the detection accuracy of the proposed cumulants based sensing method at very low SNR conditions. In the next section, the proposed policy-based CR and the two-stage spectrum sensing is discussed in detail.

6.3. Proposed policy-based cognitive radio

The proposed policy-based cognitive radio with its various components is shown in Figure 6.1.

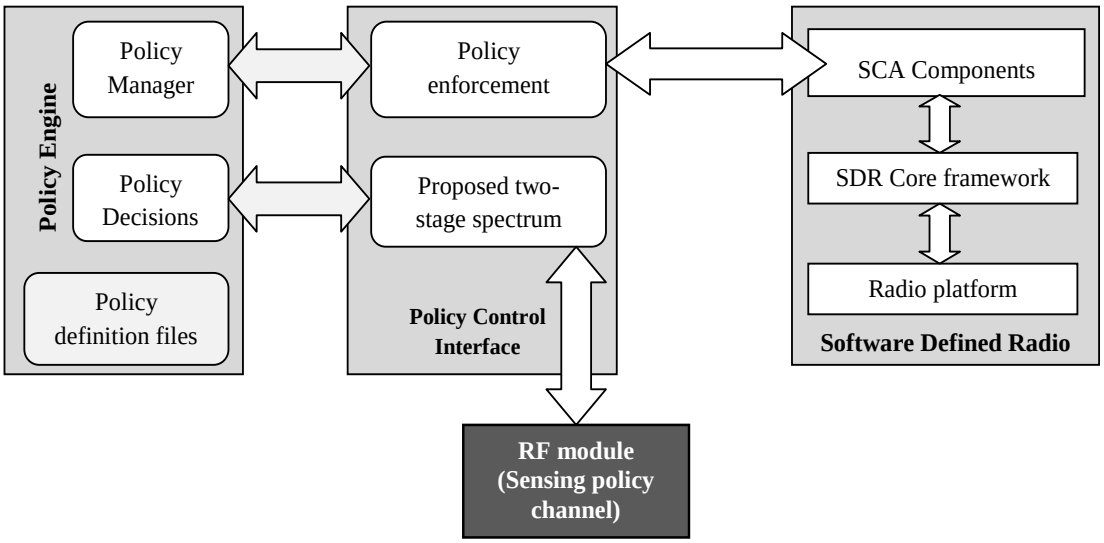

Figure 6.1. Proposed cognitive radio scheme with policy engine and spectrum sensing module.

The proposed model comprises of three main components for deployment of a CR namely: policy engine, policy control interface and the SCA-based SDR. Figure 6.1 shows that the policy engine serves three main policy management functions: policy definition files, policy decisions, and policy enforcement. The policy definition files maintain all the policies that need to be enforced to decide which waveform to be instantiated in the SDR. It also performs operations such as parsing and keeping track of policies that are enabled and disabled. The policy decision function determines which of the existing policies have to be enforced. In order to make these decisions, it requires information about the communication conditions and/or the spectral scenario. It communicates with the spectrum sensing unit in the policy control interface that report real-time information on the spectrum policy channel. The policy enforcer function acts as the control interface to constrain the radio's behavior according to the policy and communicates with the SCA framework through its components. It also performs actions that are defined in the policy. The SCA framework is the core framework for an SDR. The focus of this work is on the PE and spectrum sensing, and the details regarding the SCA framework for SDRs are considered out of scope of this work. While [144] deals with an extensive set of policy models and engines for policy management and decision making for policy-based CRs, in this work the focus is on deployment of a policy engine. For the sake of simplicity, a policy engine that encompasses the most essential functions of policy definition, deployment and enforcement is proposed.

The sensing policy channel consists of different signals that have a one-to-one mapping with the policies defined in the policy definition files. In the work presented in this chapter, an open source software project named Apache Imperius is used as the PE. It uses the Simple Policy Language (SPL) for the policy definition files [157]. SPL is an object-oriented policy language that allows expression of management policies using simple condition-action rules. The PE Imperius provides an extensible set of operations for expressing these conditions and actions. JavaSPL (Imperius with Java binding) which extends SPL to interact with Java objects directly is used. The JavaSPL is wrapped to python using JPype [158] which allows full access to all the Java class libraries. The proposed two-stage spectrum sensing method is a code written in Python in the policy control interface. The policy enforcer communicates with the SCA framework and loads

the corresponding waveform defined in the policy database or the policy definition files. In the next subsections various policies and the sensing policy channel are described in detail.

6.3.1. Proposed Sensing Policy Channel

The proposed sensing policy channel consists of M discrete frequency bands with center frequencies $\{f_1, f_2, ... f_M\}$. The bandwidth of the sensing policy channel is assumed to be 1 MHz. The corresponding policies that need to be loaded for the specified frequency bands are denoted as $\{P_1, P_2, ...P_M\}$, respectively. These policies initiate the loading of waveforms $\{W_1, W_2, ...W_M\}$ respectively, when they are enforced. The SDR based CR can reconfigure between M waveforms based on the policies that are being loaded. The policy condition is defined below:

[1] Policy P_i allows the policy-based CR to operate using the waveform W_i, if it can detect a signal in f_i for all i's, given $1 \le i \le M$. For e.g. policy P_1 is loaded when a signal is detected at a center frequency f_1. P_1 instructs the policy-based CR to operate using the waveform W_1.

[2] The policy also has the information on transmission parameters such as the bandwidth and frequency of operation for a specific policy depending on which waveform instance is instantiated in the SCA framework.

[3] Although the proposed detection is called two-stage, the detection is performed at the end of second stage. The cumulant estimates (second stage) calculated are error corrected using the power values of subbands (energy detection) calculated in the first stage.

The proposed method is discussed in detail in the next subsection, to showcase the difference between the proposed method and a conventional two-stage method as in [108].

6.3.2. Proposed Spectrum Sensing Method

The overall block diagram of the detection method is illustrated in Figure 6.2.

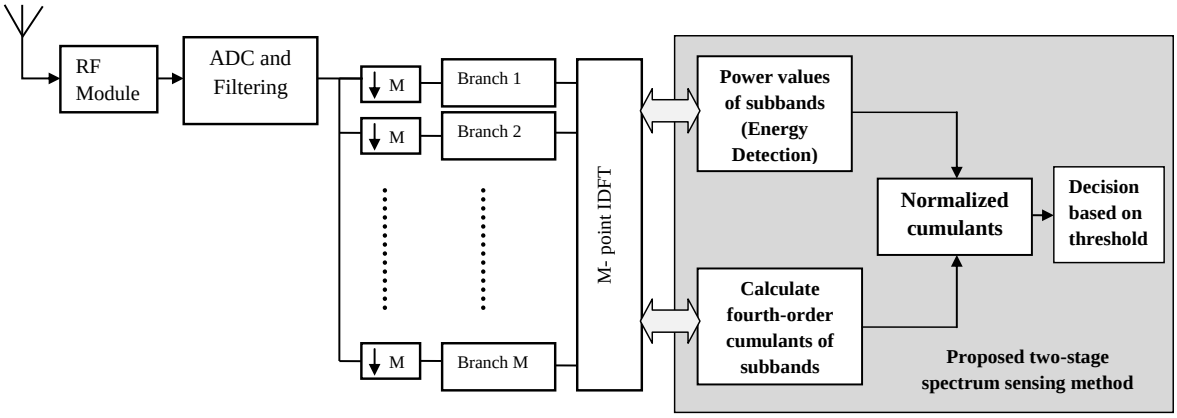

Figure 6.2. Proposed spectrum sensing module.

It is illustrated in Figure 6.2 that the filter bank is used to separate the observed sensing policy channel into uniform frequency channels. The filter bank consists of an M-channel uniform discrete Fourier transform filter bank (DFTFB) to split the sensing policy channel into multiple subbands of uniform bandwidths [50]. For simplicity sake, the number of policies and subbands are assumed to be equal to *M*. Power values, as in the case of energy detection, are calculated for all the subbands and this is considered as the first stage of the detection. The energy detector accumulates the power of *N* samples in each band in this stage to locate possible signals in the frequency locations $\{f_1, f_2, \ldots f_M\}$ in a parallel fashion. The normalized power values of the subbands obtained in the first stage are used as weights for the fourth order cumulants estimated in the next stage. Thus, at the end of both stages, a test statistic based on the new estimate of fourth order cumulants for each of the channels are compared with a threshold γ_i, to decide whether the channel is empty or occupied. It is this threshold which determines the performance metrics; probability of detection P_d, and probability of false alarm P_{fa}, of the system. The hypothesis testing performed on the test statistic is defined as

$$H_0 : r(n) = \eta(n)$$
$$H_1 : r(n) = s(n) + \eta(n) \tag{6.1}$$

where $r(n)$ is the general expression for received signal, H_0 testifies the presence of zero mean AWGN $\eta(n)$ alone, while H_1 testifies the presence of a signal $s(n)$ corrupted by AWGN, respectively. The conventional fourth order cumulant method estimates the cumulant values of the received signal. Ideally, if the signal is corrupted by AWGN, the corresponding fourth order cumulants are zero. Typically, a Gaussianity test, where the calculated cumulant values are compared with zero as threshold, is performed using the estimates of the conventional cumulants value. In low SNR cases, the energy detection fails due to the uncertainty in noise and also under the effects of fading [29]. Moreover, the values of the estimated cumulant are very low in the case of low SNRs that the detector decides that it is purely noise. By calculating the power values and using them as weights for the cumulant values of the subbands, a new set of cumulant estimates are proposed in this work. This aspect is shown in the following analysis of the proposed two-stage sensing method.

According to the properties of higher order cumulants [126], a typical pth order-qth conjugate cumulant is defined as follows

$$L_{pq}(x) \equiv cum\left(\underbrace{x,x,x,.,.,.,.,.}_{p-q},\underbrace{.,.,x^*,x^*,x^*}_{q}\right) \tag{6.2}$$

where x is a random variable, associated with the random process for the transmitted data sequence $s(n)$. x^* denotes the complex conjugate of x. $L_{pq}(x)$ is the defined as the zero-lagged cumulant value. A fourth order cumulant yields a three dimensional matrix of values. However, the most significant is the zero-lagged cumulant value. In order to reduce the complexity involved in dealing with 3-D matrix, a simple zero-lagged cumulant value was used. Expressions for the second and fourth order cumulants according to the moment-to-cumulant formula are given by the following relations respectively [149]:

$$L_{21}(x) \equiv cum\left(x,x^*\right) = E\left(|x|^2\right) \tag{6.3}$$

$$\begin{aligned} L_{42}(x) &\equiv cum\left(x,x,x^*,x^*\right) \\ &= E\left(|x|^4\right) - \left|E\left(|x|^2\right)\right|^2 - 2E^2\left(|x|^2\right) \end{aligned} \tag{6.4}$$

It can be noted that $L_{21}(x)$ is actually the power of the signal *x*. The normalized fourth order cumulant is given as

$$\overline{L_{42}}(x) \equiv \frac{L_{42}(x)}{\left(L_{21}(x)\right)^2} \tag{6.5}$$

The filter bank splits the received signal into its polyphase components and the ith branch of the polyphase filter bank has an impulse response $h_i(m)$ given by

$$h_i(m) = h(mM + i) \tag{6.6}$$

where $h(m)$ is the impulse response of the prototype filter of length L. The output signal at the ith branch is given below:

$$x_i(n) = \left(\sum_{m=0}^{L-1} h_i(m) r(n-m)\right) e^{\frac{2\pi \times i \times n}{M}}$$
$$1 \le i \le M \tag{6.7}$$

In this method, fourth-order cumulants based on higher order statistics are used for detection. Fourth-order cumulants are preferred over third-order cumulants or higher order moments because, for a random process which is symmetrically distributed, both the third-order cumulant equals zero. Moreover, some processes and signal modulations have extremely small third-order cumulant value and larger fourth-order cumulant value. Hence, fourth-order cumulants were used over the third-order cumulants. Note that the present work also utilizes higher-order cumulants instead of higher order moments for sensing. Based on practical issues, there are two reasons why cumulants are preferred over moments. Firstly, the fourth-order cumulants of AWGN are ideally zero; whereas various known signals have non-zero value. Secondly, the cumulants possess the property that the cumulant of two statistically independent random processes equals the sum of the cumulants of the individual random processes, whereas the same is not true for higher order moments. These two properties of cumulants motivated us to work with fourth-order cumulants. However, the variances of the estimates of such cumulants are large and increase as the order increases for a constant data size. This may lead to error in detection. In order to reduce the error, higher data sizes have to be considered. This in turn will increase the computational complexity, which will lead to increased sensing

time and power consumption. Calculating the value of cumulants involves computing averages of several samples from the real data over many dimensions (three in the case of a fourth order cumulant). In order to minimize the computational complexity involved in calculating a multidimensional matrix for cumulants, the zero-lag value of the cumulant is used as a test statistic in the proposed sensing scheme.

Applying the zero-lagged fourth-order cumulants on the output in (6.7), the expression for the cumulant estimate of the transmitted signal can be obtained as shown in equations (6.8)-(6.10).

$$\overline{L_{42}}\left(x_i\right) \equiv \frac{L_{42}\left(x_i\left(n\right)\right)}{\left(L_{21}\left(x_i\left(n\right)\right)\right)^2} = \frac{L_{42}\left(\left(\sum_{m=0}^{L-1} h_i\left(m\right) r(n-m)\right) e^{\frac{2\pi \times i \times n}{M}}\right)}{\left(L_{21}\left(\left(\sum_{m=0}^{L-1} h_i\left(m\right) r(n-m)\right) e^{\frac{2\pi \times i \times n}{M}}\right)\right)^2} \tag{6.8}$$

$$= \frac{L_{42}\left(\left(\sum_{m=0}^{L-1} h_i\left(m\right)\left(s(n-m)+\eta(n-m)\right)\right) e^{\frac{2\pi \times i \times n}{M}}\right)}{\left(L_{21}\left(\left(\sum_{m=0}^{L-1} h_i\left(m\right)\left(s(n-m)+\eta(n-m)\right)\right) e^{\frac{2\pi \times i \times n}{M}}\right)\right)^2} \tag{6.9}$$

$$= \frac{L_{42}\left(\left(\sum_{m=0}^{L-1} h_i\left(m\right)\left(s(n-m)\right)\right) e^{\frac{2\pi \times i \times n}{M}}\right) + L_{42}\left(\left(\sum_{m=0}^{L-1} h_i\left(m\right)\left(\eta(n-m)\right)\right) e^{\frac{2\pi \times i \times n}{M}}\right)}{\left(L_{21}\left(\left(\sum_{m=0}^{L-1} h_i\left(m\right)\left(s(n-m)\right)\right) e^{\frac{2\pi \times i \times n}{M}}\right) + L_{21}\left(\left(\sum_{m=0}^{L-1} h_i\left(m\right)\left(\eta(n-m)\right)\right) e^{\frac{2\pi \times i \times n}{M}}\right)\right)^2}$$

$$= \frac{\left(L_{42}\left(s\right)+L_{42}\left(\eta\right)\right) \times \left(\sum_{m=0}^{L-1}\left(h_i\left(m\right)\right)^4\right)}{\left(\left(L_{21}\left(s\right)+L_{21}\left(\eta\right)\right) \times \left(\sum_{m=0}^{L-1}\left(h_i\left(m\right)\right)^2\right)\right)^2} \tag{6.10}$$

Equation (6.10) was obtained by applying the cumulant operation on (6.9) [149]. If the noise is AWGN, then the fourth order cumulant is zero according to higher-order

statistics. Thus the equation can be easily modified to obtain the estimate of the cumulant of the transmitted sequence, $\overline{L_{42}}(s)$.

$$\begin{aligned}\overline{L_{42}}(x_i) &= \frac{\left(L_{42}(s)\right)}{\left(L_{21}(s)\right)^2} \times \frac{1}{\left(1+\frac{L_{21}(\eta)}{L_{21}(s)}\right)^2} \times \frac{\left(\sum_{m=0}^{L-1}\left(h_i(m)\right)^4\right)}{\left(\sum_{m=0}^{L-1}\left(h_i(m)\right)^2\right)^2} \\ &= \overline{L_{42}}(s) \times \frac{1}{\left(1+\frac{L_{21}(\eta)}{L_{21}(s)}\right)^2} \times \frac{\left(\sum_{m=0}^{L-1}\left(h_i(m)\right)^4\right)}{\left(\sum_{m=0}^{L-1}\left(h_i(m)\right)^2\right)^2}\end{aligned} \tag{6.11}$$

$$\Rightarrow \overline{L_{42}}(s) = \overline{L_{42}}(x_i) \times \left(1+\frac{L_{21}(\eta)}{L_{21}(s)}\right)^2 \times \frac{\left(\sum_{m=0}^{L-1}\left(h_i(m)\right)^2\right)^2}{\left(\sum_{m=0}^{L-1}\left(h_i(m)\right)^4\right)} \tag{6.12}$$

It is seen from (6.12) that the expression for estimated cumulant of the transmitted signal depends on three factors, namely; calculated cumulant value on the received signal, the SNR and filter coefficients of the filter bank. The effect of SNR on the cumulant value is denoted as α. When the signal power is very low compared to the noise (low SNR conditions), α can be approximated as given below:

$$\alpha = \left(1+\frac{L_{21}(\eta)}{L_{21}(s)}\right)^2 \approx \left(\frac{L_{21}(\eta)}{L_{21}(s)}\right)^2 \tag{6.13}$$

In cases where the noise variance is not known, or cannot be calculated, mitigating this error would be a tedious process. For this purpose, an algorithm where the power values of each subband normalized to the received signal power are used as weights on the cumulant value calculated on the subband is proposed. In order to estimate the cumulant value of the transmitted sequence, the wideband signal is split into *M* subbands using the DFTFB. The signal power of the received signal is calculated as P_{tot}. The power of each subband, namely P_i, is calculated. The normalized fourth order cumulant values of each subband are calculated using (5) and are used to calculate the

cumulant estimate of the transmitted sequence, denoted as $est(\overline{L_{42}(s)})$ using the weights as shown below.

$$w_i \equiv \frac{M \times P_i}{P_{tot}} \tag{6.14}$$

$$est(\overline{L_{42}(s)}) = w_i \times \overline{L_{42}}(x_i) \times \frac{\left(\sum_{m=0}^{L-1}\left(h_i(m)\right)^2\right)^2}{\left(\sum_{m=0}^{L-1}\left(h_i(m)\right)^4\right)} \tag{6.15}$$

This estimate is used to determine the presence or absence of a signal in the received spectrum. When a signal is present in a specific subband, the power value of the subband is higher than that of the power of the received signal. This is because the averaging of samples is performed over a smaller bandwidth in the case of a subband, as compared to the wideband bandwidth of the input signal. Thus the weight, which is the ratio of the power of the subband to the power of the received signal, has a value more than unity. This improves the value of the cumulant when the signal is present. When there is no signal, however, the value of the weight is dependent only on the variance of the noise and this will not increase the estimated cumulant value of the noise.

In order to understand this effect, the proposed method is analyzed through simulations and compared with various conventional methods of spectrum sensing in the next section.

6.4. Simulation Results and experimental analysis

In this section, the proposed method is validated through simulations. Two sets of simulations are performed: the effect of the proposed normalization process, and the performance comparisons in terms of probability of detection and false alarm. An experimental setup showing the functionality of the proposed policy-based CR is also illustrated in the latter part of this section.

6.4.1. Analysis of the Proposed Two-stage Sensing Method

In this subsection, simulations are presented to analyze the proposed sensing scheme for performance comparisons. Case 1 shows how the proposed cumulant estimates are error-corrected for cases of low SNRs. Case 2 deals with the detection probability of the proposed sensing method.

Case 1: A specific modulation scheme was selected for the input signal, but the number of channels was randomly chosen. Three sets of simulations involving BPSK, 16-QAM and 64-QAM were selected separately at channels 3 and 6. Figure 6.3 shows the estimated cumulant value for the proposed method as compared to the conventional cumulant method, both plotted against the channel numbers for an SNR of -10 dB. The number of observation samples for each block is 1024 samples. The number of Monte Carlo simulation is set as 3000.

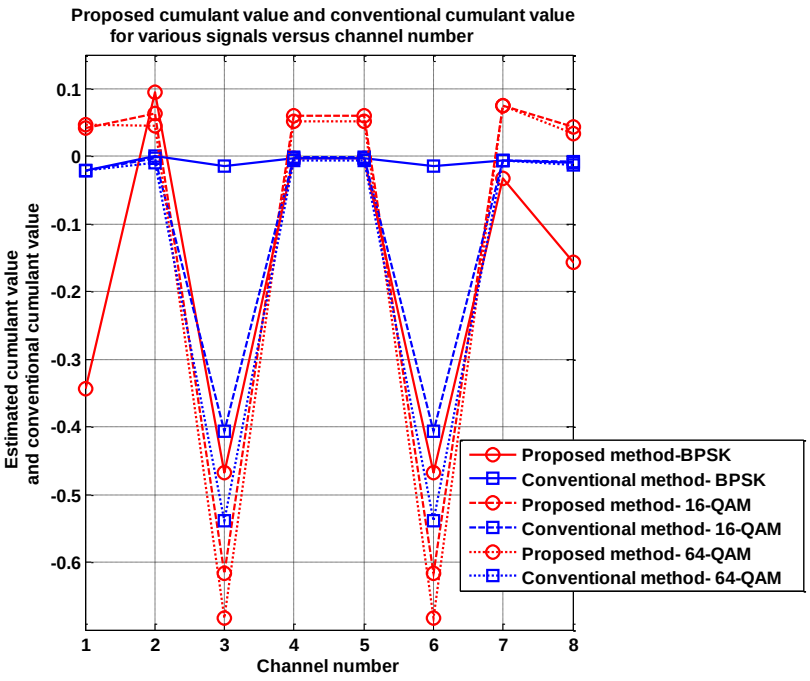

Figure 6.3. Proposed cumulant value and conventional cumulant value plotted against the channel numbers for BPSK, 16-QAM and 64-QAM signals at SNR=-10 dB.

It is evident from Figure 6.3 that at a low SNR of -10 dB, the cumulant values of the modulations are small and close to zero, which would force the spectrum sensing unit to decide wrongly that there is no signal present. However, by employing the proposed

detection scheme, it is seen that the cumulant values are improved. The true fourth order zero-lagged cumulant values for {BPSK, 16-QAM, 64-QAM} are {-2, -0.68, -0.6191}, respectively [126]. This will reduce the error in detection at the second stage of sensing in cases of low SNRs. The proposed two-stage method and the algorithm based on weights helps in converging the value of the estimated cumulant closer to the true value of the cumulant for various types of signals analyzed. It is also clear from Figure 6.3 that the improvement in the cumulant value for 64-QAM is better than that of 16-QAM and BPSK. This is because all the symbols of these three constellations were considered with a constant minimum distance between the symbols as two. Since 64-QAM has 64 symbols, it is spread out more than 16-QAM or BPSK and hence, the convergence probability of a received symbol into one of those 64 symbols is high. Intuitively, for a constant average power, the constellation with more symbols has shorter distance between their symbols. This would mean a high symbol error rate. For a fair comparison between modulation schemes, symbols are chosen such that the minimum distance between them is a constant for all modulations.

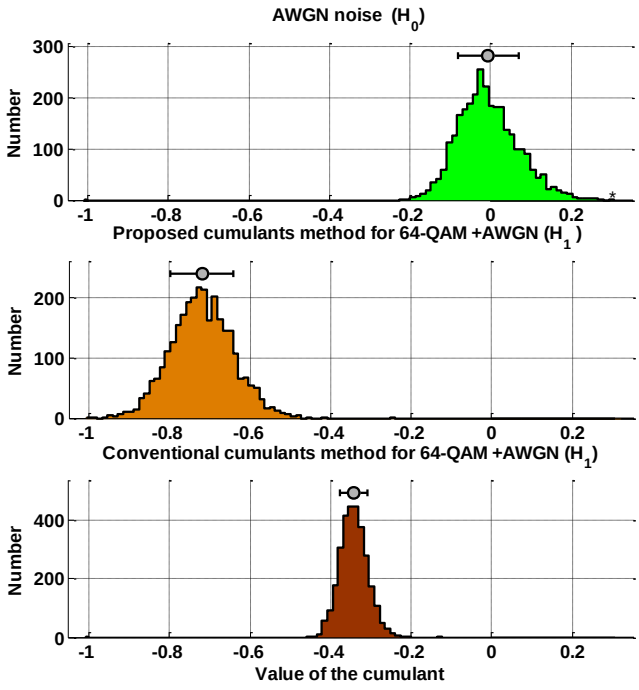

Figure 6.4. Histogram comparisons of the proposed cumulant value and the conventional cumulant value for the binary hypothesis for a 64-QAM signal.

The positive effect of the normalization process can be illustrated using the histogram of the estimated cumulant value. 3000 simulations were conducted and the

histogram of the proposed cumulant value and conventional cumulant value for a 64-QAM signal (H_1), and AWGN (H_0) are plotted in Figure 6.4. In the case of only AWGN, the value of cumulant does not change drastically from its true value of zero. However, in the case of a signal immersed in AWGN the value of the cumulant is shown to have improved. The impact of this improvement in the cumulant value is elucidated below through simulations. Figure 6.5(a), (b) and (c) show the performance improvement in the probability of detection for the proposed two-stage method over the conventional cumulants method versus SNR for a 64-QAM, 16-QAM and BPSK signal, respectively. The number of simulations conducted is set at 3000, with a signal block of 1024 symbols per simulation. The threshold for the test statistic was calculated by keeping the probability of false alarm at 0.1 for the conventional cumulants method. This calculated threshold was used to perform detection. It is evident from three plots that the false alarm rate of the conventional cumulants method is at 0.1. Figure 6.5(a) suggests that the proposed method and the conventional method provide a high detection ability of 99.87% for SNRs ranging from -20 dB to 0 dB for a 64-QAM signal. However, the false alarm rate of the proposed method reaches zero from -12 dB onwards.

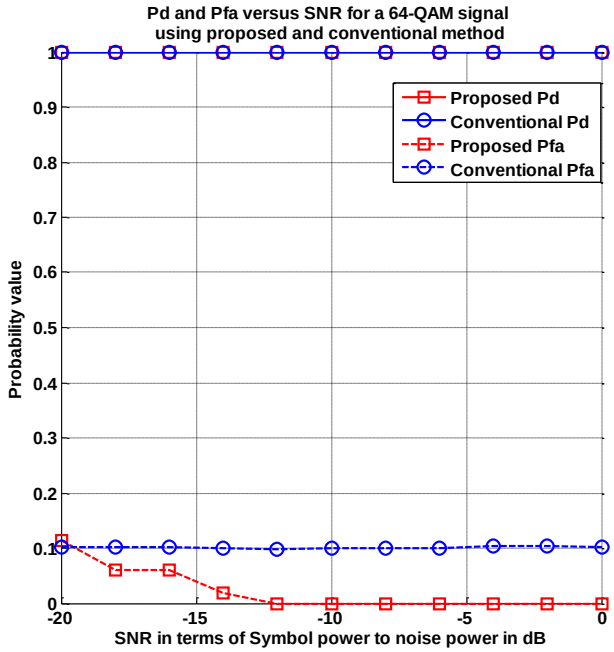

Figure 6.5(a). Probability of detection and false alarm versus SNR for a 64-QAM signal using the conventional and proposed cumulants method.

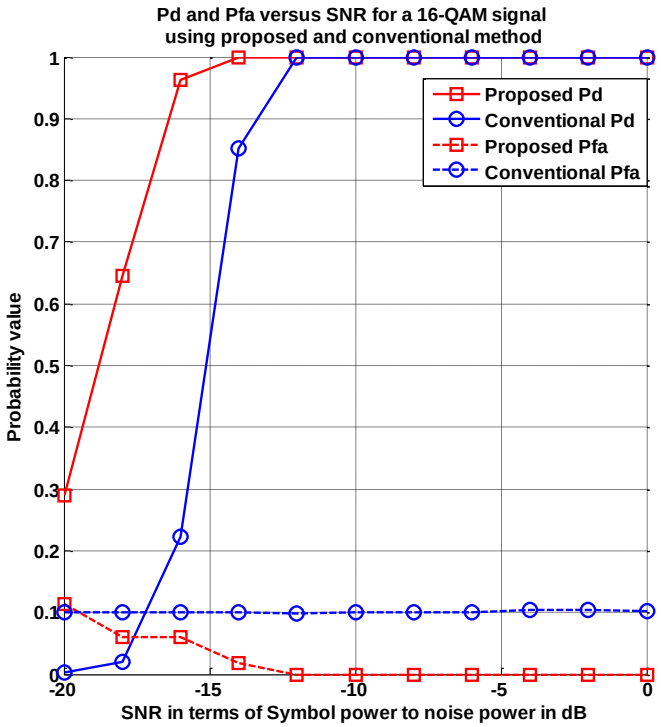

Figure 6.5(b). Probability of detection and false alarm versus SNR for a 16-QAM signal using the conventional and proposed cumulants method.

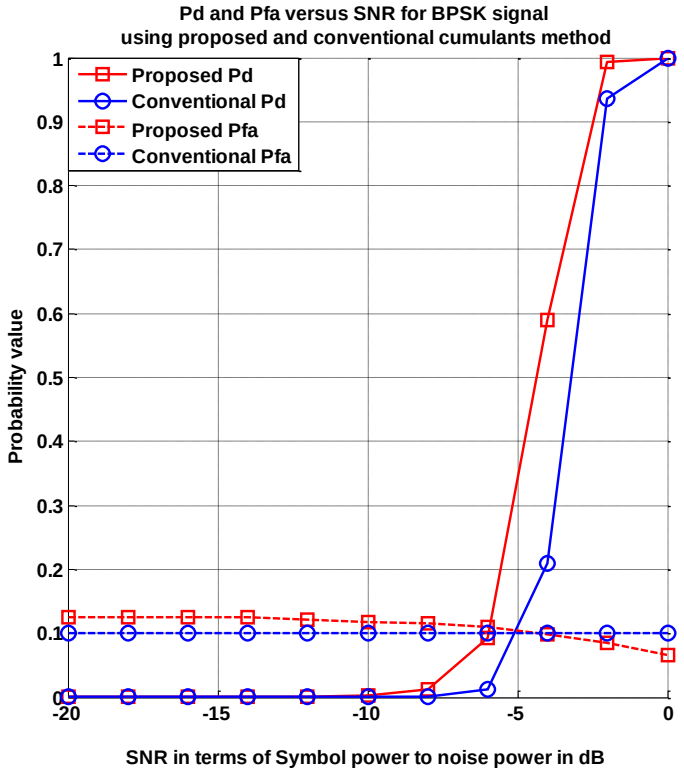

Figure 6.5(c). Probability of detection and false alarm versus SNR for a BPSK signal using the conventional and proposed cumulants method.

Figure 6.5(b) shows that the present method outperforms the conventional cumulants method for SNR values lower than -12 dB at a lower false alarm rate. At an SNR of -16 dB the proposed cumulants method gives 75% improvement in the detection ability when compared with the conventional cumulants method. Figure 6.5(c) shows the performance comparison of the proposed two-stage method and the conventional cumulants method for a BPSK signal. The performance has a flooring effect on the detection ability at lower SNR values, i.e. the probability of detection is zero for values of SNR less than -10 dB for both the methods. According to the central limit theorem, this flooring effect is because of the lower number of samples taken for each simulation. The probability of detection depends on the number of samples considered for simulation. For a fair comparison, the number of symbols was taken as 1024 for all the modulation schemes. The proposed cumulant method gives 80% detection ability at an SNR of -4 dB which is 60% more than the conventional cumulants method for the same false alarm rate of 0.1.

Case 2: The proposed two-stage method was simulated for detecting OFDM signals with signal parameters given in [108].

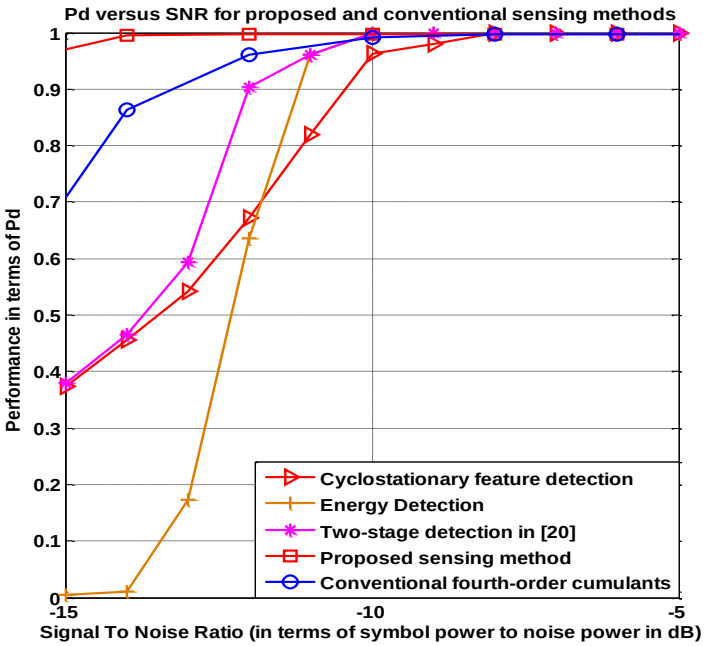

Figure 6.6. Probability of detection versus SNR for various conventional methods and the proposed method.

The noise uncertainty is assumed to be known to the receiver for a fair comparison between these methods. The performance of the sensing method was evaluated in terms of the variation of its probability of detection versus the SNR, as compared to the probability of detection of various other sensing methods and is plotted in Figure 6.6. The proposed method outperforms the conventional cumulants methods by approximately 27%, for an SNR as low as -15 dB. It also outperforms the two-stage method proposed in [108] by approximately 58%. The proposed method gives a detection ability of 96.7% for an SNR of -15 dB for the OFDM signals considered.

6.4.3. Experimental Setup and Analysis

In this subsection, the experimental setup for the proposed policy engine and spectrum sensing is elucidated. These experiments are designed to evaluate the performance of the proposed scheme in a real world scenario. In order to capture and analyze the signals, a USRP2 [159] board is used with an indoor Thomson ANTD120 DVB-T antenna as mentioned in the Chapter 3 (Refer Figure 3.6(b) for experimental setup) . The hardware setup required to capture the signal is summarized in Table 6.1.

TABLE 6.1 HARDWARE CONFIGURATION FOR OVER-THE-AIR TESTS USING USRP2

Processor	**Intel Pentium 2.26 GHz (Core 2 Duo), 4 GB RAM**
OS	Ubuntu 10.04 LTS
GNU Radio	3.3 or later
SDR RF hardware	USRP2
RX Antenna	Thomson ANTD120 DVB-T (470 MHz to 862 MHz)

In these over-the-air tests, signals were sent in the sensing policy channel using the signal generator with an antenna connected to its RF output and received by the USRP2 board which is connected to the processor where the detection is performed. The signal generator transmits the signal at known signal power level of -20 dBm. The receiving antenna, which is connected to the USRP2, is positioned at a distance of approximately 3m from the transmitting antenna. This setup is shown in the Figure 3.6(a) and Figure 3.6(b) in Chapter 3. In these tests, there is no control over the noise channel.

The noise need not be purely AWGN and there is also the effect of multipath on the transmitted signal although a clear line of sight was provided during experiments. To perform energy detection in such a case, a clear idea about the noise characteristics such as variance, and hence the noise power is necessary. The frequency band of operation was chosen arbitrarily as 649.5 MHz to 650.5 MHz in the TV white space region. This region of spectrum corresponds to the sensing policy channel, which determines the policy to be loaded onto the SDR. The main objective of the experiment was to control policies for an SDR based CR using the spectrum sensing unit. Our main challenges, therefore, were to implement an operational PE along with signal processing on the received signal in the sensing policy channel. The number of policies was varied to check the performance of the proposed system in terms of average decision time (ADT). It is calculated by performing 1000 experiments for a specific number of policy changes and calculating the time taken to instantiate the policy each time. This is averaged over the number of experiments to give the ADT for a specific number of policy changes. Similarly, experiments for different number of policy changes were conducted and ADT was calculated and tabulated in Table 6.2. XG DARPA in [146] performed similar experiments to obtain the average decision time for policy enforcement. However, they considered dynamic frequency selection (DFS) as a benchmarking policy as it is currently the only policy defined by FCC for SDRs. In Table 6.2, the ADTs of both the methods are shown. It is clear that the proposed policy engine combined with the two-stage based spectrum sensing provides sensing and policy management by utilizing slightly more time for decision as compared to an existing methodology for DSA.

TABLE 6.2 COMPARISON OF THE AVERAGE DECISION TIME REQUIREMENT FOR THE PROPOSED POLICY ENGINE AND XG DARPA ENGINE [146]

Number of policies	**Average decision time (ms)**	
	Proposed method	**XG DARPA [146]**
1	23.24	21
2	25.78	22
4	29.3	25
8	31.62	29

The ADT includes the time taken to sense the signals in the sensing policy channel and the time taken for the policy to be enforced in the PE. The advantage of the proposed method is that, it performs detection with high accuracy at the cost of a slight increase in the average policy decision time when compared with the conventional policy based radio. The proposed method also outperforms the conventional cumulants methods in terms of detection accuracy, by approximately 27%, for an SNR as low as -15 dB.

6.5. Summary

In this work, a policy-based CR that loads policies based on the sensing of a specific channel known as sensing policy channel was presented. The sensing policy channel consists of signals at various pre-defined frequencies that are sensed in order to determine which waveform is to be loaded onto the SDR. This is expected to have a profound impact on the deployment of CR as many standards can operate in a reconfigurable fashion using the proposed method. By providing a dedicated channel for sensing, a policy strategy for CR based on sensing was elucidated. It allows policies to be dynamically changed and controlled. The proposed PE concept is implemented using an off-the-shelf Java Imperius policy engine and the SCA architecture. The proposed sensing method is a two-stage filter bank based energy detector and higher order cumulants. The filter bank used for channelization is used for spectrum sensing as well, resulting in complexity reduction. The two-stage spectrum sensing method involves calculation of HOS based fourth-order cumulants. These cumulant values are normalized using weights obtained by the power values of the corresponding subbands. Applying binary hypothesis testing, it is shown through simulations that the normalization method helps in improving the cumulant value to its true value. This improvement is shown, through simulations, to increase the detection ability of the proposed cumulants over the conventional cumulants methods for BPSK, 16-QAM and 64-QAM signals. The proposed cumulants method shows an improvement of 27% in the probability of detection for an OFDM signal at an SNR of -15 dB for a constant false alarm rate of 0.1, when compared with the conventional cumulants method. It is also shown to outperform various conventional methods such as energy detection, cyclostationary feature detection and the conventional two-stage sensing method. In this work, the fourth-order zero-lag cumulant was

considered for high sensing performance. The performance of the sensing method comes at the cost of the computational complexity involved in calculating higher order moments. However, the average decision time of the proposed method indicates that the proposed method takes only slightly more time than the conventional XG DARPA policy based SDR. Spectrum sensing based policy management for CRs is considered in this work. The proposed methods have been shown to be better or on par in performance with various existing methods in the literature.

In this chapter, a prototype implementation of a cognitive radio using spectrum sensing has been explained with an off the shelf policy engine. The usage of zero lag single valued fourth-order cumulants ensured higher accuracy for detection. However, it is computationally complex because higher-order moments are calculated for all the cumulant estimates. The present work does not focus on reducing the complexity of the method but on improving the performance of sensing. The two-stage method in [108] can be used with our method to reduce the complexity. It is shown in [108] that in case of scenarios where the SNR is high, the detection performance of energy detection alone is equivalent to that of complex methods such as cyclostationary feature detection. Thus, if the SNR is known to the receiver, the second stage can be used sparingly to detect the signal. The complexity incurred in using two stages for sensing can be minimized in this manner. In [108], the authors perform a two-stage spectrum sensing using energy detection in the first stage and cyclostationary feature detection in the second stage. In contrast, the proposed two-stage spectrum sensing algorithm uses fourth-order cumulants in the second stage. The future work needs to focus on reducing the computational complexity of the proposed method. In the next chapter, the conclusion of this thesis work is given in detail along with a few possible areas of future development.

Chapter 7

Conclusions and Future Work

The use of radio frequencies has increased dramatically during the past few decades. As a result, the radio frequency spectrum is becoming more and more crowded. Efficient and reliable operation in this crowded electromagnetic spectrum environment calls for flexible and intelligent automatic systems capable of adapting to the existing radio environment. In order to facilitate learning and adaptation, these systems must observe the radio environment. That is, they must sense the spectrum and become aware of its state. Cognitive radios (CRs) are future communication devices that are capable of learning from the environment. Spectrum sensing operations such as detection, spectrum estimation, waveform or modulation recognition, are examples of tasks that future communication and radar systems, such as cognitive radios and radars, need to perform for optimum performance.

The thesis focused primarily on two problems of signal processing for wireless communications namely, detection and classification. It also focused on implementing a prototype for cognitive radio by enabling policies based on spectrum sensing. The primary challenges in these fields include the low SNR levels, the non-Gaussian nature of the noise and the interference from other equipments and devices. The contributions of the work presented in this thesis to these fields and the inferences drawn are described below.

7.1. Conclusions

The main contribution of the work was on improved sensing and classification methods for cognitive radios and military radios. An energy detector based on tree-structured discrete Fourier transform filter bank (TDFTFB) was proposed for detecting the frequency edges of channels for accurate hole detection. Simulation results were presented to show that the proposed architecture performs better than the conventional DFTFB based spectrum sensor. The advantage of the proposed method is that, it works with limited knowledge about the signal and noise. The noise was assumed to be Gaussian in nature, to serve as a simple starting point for the detection problem addressed in this thesis.

The second contribution was an integrated scheme for spectrum sensing and automatic modulation classification in cognitive radios. Spectrum sensing was done using the proposed cumulants derived using fractional lower order statistics. The performance of the proposed method was compared with the conventional method based on higher order statistics (HOS) for various noise conditions. It was shown that the proposed method performs well in both Gaussian and non-Gaussian conditions as compared to the conventional method. An experimental data acquisition setup was employed to obtain real time signals from the wideband spectrum to analyze the noise characteristics. A new pattern recognition based automatic modulation classification algorithm based on fractional lower-order statistics (FLOS) and cumulants was proposed. The advantage of the proposed method is that the same statistic used for detection is used for classification. The challenge in designing a classifier is the lack of prior knowledge about the signal and channel information. In the proposed method, the detection and classification was performed without any prior knowledge about the signal, noise or fading in the channel. The main advantage of the proposed scheme is that, it is designed for a wide class of noises while most of the literature assumes noise to be Gaussian in nature.

The third contribution was a policy-based CR that loads policies based on the sensing of a specific channel known as sensing policy channel. The sensing policy channel consists of signals at various pre-defined frequencies that are sensed in order to

determine which waveform has to be loaded onto the software defined radio. Using the proposed model, many standards can operate in a reconfigurable fashion. By providing a dedicated channel for sensing, a policy strategy for CR based on sensing was elucidated. It allows policies to be dynamically changed and controlled. The proposed concept was implemented using an off-the-shelf Java Imperius policy engine and the SCA architecture.

The last contribution was a two-stage detection method using filter banks and higher order statistics. The filter bank used for channelization was used for spectrum sensing as well, resulting in complexity reduction. The two-stage spectrum sensing method involves calculation of HOS based fourth order cumulants. These cumulant values are normalized using weights obtained by the power values of the corresponding subbands. Applying binary hypothesis testing, it is shown through simulations that the normalization method helps in improving the detection accuracy.

7.2. Future work

Possible future work includes

- Optimization of hardware resources is important in the case of cognitive radio as spectrum sensing forms a major part in the CR. Thus, there is a need to find less complex ways of implementing the proposed methods in hardware with minimum power consumption and optimum performance. The proposed method in Chapter 4 is a multi-stage DFTFB, which has filtering and FFT transform operations at each stage. As the number of stages increases, the number of filter banks and FFT also will increase. This increases the complexity of the proposed method drastically. The complexity is high not only because of the number of filter banks involved, but also because these filter banks are operated in a parallel fashion. In parallel implementation, the filter banks occupy more area as several inputs are processed in parallel and outputs are produced simultaneously (in a single clock period) by replicating the hardware. In order to reduce the complexity in terms of area in the FPGA, the implementation can be done in a serial manner by means of

pipelining the output, rather than a parallel fashion. This would reduce the complexity incurred in implementing such a system, however it affects the operational speed of the filter bank. Also, when a serial implementation is done, it needs a separate memory block to store the input signal samples coming at a high sampling rate. Serial implementation of the proposed TDFTFB is a good scope for future work, as optimizing the hardware forms a major role in developing a cognitive radio. Hybrid implementations can also be a good future direction, in terms of optimizing the hardware implementation. It is important to implement and realize the proposed architectures and algorithms in hardware platform such as FPGA to analyze the complexity incurred in real-time. Although, this thesis involved a few realizations, the CR as a whole needs to be realized using the proposed architectures and algorithms. It also needs to be compared with other existing methods in terms of power consumption and speed of operation. The implementation results include the estimate of area, power and delay metrics, which play a major role in validating the functionality of the proposed methods.

- CRs are expected to optimize available resources (e.g. power, bandwidth, etc.) and to adapt each layer of the network layers according to the sensed environment. Several potential applications of CR are in military and public safety where there are inherent necessity for interoperability amongst various existing standards and guaranteed level of Quality of Service (QoS) for secure, reliable, and robust communications. In commercial applications, QoS includes service availability of and reliable/fast data transfer [4]. In addition, for military and public safety applications, the CRs are expected to perform fixed and on-the move communications between highly diverse elements in a very harsh spectral environment, which is susceptible to jamming attacks and interferences [5]. In military applications, there is no information about the enemy signal and hence the CR receiver needs to identify the modulation format employed in the signal. Automatic modulation classification (AMC) method was addressed in this thesis to identify the modulation format employed in the received signal. After spectrum sensing and modulation classification, the CR must be able to adjust its parameters according to the sensing information. In a typical wireless

communication channel, noise and multipath fading corrupt the transmitted signals. Multipath fading not only affects the performance of symbol detection by causing inter symbol interference (ISI) but also affects the performance of the AMC. An equalizer is usually used to remove ISI from the received signal, thus improving the symbol detection performance. However, in a CR scenario it is difficult to design an equalizer because of lack of training or pilot sequences when compared to a conventional wireless communication system, where training or pilot sequences are usually available for designing the equalizer. In the latter case, equalizer parameters are generally adapted by minimizing the well-known cost function mean square error (MSE). Whereas, in the CR scenario, there is a need for adaptive blind equalization algorithms due to the lack of training sequences. Since the blind equalizers affect the performance of AMC as well, robust blind equalizers can be designed by considering the performance of AMC while adapting equalizer parameters. For this purpose, an adaptive communication system is imperative. A blind equalizer is another important signal-processing component that a CR must possess.

- A CR must be able to reconfigure its components in order to facilitate use of various technologies. An ideal CR must be a fully reconfigurable radio that changes its communication parameters depending on network and/or user demands. In reality, full reconfiguration of a radio is a huge task. Partial reconfiguration is a solution for such a scenario. For this purpose, Software Defined Radio (SDR) is used for CR implementation. SDR refers to a set of techniques that permit the reconfiguration of a communication system without changing/adding any hardware system element. The goal of SDR is to produce communication devices, which can support several different services on a single platform as mentioned in Chapter six of this thesis. Enabling cognitive abilities in a radio with the help of partial reconfiguration offered by SDR platforms is an interesting future direction.

- CRs must be able to perform sensing in a dynamic and fast manner. Cooperative sensing is one field of research that enables usage of cognitive users in a primary user scenario. From the results on cooperative sensing presented in [55] it can be concluded that the highest increase in probability of detection is observed when two or more cooperating radios were considered for spectrum sensing. Cooperative sensing will also help CRs share the workload on spectrum sensing, if they are in the same spectral environment. There is a lot of work done in literature on cooperative sensing. An investigation into how the cognitive radio networks work by cooperating with one another could provide an interesting future direction.

References

[1] F. C. Commission, "Spectrum policy task force report," in *Proceedings of the Federal Communications Commission*, ed. Washington DC, November 2002.

[2] J. Mitola, III and G. Q. Maguire, Jr., "Cognitive radio: making software radios more personal," *Personal Communications, IEEE*, vol. 6, pp. 13-18, 1999.

[3] T. C. Clancy, "Formalizing the interference temperature model," *Wirel. Commun. Mob. Comput.*, vol. 7, pp. 1077-1086, 2007.

[4] H. Arslan, "Applications of Cognitive Radio," in *Cognitive Radio, Software Defined Radio and Adaptive Wireless Systems*, ed: Springer, 2007, pp. 383-420.

[5] Z. Qing and B. M. Sadler, "A Survey of Dynamic Spectrum Access," *Signal Processing Magazine, IEEE*, vol. 24, pp. 79-89, 2007.

[6] M. M. Buddhikot, "Understanding Dynamic Spectrum Access: Models,Taxonomy and Challenges," in *New Frontiers in Dynamic Spectrum Access Networks, 2007. DySPAN 2007. 2nd IEEE International Symposium on*, 2007, pp. 649-663.

[7] W. Lehr and J. Crowcroft, "Managing shared access to a spectrum commons," in *New Frontiers in Dynamic Spectrum Access Networks, 2005. DySPAN 2005. 2005 First IEEE International Symposium on*, 2005, pp. 420-444.

[8] I. F. Akyildiz, W.Y. Lee, M. C. Vuran, and S. Mohanty, "Next generation/ dynamic spectrum access/cognitive radio wireless networks: A survey," *Computer Networks,* vol. 50, pp. 2127-2159, Sept 2006.

[9] F. C. Commission, "Notice of proposed rule making and order: Facilitating oppurtunities for flexible, efficient, and reliable spectrum use employing cognitive radio technologies," vol. ET Docket No. 03-108, ed, Feb 2005.

[10] S. M. D Cabric, D Willkomm, R Brodersen, A Wolisz, "A cognitive radio approach for usage of virtual unlicensed spectrum," in *Proc. IST Mobile and Wireless Communications Summit*, Dresden, 2005.

[11] D. Cabric and R. W. Brodersen, "Physical layer design issues unique to cognitive radio systems," in *Personal, Indoor and Mobile Radio Communications, 2005. PIMRC 2005. IEEE 16th International Symposium on*, 2005, pp. 759-763 Vol. 2.

[12] D. Cabric, S. M. Mishra, and R. W. Brodersen, "Implementation issues in spectrum sensing for cognitive radios," in *Signals, Systems and Computers, 2004. Conference Record of the Thirty-Eighth Asilomar Conference on*, 2004, pp. 772-776 Vol.1.

[13] A. Ghasemi and E. S. Sousa, "Spectrum sensing in cognitive radio networks: requirements, challenges and design trade-offs," *Communications Magazine, IEEE,* vol. 46, pp. 32-39, 2008.

[14] S. Haykin, "Cognitive radio: brain-empowered wireless communications," *Selected Areas in Communications, IEEE Journal on,* vol. 23, pp. 201-220, 2005.

[15] S. Haykin, "Fundamental Issues in Cognitive Radio," in *Cognitive Wireless Communication Networks*, E. Hossain and V. Bhargava, Eds., ed: Springer US, 2007, pp. 1-43.

[16] Z. Qing, R. Wei, and A. Swami, "Spectrum Opportunity Detection: How Good Is Listen-before-Talk?," in *Signals, Systems and Computers, 2007. ACSSC 2007. Conference Record of the Forty-First Asilomar Conference on*, 2007, pp. 767-771.

[17] Z. Qing, "Spectrum Opportunity and Interference Constraint in Opportunistic Spectrum Access," in *Acoustics, Speech and Signal Processing, 2007. ICASSP 2007. IEEE International Conference on*, 2007, pp. III-605-III-608.

[18] T. X. Brown, "An analysis of unlicensed device operation in licensed broadcast service bands," in *New Frontiers in Dynamic Spectrum Access Networks, 2005. DySPAN 2005. 2005 First IEEE International Symposium on*, 2005, pp. 11-29.
[19] J. Proakis, *Digital Communications*: McGraw-Hill, 2001.
[20] A. Sahai, N. Hoven, and R. Tandra, "Some Fundamental Limits on Cognitive Radio," in *the 42sd Allerton Conference on Communication, Control and Computing*, 2004.
[21] S.-Y. Chang, "Analysis of proposed sensing schemes for IEEE802. 22 WRAN," ed: IEEE.
[22] D. Cabric, A. Tkachenko, and R. W. Brodersen, "Spectrum Sensing Measurements of Pilot, Energy, and Collaborative Detection," in *Military Communications Conference, 2006. MILCOM 2006. IEEE*, 2006, pp. 1-7.
[23] D. Cabric, "Addressing feasibility of cognitive radios," *Signal Processing Magazine, IEEE*, vol. 25, pp. 85-93, 2008.
[24] S. V. Nagaraj, "Entropy-based spectrum sensing in cognitive radio," *Signal Processing*, vol. 89, pp. 174-180, 2009.
[25] M. Muterspaugh, H. Liu, and W. Gao, "Thomson proposal outline for WRAN," *IEEE 802.22-05/0096r1*, 2005.
[26] C. Cordeiro, "A cognitive PHY/MAC proposal for IEEE 802.22 WRAN systems," ed: IEEE, 2005.
[27] C. Hou-Shin, G. Wen, and D. G. Daut, "Signature Based Spectrum Sensing Algorithms for IEEE 802.22 WRAN," in *Communications, 2007. ICC '07. IEEE International Conference on*, 2007, pp. 6487-6492.
[28] H. Urkowitz, "Energy detection of unknown deterministic signals," *Proceedings of the IEEE*, vol. 55, pp. 523-531, 1967.
[29] T. Y. H. Arslan, "A Survey of Spectrum Sensing Algorithms for Cognitive Radio Applications," *IEEE Communications Surveys & Tutorials*, vol. 11, pp. 116-130, 2009.
[30] P. Stoica and R. Moses, *Introduction to Spectral Analysis*: {Prentice Hall}, 1997.
[31] S. P. Fazeli-Dehkordy, K.N.; Pasupathy, S, "Two stage spectrum detection in cognitive radio networks," presented at the IEEE International Conference on Acoustics Speech and Signal Processing (ICASSP), 2010.
[32] P. D. Welch, "The use of fast Fourier transform for the estimation of power spectra: A method based on time averaging over short, modified periodograms," *Audio and Electroacoustics, IEEE Transactions on*, vol. 15, pp. 70-73, 1967.
[33] D. J. Thomson, "Spectrum estimation and harmonic analysis," *Proceedings of the IEEE*, vol. 70, pp. 1055-1096, 1982.
[34] A. Sonnenschein and P. M. Fishman, "Radiometric detection of spread-spectrum signals in noise of uncertain power," *Aerospace and Electronic Systems, IEEE Transactions on*, vol. 28, pp. 654-660, 1992.
[35] R. Tandra and A. Sahai, "SNR Walls for Signal Detection," *Selected Topics in Signal Processing, IEEE Journal of*, vol. 2, pp. 4-17, 2008.
[36] K. Young Min, Z. Guanbo, S. Sung Hwan, and K. Jae Moung, "An Alternative Energy Detection Using Sliding Window for Cognitive Radio System," in *Advanced Communication Technology, 2008. ICACT 2008. 10th International Conference on*, 2008, pp. 481-485.
[37] D. J. Torrieri, "Principles of military communication systems," *Dedham, MA, Artech, 1981. 340 p.*, vol. 1, 1981.
[38] H. Kim and K. G. Shin, "In-band spectrum sensing in cognitive radio networks: energy detection or feature detection?," in *Proceedings of the 14th ACM international conference on Mobile computing and networking*, 2008, pp. 14-25.
[39] M. Jun and L. Ye, "Soft Combination and Detection for Cooperative Spectrum Sensing in Cognitive Radio Networks," in *Global Telecommunications Conference, 2007. GLOBECOM '07. IEEE*, 2007, pp. 3139-3143.

[40] A. Ghasemi and E. S. Sousa, "Opportunistic spectrum access in fading channels through collaborative sensing," *Journal of Communications,* vol. 2, pp. 71-82, 2007.
[41] F. F. Digham, M. S. Alouini, and M. K. Simon, "On the energy detection of unknown signals over fading channels," in *Communications, 2003. ICC '03. IEEE International Conference on*, 2003, pp. 3575-3579 vol.5.
[42] M. I. Skolnik, "Introduction to radar systems," 2001.
[43] J. Lehtomaki, *Analysis of energy based signal detection* vol. 68, 2005.
[44] J. J. Lehtomaki, M. Juntti, and H. Saarnisaari, "CFAR strategies for channelized radiometer," *Signal Processing Letters, IEEE,* vol. 12, pp. 13-16, 2005.
[45] S. M. Mishra, R. W. Brodersen, S. T. Brink, and R. Mahadevappa, "Detect and avoid: an ultra-wideband/WiMAX coexistence mechanism [Topics in Radio Communications]," *Communications Magazine, IEEE,* vol. 45, pp. 68-75, 2007.
[46] C. Cordeiro, M. Ghosh, D. Cavalcanti, and K. Challapali, "Spectrum Sensing for Dynamic Spectrum Access of TV Bands," in *Cognitive Radio Oriented Wireless Networks and Communications, 2007. CrownCom 2007. 2nd International Conference on*, 2007, pp. 225-233.
[47] H. Urkowitz, "Energy Detection of a Random Process in Colored Gaussian Noise," *Aerospace and Electronic Systems, IEEE Transactions on,* vol. AES-5, pp. 156-162, 1969.
[48] S. A. Kassam and J. B. Thomas, *Signal detection in non-Gaussian noise* vol. 5: Springer-Verlag New York, 1988.
[49] J. Moragues, L. Vergara, J. Gosálbez, and I. Bosch, "An extended energy detector for non-Gaussian and non-independent noise," *Signal Processing,* vol. 89, pp. 656-661, 2009.
[50] B. Farhang-Boroujeny, "Filter Bank Spectrum Sensing for Cognitive Radios," *Signal Processing, IEEE Transactions on,* vol. 56, pp. 1801-1811, 2008.
[51] N. M. Neihart, S. Roy, and D. J. Allstot, "A Parallel, Multi-Resolution Sensing Technique for Multiple Antenna Cognitive Radios," in *Circuits and Systems, 2007. ISCAS 2007. IEEE International Symposium on*, 2007, pp. 2530-2533.
[52] A. Pandharipande and J. P. M. G. Linnartz, "Performance Analysis of Primary User Detection in a Multiple Antenna Cognitive Radio," in *Communications, 2007. ICC '07. IEEE International Conference on*, 2007, pp. 6482-6486.
[53] S. M. Kay and S. L. Marple, Jr., "Spectrum analysis—A modern perspective," *Proceedings of the IEEE,* vol. 69, pp. 1380-1419, 1981.
[54] P. Stoica and R. L. Moses, *Spectral analysis of signals*: Pearson/Prentice Hall Upper Saddle River, NJ, 2005.
[55] H. Sarvanko, M. Mustonen, A. Hekkala, A. Mammela, M. Matinmikko, and M. Katz, "Cooperative and noncooperative spectrum sensing techniques using Welch’s periodogram in cognitive radios," in *Cognitive Radio and Advanced Spectrum Management, 2008. CogART 2008. First International Workshop on*, 2008, pp. 1-5.
[56] C. M. Spooner, "Multi-Resolution White-Space Detection for Cognitive Radio," in *Military Communications Conference, 2007. MILCOM 2007. IEEE*, 2007, pp. 1-9.
[57] T. Zhi and G. B. Giannakis, "A Wavelet Approach to Wideband Spectrum Sensing for Cognitive Radios," in *Cognitive Radio Oriented Wireless Networks and Communications, 2006. 1st International Conference on*, 2006, pp. 1-5.
[58] T. Zhi and G. B. Giannakis, "Compressed Sensing for Wideband Cognitive Radios," in *Acoustics, Speech and Signal Processing, 2007. ICASSP 2007. IEEE International Conference on*, 2007, pp. IV-1357-IV-1360.
[59] Y. L. Polo, W. Ying, A. Pandharipande, and G. Leus, "Compressive wide-band spectrum sensing," in *Acoustics, Speech and Signal Processing, 2009. ICASSP 2009. IEEE International Conference on*, 2009, pp. 2337-2340.

[60] W. Ying, A. Pandharipande, Y. L. Polo, and G. Leus, "Distributed compressive wide-band spectrum sensing," in *Information Theory and Applications Workshop, 2009*, 2009, pp. 178-183.

[61] Y. Hur, J. Park, W. Woo, K. Lim, C. H. Lee, H. S. Kim, and J. Laskar, "A wideband analog multi-resolution spectrum sensing (MRSS) technique for cognitive radio (CR) systems," in *Circuits and Systems, 2006. ISCAS 2006. Proceedings. 2006 IEEE International Symposium on*, 2006, p. 4 pp.

[62] Y. Youngwoo, J. Hyoungsuk, J. Hoiyoon, and L. Hyuckjae, "Discrete Wavelet Packet Transform based Energy Detector for Cognitive Radios," in *Vehicular Technology Conference, 2007. VTC2007-Spring. IEEE 65th*, 2007, pp. 2641-2645.

[63] J. J. Lehtomaki, J. Vartiainen, M. Juntti, and H. Saarnisaari, "CFAR Outlier Detection With Forward Methods," *Signal Processing, IEEE Transactions on*, vol. 55, pp. 4702-4706, 2007.

[64] J. J. Lehtomäki, J. Vartiainen, M. Juntti, and H. Saarnisaari, "Spectrum sensing with forward methods," in *Proceedings of the 2006 IEEE conference on Military communications*, 2006, pp. 2217-2223.

[65] J. Vartiainen, H. Sarvanko, J. Lehtomaki, M. Juntti, and M. Latva-aho, "Spectrum Sensing with LAD-Based Methods," in *Personal, Indoor and Mobile Radio Communications, 2007. PIMRC 2007. IEEE 18th International Symposium on*, 2007, pp. 1-5.

[66] J. H. K. J. W. Lee, H. J. Oh and S. H. Hwang, "Energy Detector using Adaptive-Fixed Thresholds in Cognitive Radio Systems," presented at the 14th Asia-Pacific Conference on Communications,APCC 2008, Tokyo, Oct 2008.

[67] J. H. K. J. W. Lee, H. J. Oh and S. H. Hwang, "Energy detector using a hybrid threshold in cognitive radio system," *IEICE transactions on communications*, vol. E92-B, pp. 3079-3083, Oct 2009.

[68] e. a. Shi, "Signal detection in cognitive radio systems," US Patent, 2010.

[69] K. J. H H Choi, Y Cheong, "Adaptive Sensing Threshold Control Based on Transmission Power in Cognitive Radio Systems," presented at the Cognitive Radio Oriented Wireless Networks and Communications, Singapore, May, 2008.

[70] S. R.-P. Tsung-Han Yu, Dejan Markovic´, and Danijela Cˇ abric, " Cognitive Radio Wideband Spectrum Sensing Using Multitap Windowing and Power Detection with Threshold Adaptation," presented at the IEEE International Communications Conference, 2010.

[71] Z. X. Jiang ZHu, Furong Wang, B Huang, B Zhang, "Double threshold energy detection of cooperative spectrum sensing in cognitive radio," presented at the Cognitive Radio Oriented Wireless Networks and Communications, Singapore, May 2008.

[72] e. a. C. Song, "Adaptive Two thresholds based energy detection for cooperative spectrum sensing," presented at the IEEE Consumer Communications and Networking Conference , CCNC, 2010.

[73] W. A. Gardner, "Signal interception: a unifying theoretical framework for feature detection," *Communications, IEEE Transactions on*, vol. 36, pp. 897-906, 1988.

[74] W. A. Gardner and C. M. Spooner, "Signal interception: performance advantages of cyclic-feature detectors," *Communications, IEEE Transactions on*, vol. 40, pp. 149-159, 1992.

[75] W. A. Gardner and C. M. Spooner, "Detection and source location of weak cyclostationary signals: simplifications of the maximum-likelihood receiver," *Communications, IEEE Transactions on*, vol. 41, pp. 905-916, 1993.

[76] L. Izzo, L. Paura, and M. Tanda, "Signal interception in non-Gaussian noise," *Communications, IEEE Transactions on*, vol. 40, pp. 1030-1037, 1992.

[77] P. Rostaing, E. Thierry, and T. Pitarque, "Asymptotic performance analysis of the single-cycle detector," in *Proc. IEEE European Signal Processing Conference (EUSIPCO'96)*, 1996, pp. 10-13.

[78] H. Bolcskei, "Blind estimation of symbol timing and carrier frequency offset in wireless OFDM systems," *Communications, IEEE Transactions on*, vol. 49, pp. 988-999, 2001.

[79] W. A. Gardner, W. Brown, and C. Chih-Kang, "Spectral Correlation of Modulated Signals: Part II--Digital Modulation," *Communications, IEEE Transactions on*, vol. 35, pp. 595-601, 1987.

[80] W. A. Gardner, A. Napolitano, and L. Paura, "Cyclostationarity: Half a century of research," *Signal Processing*, vol. 86, pp. 639-697, 2006.

[81] A. Napolitano and C. M. Spooner, "Cyclic spectral analysis of continuous-phase modulated signals," *Signal Processing, IEEE Transactions on*, vol. 49, pp. 30-44, 2001.

[82] M. Oner and F. Jondral, "On the extraction of the channel allocation information in spectrum pooling systems," *Selected Areas in Communications, IEEE Journal on*, vol. 25, pp. 558-565, 2007.

[83] P. Rostaing, E. Thierry, and T. Pitarque, "Asymptotic performance analysis of cyclic detectors," *Communications, IEEE Transactions on*, vol. 47, pp. 10-13, 1999.

[84] E. Serpedin, F. Panduru, I. Sarı, and G. B. Giannakis, "Bibliography on cyclostationarity," *Signal Processing*, vol. 85, pp. 2233-2303, 2005.

[85] G. Loo Peng, L. Zhongding, and F. Chin, "Feature Detector for DVB-T Signal in Multipath Fading Channel," in *Cognitive Radio Oriented Wireless Networks and Communications, 2007. CrownCom 2007. 2nd International Conference on*, 2007, pp. 234-240.

[86] P. Marques, J. Bastos, and A. Gameiro, "Sensing UMTS Bands Using Cyclostationary Features and Cooperation Between Opportunistic Terminals," in *Cognitive Radio Oriented Wireless Networks and Communications, 2008. CrownCom 2008. 3rd International Conference on*, 2008, pp. 1-5.

[87] O. A. Y. Ojeda and J. Grajal, "Detection of unknown signals based on spectral correlation measurements," *EUSIPCO 2006*, 2006.

[88] R. S. Roberts, W. A. Brown, and H. H. Loomis, "Computationally efficient algorithms for cyclic spectral analysis," *Signal Processing Magazine, IEEE*, vol. 8, pp. 38-49, 1991.

[89] C. Hou-Shin, G. Wen, and D. G. Daut, "Spectrum Sensing Using Cyclostationary Properties and Application to IEEE 802.22 WRAN," in *Global Telecommunications Conference, 2007. GLOBECOM '07. IEEE*, 2007, pp. 3133-3138.

[90] A. Fehske, J. Gaeddert, and J. Reed, "A new approach to signal classification using spectral correlation and neural networks," in *New Frontiers in Dynamic Spectrum Access Networks, 2005. DySPAN 2005. 2005 First IEEE International Symposium on*, 2005, pp. 144-150.

[91] T. Yucek and H. Arslan, "Spectrum Characterization for Opportunistic Cognitive Radio Systems," in *Military Communications Conference, 2006. MILCOM 2006. IEEE*, 2006, pp. 1-6.

[92] S. Chaudhari, V. Koivunen, and H. V. Poor, "Autocorrelation-Based Decentralized Sequential Detection of OFDM Signals in Cognitive Radios," *Signal Processing, IEEE Transactions on*, vol. 57, pp. 2690-2700, 2009.

[93] S. Chaudhari, J. Lunden, and V. Koivunen, "Collaborative autocorrelation-based spectrum Sensing of OFDM signals in cognitive radios," in *Information Sciences and Systems, 2008. CISS 2008. 42nd Annual Conference on*, 2008, pp. 191-196.

[94] S. Chaudhari, V. Koivunen, and H. V. Poor, "Distributed Autocorrelation-Based Sequential Detection of OFDM Signals in Cognitive Radios," in *Cognitive Radio Oriented Wireless Networks and Communications, 2008. CrownCom 2008. 3rd International Conference on*, 2008, pp. 1-6.

[95] A. Sahai, R. Tandra, S. M. Mishra, and N. Hoven, "Fundamental design tradeoffs in cognitive radio systems," in *Proceedings of the first international workshop on Technology and policy for accessing spectrum*, 2006, p. 2.

[96] H. Tang, "Some physical layer issues of wide-band cognitive radio systems," in *New Frontiers in Dynamic Spectrum Access Networks, 2005. DySPAN 2005. 2005 First IEEE International Symposium on*, 2005, pp. 151-159.

[97] "Supplement to IEEE Standard for Information Technology- Telecommunications and Information Exchange Between Systems- Local and Metropolitan Area Networks- Specific Requirements- Part 11: Wireless LAN Medium Access Control (MAC) and Physical Layer (PHY) Specifications: Higher-Speed Physical Layer Extension in the 2.4 GHz Band," *IEEE Std 802.11b-1999*, pp. i-90, 2000.

[98] S. Geirhofer, T. Lang, and B. M. Sadler, "A Measurement-Based Model for Dynamic Spectrum Access in WLAN Channels," in *Military Communications Conference, 2006. MILCOM 2006. IEEE*, 2006, pp. 1-7.

[99] S. Geirhofer, L. Tong, and B. M. Sadler, "Dynamic spectrum access in WLAN channels: empirical model and its stochastic analysis," in *Proceedings of the first international workshop on Technology and policy for accessing spectrum*, 2006, p. 14.

[100] X. Xiang, X. Chi, W. Pan, and Y. Wang, "An Adaptive Spectrum Sensing Algorithm Based on Eigenvalue Decomposition," in *Image and Signal Processing, 2009. CISP '09. 2nd International Congress on*, 2009, pp. 1-5.

[101] Z. Yonghong and L. Ying-Chang, "Eigenvalue-based spectrum sensing algorithms for cognitive radio," *Communications, IEEE Transactions on*, vol. 57, pp. 1784-1793, 2009.

[102] E. E. Azzouz and A. K. Nandi, *Automatic Modulation Recognition of Communication Signals*: Kluwer Academic Publishers, 1996.

[103] Z. Yonghong, C. L. Koh, and L. Ying-Chang, "Maximum Eigenvalue Detection: Theory and Application," in *Communications, 2008. ICC '08. IEEE International Conference on*, 2008, pp. 4160-4164.

[104] Z. Yonghong and L. Ying-Chang, "Spectrum-Sensing Algorithms for Cognitive Radio Based on Statistical Covariances," *Vehicular Technology, IEEE Transactions on*, vol. 58, pp. 1804-1815, 2009.

[105] J. Wang and G. Bi, "Spectrum Sensing in Cognitive Radios Based on Multiple Cumulants," *Signal Processing Letters, IEEE*, vol. 17, pp. 723-726, 2010.

[106] L. Ling, N. M. Neihart, S. Roy, and D. J. Allstot, "A two-stage sensing technique for dynamic spectrum access," *Wireless Communications, IEEE Transactions on*, vol. 8, pp. 3028-3037, 2009.

[107] S. Maleki, A. Pandharipande, and G. Leus, "Two-stage spectrum sensing for cognitive radios," in *Acoustics Speech and Signal Processing (ICASSP), 2010 IEEE International Conference on*, 2010, pp. 2946-2949.

[108] P. R. Nair, A. P. Vinod, K. G. Smitha, and A. K. Krishna, "Fast two-stage spectrum detector for cognitive radios in uncertain noise channels," *Communications, IET*, vol. 6, pp. 1341-1348, 2012.

[109] K. L. Blackard, T. S. Rappaport, and C. W. Bostian, "Measurements and models of radio frequency impulsive noise for indoor wireless communications," *Selected Areas in Communications, IEEE Journal on*, vol. 11, pp. 991-1001, 1993.

[110] M. Shao and C. L. Nikias, "Signal processing with fractional lower order moments: stable processes and their applications," *Proceedings of the IEEE*, vol. 81, pp. 986-1010, 1993.

[111] C. L. Nikias and M. Shao, *Signal processing with alpha-stable distributions and applications*: Wiley-Interscience, 1995.

[112] M. Fähnle, "Software-Defined Radio with GNU Radio and USRP/2 Hardware Frontend: Setup and FM/GSM Applications," Bachelor Thesis, Institute of Communication Technology, University of Applied Sciences, Ulm, Germany, 2010.

[113] A. Verduin, "GNU Radio Wireless protocol analysis approach," Master Thesis, Universiteit van Amsterdam, 2008.

[114] A. Mayer, L. Maurer, G. Hueber, T. Dellsperger, T. Christen, T. Burger, and C. Zhiheng, "RF Front-End Architecture for Cognitive Radios," in *Personal, Indoor and Mobile Radio Communications, 2007. PIMRC 2007. IEEE 18th International Symposium on*, 2007, pp. 1-5.

[115] A. Mayer, L. Maurer, G. Hueber, B. Lindner, C. Wicpalek, and R. Hagelauer, "Novel Digital Front End Based Interference Detection Methods," in *Wireless Technologies, 2007 European Conference on*, 2007, pp. 70-73.

[116] G. Hueber, R. Stuhlberger, and A. Springer, "Concept for an adaptive digital front-end for multi-mode wireless receivers," in *Circuits and Systems, 2008. ISCAS 2008. IEEE International Symposium on*, 2008, pp. 89-92.

[117] Y. P. Hur, J.; Woo, W.; Lim, K.; Lee, C.-H.; Kim, H.S.; Laskar, J.;, "A wideband analog multi-resolution spectrum sensing (MRSS) technique for cognitive radio (CR) systems " presented at the IEEE International Symposium on Circuits and Systems, 2006.

[118] Q. Zhi, C. Shuguang, A. H. Sayed, and H. V. Poor, "Wideband Spectrum Sensing in Cognitive Radio Networks," in *Communications, 2008. ICC '08. IEEE International Conference on*, 2008, pp. 901-906.

[119] B. M. Sadler and A. Swami, "Analysis of multiscale products for step detection and estimation," *Information Theory, IEEE Transactions on*, vol. 45, pp. 1043-1051, 1999.

[120] R. Mahesh, A. P. Vinod, E.-K. Lai, and A. Omondi, "Filter Bank Channelizers for Multi-Standard Software Defined Radio Receivers," *Journal of Signal Processing Systems*, vol. 62, pp. 157-171, 2011/02/01 2011.

[121] T. M. Taher, R. B. Bacchus, K. J. Zdunek, and D. A. Roberson, "Long-term spectral occupancy findings in Chicago," in *New Frontiers in Dynamic Spectrum Access Networks (DySPAN), 2011 IEEE Symposium on*, 2011, pp. 100-107.

[122] M. Ghozzi, F. Marx, M. Dohler, and J. Palicot, "Cyclostatilonarilty-Based Test for Detection of Vacant Frequency Bands," in *Cognitive Radio Oriented Wireless Networks and Communications, 2006. 1st International Conference on*, Mykonos, Greece, 2006, pp. 1-5.

[123] Y. Z. Y C Liang, E C Y Peh, A T Hoang, "Sensing Throughput TradeOff for Cognitive Radio Networks," *IEEE Transactions on Wireless Communications*, vol. 7, pp. 1326-1337, April 2008.

[124] H. Chung-Yu and A. Polydoros, "Likelihood methods for MPSK modulation classification," *Communications, IEEE Transactions on*, vol. 43, pp. 1493-1504, 1995.

[125] O. A. Dobre, Y. Bar-Ness, and S. Wei, "Higher-order cyclic cumulants for high order modulation classification," in *Military Communications Conference, 2003. MILCOM '03. 2003 IEEE*, 2003, pp. 112-117 Vol.1.

[126] W. Hsiao-Chun, M. Saquib, and Y. Zhifeng, "Novel Automatic Modulation Classification Using Cumulant Features for Communications via Multipath Channels," *Wireless Communications, IEEE Transactions on*, vol. 7, pp. 3098-3105, 2008.

[127] M. Rupi, P. Tsakalides, E. D. Re, and C. L. Nikias, "Constant modulus blind equalization based on fractional lower-order statistics," *Signal Process.*, vol. 84, pp. 881-894, 2004.

[128] P. Panagiotou, A. Anastasopoulos, and A. Polydoros, "Likelihood ratio tests for modulation classification," in *MILCOM 2000. 21st Century Military Communications Conference Proceedings*, Los Angeles, CA, 2000, pp. 670-674 vol.2.

[129] L. Rugini, P. Banelli, and G. Leus, "Small Sample Size Performance of the Energy Detector," *Communications Letters, IEEE*, vol. 17, pp. 1814-1817, 2013.

[130] R. A. Gonzalo, *Nonlinear Signal Processing: A Statistical Approach*: John Wiley and Sons, 2004.

[131] X. Li, L. Jin, and S. Wang, "A Simplified Non-Gaussian Mixture Model for Signal LO Detection in a-Stable Interference," in *Image and Signal Processing, 2008. CISP '08. Congress on*, 2008, pp. 403-407.

[132] M. Xinyu and C. L. Nikias, "Parameter estimation and blind channel identification in impulsive signal environments," *Signal Processing, IEEE Transactions on*, vol. 43, pp. 2884-2897, 1995.

[133] O. A. Dobre, A. Abdi, Y. Bar-Ness, and W. Su, "Survey of automatic modulation classification techniques: classical approaches and new trends," *Communications, IET*, vol. 1, pp. 137-156, 2007.

[134] K. Kyouwoong, I. A. Akbar, K. K. Bae, U. Jung-Sun, C. M. Spooner, and J. H. Reed, "Cyclostationary Approaches to Signal Detection and Classification in Cognitive Radio," in *New Frontiers in Dynamic Spectrum Access Networks, 2007. DySPAN 2007. 2nd IEEE International Symposium on*, 2007, pp. 212-215.

[135] O. A. Dobre, A. Abdi, Y. Bar-Ness, and W. Su, "Cyclostationarity-Based Blind Classification of Analog and Digital Modulations," in *Military Communications Conference, 2006. MILCOM 2006. IEEE*, 2006, pp. 1-7.

[136] A. Polydoros and K. Kim, "On the detection and classification of quadrature digital modulations in broad-band noise," *Communications, IEEE Transactions on*, vol. 38, pp. 1199-1211, 1990.

[137] S. Z. Hsue and S. S. Soliman, "Automatic modulation classification using zero crossing," *Radar and Signal Processing, IEE Proceedings F*, vol. 137, pp. 459-464, 1990.

[138] K. C. Ho, W. Prokopiw, and Y. T. Chan, "Modulation identification of digital signals by the wavelet transform," *Radar, Sonar and Navigation, IEE Proceedings -*, vol. 147, pp. 169-176, 2000.

[139] C. M. Jarque and A. K. Bera, "A Test for Normality of Observations and Regression Residuals," *International Statistical Review / Revue Internationale de Statistique*, vol. 55, pp. 163-172, 1987.

[140] S. Kay, *Fundamentals of Statistical Signal Processing, Volume 2: Detection Theory*: Prentice-Hall Inc, 1993.

[141] C. Nikias and A. Petropulu, *Higher Order Spectra Analysis: A Non-Linear Signal Processing Framework (Prentice Hall Signal Processing Series)*: Prentice Hall PTR, 1993.

[142] A. Swami and B. M. Sadler, "Hierarchical digital modulation classification using cumulants," *Communications, IEEE Transactions on*, vol. 48, pp. 416-429, 2000.

[143] T. A. Drumright and D. Zhi, "QAM constellation classification based on statistical sampling for linear distortive channels," *Signal Processing, IEEE Transactions on*, vol. 54, pp. 1575-1586, 2006.

[144] B. A. Fette, *Cognitive radio technology*: Academic Press, 2009.

[145] D. Elenius, G. Denker, M. O. Stehr, R. Senanayake, C. Talcott, and D. Wilkins, "CoRaL--Policy Language and Reasoning Techniques for Spectrum Policies," in *Policies for Distributed Systems and Networks, 2007. POLICY '07. Eighth IEEE International Workshop on*, 2007, pp. 261-265.

[146] F. Perich and M. McHenry, "Policy-based spectrum access control for dynamic spectrum access network radios," *Web Semantics: Science, Services and Agents on the World Wide Web*, vol. 7, pp. 21-27, 2009.

[147] A. Uszok, J. Bradshaw, R. Jeffers, N. Suri, P. Hayes, M. Breedy, L. Bunch, M. Johnson, S. Kulkarni, and J. Lott, "KAoS policy and domain services: toward a description-logic approach to policy representation, deconfliction, and enforcement," in *Policies for Distributed Systems and Networks, 2003. Proceedings. POLICY 2003. IEEE 4th International Workshop on*, 2003, pp. 93-96.

[148] A. Uszok, J. M. Bradshaw, M. Johnson, R. Jeffers, A. Tate, J. Dalton, and S. Aitken, "KAoS policy management for semantic Web services," *Intelligent Systems, IEEE,* vol. 19, pp. 32-41, 2004.
[149] G. N. Stone, B. Lundy, and G. G. Xie, "Network policy languages: a survey and a new approach," *Network, IEEE,* vol. 15, pp. 10-21, 2001.
[150] (17 October 2012). *http://www.w3.org*.
[151] D. R. Stephens, B. Salisbury, and K. Richardson, "JTRS infrastructure architecture and standards," in *Military Communications Conference, 2006. MILCOM 2006. IEEE,* 2006, pp. 1-5.
[152] R. Orfali and D. Harkey, *Client/server programming with Java and CORBA (2nd ed.)*: John Wiley \\& Sons, Inc., 1998.
[153] E. S. S. Amir Ghasemi, "Spectrum Sensing in Cognitive Radio Networks: Requirements, Challenges and Design Trade-offs," *IEEE Communications Magazine,* vol. 46, 2008.
[154] Z. Khalaf, A. Nafkha, J. Palicot, and M. Ghozzi, "Hybrid spectrum sensing architecture for cognitive radio equipment," in *Telecommunications (AICT), 2010 Sixth Advanced International Conference on*, 2010, pp. 46-51.
[155] N. M. N. L. Luo, S. Roy, D. J Allsot, "A Two Stage Sensing Technique for Dynamic Spectrum Access," *IEEE Transactions on Wireless Communications,* vol. 8, pp. 3028-3037, 2009.
[156] G. B. Giannakis and M. K. Tsatsanis, "Signal detection and classification using matched filtering and higher order statistics," *Acoustics, Speech and Signal Processing, IEEE Transactions on,* vol. 38, pp. 1284-1296, 1990.
[157] (17 October 2012). *http://incubator.apache.org/imperius/*.
[158] (17 October 2012). *http://jpype.sourceforge.net/*.
[159] (17 October 2012). *http://gnuradio.org/redmine/projects/gnuradio/wiki/USRP2*.